Republic of Iraq

Ministry of Higher Education & Scientific Research

University of Kerbala

College of Engineering

Civil Engineering Department

Strengthening of Rubberized Reinforced Concrete beams subjected to repeated loads by NSM-CFRP Bars

A Thesis Submitted to the Council of the Faculty of the College of the Engineering/University Of Kerbala in Partial Fulfillment of the Requirements for the Master Degree in Civil Engineering

By:

Shahad Adnan Abd Al-kadum

Supervisor

Asst. Prof. Dr. Ali Ghanim Abbas Al-Khafaji

April 2025 Shawwal 1446

Republic of Iraq

Ministry of Higher Education & Scientific Research

University of Kerbala

College of Engineering

Civil Engineering Department

Strengthening of Rubberized Reinforced Concrete beams subjected to repeated loads by NSM-CFRP Bars

A Thesis Submitted to the Council of the Faculty of the College of the Engineering/University Of Kerbala in Partial Fulfillment of the Requirements for the Master Degree in Civil Engineering

By:

Shahad Adnan Abd Al-kadum

Supervisor

Asst. Prof. Dr. Ali Ghanim Abbas Al-Khafaji

April 2025

Shawwal 1446

بسم الله الرحمن الرحيم

"وَأَن لَّيْسَ لِلإِنسَانِ إِلاَّ مَا سَعَى، وَأَنَّ سَعْيَهُ سَوْفَ يُرَى".

صدق الله العلي العظيم

(النجم: الآية 39 و40)

Examination committee certification

We certify that we have read the thesis entitled " Strengthening of Rubberized Reinforced Concrete beams subjected to repeated loads by NSM-CFRP Bars " and as an examining committee, we examined the student "Shahad Adnan Abd Al-kadum" in its content and in what is connected with it and that, in our opinion, it is adequate as a thesis for the degree of Master of Science in Civil Engineering.

Supervisor

ignature:
lame : Assist. Prof. Dr. Ali Ghanim Abbas
ate: / / 2025

Member

ignature:
ame : Assist. Prof. Dr. Muthanna Hussein Mohsin
ate: / / 2025

Member

Signature:
Name : Assist. Prof. Dr. Mushtaq Sadiq
Date: / / 2025

Chairman

Signature:
Name : Prof. Dr. Sadjad Amir Hemzah
Date: / / 2025

Signature:
Name : Assist. Prof. Dr. Aysar Tuama Al-Awadi
Head of the Department of Civil Engineering
Date: / / 2025

Signature:
Name : Prof. Dr. Haider Nazem Aziz
Dean of the Engineering College
Date: 28/ 5/ 2025

Supervisor certificate

We certify that the thesis entitled " **Strengthening of Rubberized Reinforced Concrete beams subjected to repeated loads by NSM-CFRP Bars** " was prepared by **Shahad Adnan Abd Al-kadum** under our supervision at the Department of Civil Engineering, Faculty of Engineering, University of Kerbala as a partial of fulfilment of the requirements for the Degree of Master of Science in Civil Engineering.

Signature:

Assist. Prof. Dr. Ali Ghanim Abbas

Date: / / 2025

Linguistic certificate

I certify that the thesis entitled " **Strengthening of Rubberized Reinforced Concrete beams subjected to repeated loads by NSM-CFRP Bars** " which has been submitted by **Shahad Adnan Abd Al-kadum,** has been proofread, and its language has been amended to meet the English style.

Signature:

Dr. Kamal Darweesh Ibrahim

Date: 11/5/2025

Undertaking

I certify that research worken titled "" **Strengthening of Rubberized Reinforced Concrete beams subjected to repeated loads by NSM-CFRP Bars** " is my own work. The work has not been presented elsewhere for assessment. Where material has been used from other sources, it has been properly acknowledged / referred.

Signature:

Shahad Adnan Abd Al-kadum

Date: 11/ 5/ 2025

Dedication

To the Master of all beings, to the one whom God sent as a mercy to the world, to the one who was the light that illuminated the darkness of ignorance, to the one who saved humanity and guided it to the path of guidance, to the beloved Mustafa, Muhammad (peace be upon him and his family)

To the two lights that shone from the House of Prophethood to the Lady of Women Fatima al-Zahra (peace be upon her), and to the Master of Guardians and Commander of the Faithful Ali ibn Abi Talib (peace be upon him)

To the light that dispels the darkness of this world, to the hope that hearts yearn for, to the Imam of our time, the awaited Mahdi (may God hasten his noble reappearance)

To the one who left this world but whose soul still fills my life with love and supplication, to my beloved father (may Allah have mercy on him), who always wished to see me at stage, to his pure soul, and I ask God to make it in the balance of his good deeds

To the one who overwhelmed me with her supplications, to my beloved mother

To my sisters and brother, to my husband's family, and to my colleaguse on the path, my dear husband, who stood by my side and endured with me the challenges and difficulties, and it was a great help to me, to my beloved daughter Zahraa who shared this path with me since she was a few months old.

To all of you, I dedicate this work, hoping Allah will make it a blessed step on the path of knowledge and learning

Acknowledgments

In the name of Allah, the Most Gracious, the Most Merciful, Praise be to Allah, who has granted me success and enabled me to complete this thesis. I would like to take this opportunity to extend my sincere thanks and gratitude to my supervisor [Prof. Dr. Ali Ghanim Abbas Al-Khafaji] for his valuable support, guidance, and constant patience, which played a major role in developing this research. It was an honor for me to be under his supervision.

I would also like to express my sincere gratitude and appreciation to my dear husband, Engineer Ali Ihsan, who was my greatest support during this academic journey. His presence by my side was a source of strength and inspiration, and he spared no effort in encouraging, motivating, and working with me to continue despite the challenges.

I would also like to extend my sincere thanks and appreciation to the Engineering Projects Department of the Al-Abbas's (p) Holy Shrine for its valuable support and facilitation of services that contributed greatly to the completion of this research. Your generous cooperation and the provision of the necessary resources and capabilities played a prominent role in facilitating my research process, which was positively reflected in the quality of this study.

I extend my sincere thanks and appreciation to Eng. Ahmed Zaki, Eng. Nour El-Hoda Kazem, and Eng. Khaled Rashid Al-Shalabi, for their valuable support and assistance during the research and experimentation stages. I also express my deep gratitude to my dear family and friends for their unlimited support and continuous encouragement. Without their patience and constant motivation, this achievement would not have been achieved. My sincere thanks and appreciation to all of you.

Abstract

This study examines the behavior of rubberized reinforced concrete beams subjected to repeated loading, strengthened using Near-Surface Mounted (NSM) Carbon Fiber Reinforced Polymer (CFRP) bars and strips. The research addresses the growing environmental issue of waste from discarded vehicle tires, which are challenging to dispose of due to their non-biodegradable nature. By recycling tire rubber and incorporating it as a partial replacement for coarse and fine aggregates in concrete, the study aims to mitigate tire waste and evaluate its impact on concrete properties and structural performance.

The experimental program involved volumetric replacement of fine and coarse aggregates with rubber particles at ratios of 10% and 20%, individually and in combination. Fourteen beam specimens (250 × 150 × 1600 mm) were prepared, including two control beams (one tested under monotonic loading and the other under repeated loading) and twelve strengthened beams. These were divided into two groups: six beams strengthened with NSM-CFRP bars and six with NSM-CFRP strips. Repeated loading tests followed a protocol of 30 cycles, starting with 30%, 60%, and 80% of the ultimate load, followed by loading to failure.

Results indicated that replacing aggregates with rubber significantly reduced mechanical properties, including compressive strength, tensile strength, and flexural strength by 51.66%, 22.59%, and 38%, respectively, at a 20% replacement ratio. The ultimate load capacity of rubberized concrete was lower, especially at higher replacement levels of aggregates. Strengthening with NSM-CFRP strips enhanced ultimate load capacity under repeated loading more than NSM-CFRP bars. Numerical modeling using ABAQUS demonstrated good agreement with experimental results, with

minor deviations. The analysis revealed that increasing CFRP bar diameters from 6 mm to 8 mm improved ultimate load by 2.25%, while increasing strip thickness from 1.2 mm to 2 mm resulted in a marginal improvement of 0.74%, suggesting limited cost-efficiency for thicker strips.

This research highlights the potential of rubberized concrete as a sustainable material and the effectiveness of NSM-CFRP strengthening systems in improving the performance of concrete beams under repeated loading conditions.

Table of Contents

List of Tables

List of Figures

List of Plate

List of Abbreviations

ACI	American Concrete Institute.
ASTM	American society for testing materials
C	Coarse aggregate
CDP	Concrete damage plasticity
CFRP	Carbon fiber reinforced polymer.
CRC	Crumbled Rubber Concrete
F	Fine aggregate
FEA	Finite element analysis.
FRP	Fiber-reinforced polymer.
GFRP	Glass fiber reinforced polymer.
IQS	Iraqi Specification.
kN	Kilo Newton.
mm	Millimeter.
MPa	Mega Pascal.
N	Normal concrete
No	Number.
NSM	Near-surface mounted.
PCC	Portland cement concrete
RC	Reinforced concrete.
SFR	steel fiber concrete

List of Symbols

A	Area.
b	Section Width of Prism
D	Section Diameter
d	Section Depth of Prism
h	Section Height
L	Supports Distance
F	Applied Force
P	Total Failure Load
fc	Compression Resistance According to British Standard.
fc'	Compression Resistance According to American Standard
fr	Flexural Stress
ft	Tensile Stress

Chapter One: Introduction

1.1 General

The high daily production rate of rubber waste tires presents various environmental waste disposal difficulties, which is why many scientists and researchers are attempting to develop sustainable alternative building materials that can sustain growth over the long term.

Numerous studies have demonstrated that compared to regular concrete, tire-rubbed concrete, or Rubcrete, is lower in density and more ductile. Because of this, scrap tire rubber has a lower specific gravity and a higher absorption of energy than rocks, making it a suitable substitute for some of the aggregates in rubberized concrete (rubcrete). The primary issue with utilizing this type of rubcrete mix is the rubber's reduction of the concrete's hardened qualities (compressive and tensile strength values) in comparison to regular concrete. Thus, if these undesirable characteristics are addressed, a new cementation rubber composite that is more ductile and useful in concrete constructions will be produced (Ali and Hasan, 2019a) .

Carbon fiber reinforced polymer (CFRP), repurposed for structural strengthening, is quickly gaining popularity as an alternative method for strengthening concrete structures . It is an anisotropic composite material with all of the carbon fibers pointing in the same direction within a polymer matrix. Because of the carbon fibers' structural strength and the adhesive binder, the polymer is often an epoxy resin. To alter the material's molecular structure and improve its mechanical qualities, the two components are chemically and physically bonded together at the interface. It is the responsibility of each component to guarantee that the material's qualities are tuned to provide

satisfactory performance when used as a whole. The fibers increase the material's strength and rigidity, while the matrix shields it from the elements (Goldstone, 2012).

On the other side, repeated loads refer to loads that are applied to a structure or material multiple times over its lifetime. These loads may be of constant or varying magnitude but are applied repeatedly in a cyclic manner. A comprehensive understanding of the behavior of reinforced concrete (RC) structures and their components subjected to cyclic loading is essential for the accurate design and analysis of such systems (Zhu *et al.*, 2022a) ,this emphasizes the significance of researching how concrete beams behave under repeated loads., as it contributes to improving their design and ensuring their ability to withstand different operating conditions, which enhances the safety and efficiency of engineering structures in the long term.

1.2 Rubberized concrete (Rubcrete)

One of the most often utilized elements in concrete manufacturing are aggregates, both fine and coarse. On the other hand, this material can become rare. A major step toward creating sustainable concrete is the partial addition of rubber particles to concrete mixtures. Numerous studies have tried to develop an efficient rubcrete mixture that incorporates a significant amount of rubber waste. In order to create rubcrete, waste tire rubber particles are substituted for natural aggregates, either by volume or by weight (fine and coarse) in typical concrete compositions (Sibiyone and Sundar, 2017). Therefore, the most frequent waste material utilized to create rubcrete is scrap tire rubber. In civil engineering, there are numerous financial and environmental advantages to using rubber scrap tires. It produces a substance that is ecologically significant, conserves natural resources .

1.2.1 Waste tires

Since rubber takes several years to break down naturally and lingers in the environment for extended periods of time, waste rubber tires are a major environmental concern (Plate 1-1). This is because of the tire's intricately woven three-dimensional structure and the several compounds that are included in its formulation. The majority of tires that reach the end of their useful life are either burned for energy recovery or dumped as garbage in landfills, especially if the rubber is severely damaged. The circular economy and the environment no longer tolerate any of these solutions. However, because recycled used tires have a great potential to be a valuable supply of raw materials, tremendous progress has been made in making used tires sustainable (Fazli and Rodrigue, 2020).

Plate 1-1: Scrap tires (Alfayez, Suleiman and Nehdi, 2020)

The process of treating discarded tires requires first cutting and grinding them into tiny pieces and then using a cracker mill to shred the tire partials into smaller bits by passing them between spinning steel cylinders with reinforced grooves. This process creates particles of various sizes and shapes. These particles are commonly referred to as chip rubbers (Kadhim and Kadhim, 2023).

1.2.2 Waste tires rubber classification

Based on their size, leftover tire rubber is categorized as follows:
1. Chipped rubber (shredded) is widely used to replace coarse aggregate due to its large size. For this type of rubber, two steps of shredding and cutting are necessary. The first step reduces the size of rubber particles until they achieve a particular dimension of 430-300 mm length and 230-150 mm wide. A rubber cube with 150-100 mm dimensions on each side is produced in the second stage. Chips particles with dimensions of 5 to 76 mm are produced if the cutting process is continued.
2. Crumb rubber is a substitute material for fine aggregate. It is produced in a facility equipped with specialized mills that reduce chip rubber particles to a size range of 4.75 to 0.425 mm.
3. Ground rubber, the most effective rubber type for cement replacement, necessitates complex micro-milling to achieve a particle size range of 0.475 mm to 0.075 mm.

The many waste tire kinds are shown in Table 1-1 and Plate 1-2, where they are arranged according to size (Ali and Hasan, 2019b)

Table 1-1: Rubber waste tire classification (Ali and Hasan, 2019)

Items	Metric measurements (mm)	Fields of Uses
Shredded rubber	(100-340) length Width (100-230)	Gravel replacement
Chip rubber	(5 -76)	Coarse aggregate replacement
Crumb rubber	(0.425 - 4.75)	Fine aggregate replacement
Grinded rubber	(0.0075 - 0.475)	Cement replacement
Rubber fiber	(8.5-21.5) Length	Fiber reinforcements

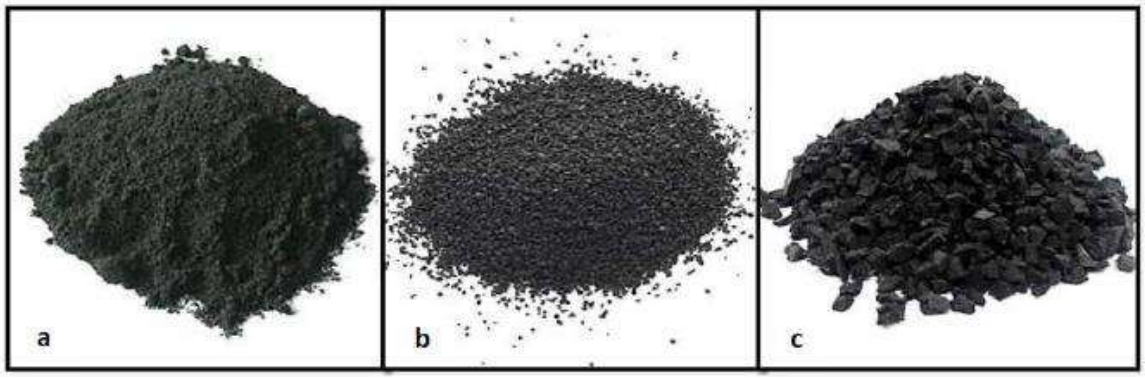

Plate 1-2: Types of tires rubber: a-grinded rubber, b-crumb rubber, and c-chip rubber (Ali and Hasan, 2019).

1.2.3 Advantages and Disadvantages of Including Recycled Tire Rubber into Concrete Mixes

There are numerous advantages and disadvantages of using rubber waste in construction methods, some of which are listed below:

Advantages

1. Generates a substance with a low unit weight.
2. Concrete will have shown ductile behavior rather than brittleness.
3. Increases toughness by absorbing energy.
4. Less shrinkage and cracking.
5. Resources found in nature are preserved.
6. It resists abrasion well.

Disadvantages

One of the biggest drawbacks of utilizing scrap rubber tires in concrete is the decrease in the material's hardened qualities, such as compressive, splitting, flexural strength, and fire resistance.

1.3 Carbon Fiber Reinforced Polymer (CFRP)

More and more civil engineers are turning to carbon fiber-reinforced polymer (CFRP) composites for various engineering projects. Civil

engineering projects are ideal for CFRP composites due to their lightweight, exceptionally durable, and mechanically superior properties. Many infrastructures, including buildings and bridges, have been constructed using CFRP composites in the last several decades . Composites made of carbon fibers that have been woven together and treated with resin are strong and durable. The resin matrix protects the material from environmental hazards, including moisture and UV rays, while the carbon fibers give high tensile strength, stiffness, and fatigue resistance. The resultant composite material's excellent strength-to-weight ratio and low density make it an ideal choice for structural applications. (Vijayan *et al.*, 2023).

1.3.1 Near surface mounting by CFRP

For flexural strengthening in the negative moment zones of slabs and girders, where externally bonded reinforcement could be severely damaged by mechanical and climatic factors, the near-surface mounting technique becomes very appealing (Hassan and Rizkalla, 2004).

As a successful substitute for the externally bonded (EB) FRP strengthening technology, the near-surface mounted (NSM) FRP strengthening approach has garnered international interest. To introduce and embed the FRP reinforcement using an adhesive, grooves must first be carved in the concrete cover of a concrete member in the NSM FRP strengthening method. Compared to the EB FRP method, the NSM FRP method offers several benefits, such as improved bonding efficiency and better protection for the FRP reinforcement (Zhang, Yu and Chen, 2017).

1.4 Repeated load

Over the course of their service life, reinforced concrete structures may be subjected to various repetitive loads, ranging from dead load to dead plus

live load. A force that is delivered repeatedly, changing the internal forces amount and occasionally their sensation. Variable loading occurs when a component experiences applied load or generated stress that is not constant but changes over time; in other words, the load or stress exhibits a pattern of variation over time. The majority of recurring loading is actually caused by:

- Change in the magnitude of applied load
- Change in direction of load application
- Change in point of load application

There are only two ways that the dynamic load might impact a material's strength. The first has to do with the rate of strain. Concrete's ultimate strength during extremely fast straining is substantially greater than it would be during slower straining. Likewise, during highly fast straining, the yield stress of reinforcing steel is much more than under modest strain rates. The failure brought on by repeated cycles of stress that are less severe than those that would result from single loading is the second way that dynamic loading may impact the static strength of materials. This process, known as "fatigue," can happen to steel and concrete reinforcement. It should be mentioned that the primary cause of weariness. As a result, both dynamic and static loads (of a cyclic nature) may cause this form of failure. Even when the actual maximum stresses were below the material's ultimate strength and frequently at stress values even below the yield strength, structural members that were subjected to such recurrent or cyclic stressing were discovered to have collapsed. One of the most distinctive features is that the failure only happened after the stresses were applied numerous times. As a result, the breakdown is known as fatigue failure

1.5 Aim and objectives of this study

The primary objectives of this research, as presented in the thesis, are outlined as follows:

1- Investigate the potential of incorporating used tire rubber in creating viable rubberized concrete mixtures for construction applications.

2- Examine the impact of different proportions of used tire rubber (10%, 20%) as a partial replacement for fine and coarse aggregates, both individually and in combination, on the performance of rubberized concrete under repeated loading, and compare these results with those from conventional concrete.

3- Explore the enhancement of rubber-modified concrete beams by applying carbon fiber reinforced polymer (CFRP) strips and bars using near-surface mounted (NSM) strengthening methods.

4- Use nonlinear finite element analysis to evaluate the repeated behavior of CFRP-reinforced concrete beams under repeated loads.

1.6 Thesis Planning

The thesis is organized into six chapters, each focusing on different aspects of the research:

Chapter One: This chapter introduces the concepts of rubberized concrete, reinforcement methods, and the effects of repeated loading. It also describes the study's main goals and methodology.

Chapter Two: This chapter reviews relevant literature, covering both experimental and theoretical studies. It also discusses previous research on strengthening reinforced concrete beams using CFRP strips and bars with a near-surface mounted reinforcement system.

Chapter Three: This chapter details the properties of the construction materials used in the study and their test results. It also describes the preparation, mixing, and pouring of the concrete beams, the use of CFRP strips and bars, and the installation and testing methods employed.

Chapter Four: The experimental results are presented and analyzed in this chapter.

Chapter Five: Reinforced concrete beams subjected to repeated loading can be modeled analytically using a nonlinear finite element approach. The chapter compares the experimental results with those obtained from the analytical model.

Chapter Six: This chapter concludes the thesis by summarizing the findings from the experimental work and the finite element analysis.

Chapter Two: Literature Review

2.1 Introduction

There are worldwide concerns due to waste tires accumulation, especially in densely populated regions. According to the technical and economic study for tire production in Iraq, an estimate of two million tires are thrown into the environment per year. They are kept as stockpiles. Illegally discarding of these tires causes environmental pollution due to the wrong disposal methods by burning large amounts of them (Kadhim and Kadhim, 2020).

Burning rubber tires releases harmful gases, including dioxin, carbon monoxide, nitrogen oxides, and sulfur, which can cause diseases like asthma, cancer, allergies, and pneumonia. Thermal breakdown produces harmful liquid compounds, contaminating groundwater and causing harm to plants, animals, and wildlife. Burial is not practical or environmentally sustainable due to rubber's long decomposition time (Jevtić, Zakić and Savić, 2012).

Batayneh, Marie and Asi, (2007) found recycling materials is a great way to dispose of waste and create a better environment. Examples of these materials include rubber, glass, metal, plastic, and demolished concrete. The term “use of this type of environmental waste” has appeared in construction as one of the proposed solutions to get rid of its negative impact by converting damaged tires into rubber crumbs using manual methods or automatic machines. They are used in creating retaining earth walls and improving soil properties in asphalt mixtures. Asphalt, as a material added to concrete or as a substitute for fine aggregate and coarse aggregate in different proportion

Research suggests adding rubber powder to cement concrete to replace waste-damaged tires. This method improves properties like flexibility, density, insulation, and crack resistance. However, it decreases compressive strength, leading to less use of this type of concrete.

This chapter covered the benefits of rubberized concrete, based on a large body of research on rubberized concrete construction and an analysis of experimental studies pertaining to thresholds in reinforced concrete. In addition to the NSM strengthening system with carbon fiber reinforced polymer bars employed in this study, it is also composed of regular and rubber concrete.

2.2 Rubberized concrete

Rubber concrete, sometimes referred to as rubber concrete, is a mixture made from tire rubber granules that are used to partially replace natural aggregate (sand and gravel) both by volume and weight. Replacement ratios are usually in proportions ranging from 1.5% to 25% by weight and from 5% to 50% by volume (Tehrani and Miller, 2018).

Recently, a number of researchers have conducted experiments to find the best way to use recycled rubber in concrete technology. The primary goal of the study was to find the optimal way to use recycled rubber and reduce rubber waste

This chapter will review research on the use of tire rubber residues in concrete.

2.2.1 Rubbers as coarse aggregates

Khorami, Ganjian and Vafaii,(2007) examine the effects of hardened concrete were by replacing coarse particles with used rubber chips at weight replacement ratios of 0, 5, 7, and 9%. The findings revealed that compressive

strength was 10% lower with a 5% rubber substitute. The decrease in compressive strength reached 19% and 30%, respectively, as the percentage of rubber replacement rose to 7% and 9%. Replacing shredded rubber reduces the tensile strength of concrete. The most significant reason for this is the lack of cohesion and bonding between the rubber and the concrete matrix. When 5-10% of the coarse aggregate is replaced with shredded rubber, the tensile strength decreases by approximately 2-12%. The flexural strength of rubberized concrete decreases by approximately 30-60% when 5-10% of the coarse aggregate is replaced with shredded rubber. The modulus of elasticity decreases when 5-10% of the coarse aggregate is replaced with shredded rubber, resulting in a strength reduction of 17-25%.

Olubunmi, Olamoju and Taiye, (2023) studied the effect of partially replacing coarse aggregate in paving blocks with plastic waste using a mixing ratio of 1:2:4 l. Coarse aggregate was replaced with sizes of 0%, 5%, 10%, and 15%. After mixing and blending, 54 cubes were generated and cured for 7, 14, and 28 days. Slump, compressive strength, and water absorption tests were performed. The results showed that 10% of coarse aggregate should be replaced with plastic waste to reduce water absorption.

2.2.2 Rubbers as fine aggregates

Antil, (2014) studied the effects of using crumb rubber with different volumetric ratios ranging from 0% to 20% as sand replacement. He observed that concrete toughness increased at a higher proportion of crumb rubber replacement. While the workability of the concrete improved by 1.08 % as a result of replacing 10% of the mixture of sand with rubber. The findings also showed that the replacement of 20% of the mixture sand by rubber, caused a

reduction of the compression, tensile, and flexural resistance by 43%, 35%, and 37 %, respectively.

Su, (2022) analyzed the cube compressive strength of concrete containing recycled aggregate as part of coarse aggregates and rubber particles as part of fine aggregate, simultaneously. The effect of content of both aggregates on concrete compressive strength was studied. 25 sets of samples were made with a constant water/cement ratio of 0.39. Cube compressive strength of different samples at the age of 28 days was obtained in accordance with the relevant standards. The influence of the replacement ratio of recycled aggregate and rubber on strength was investigated based on the analyses of testing data and microstructure inspections, respectively. Results indicate that both recycled aggregate and rubber particles weaken the compressive strength of concrete, while rubber particles play a more important role.

Soren *et al.*, (2023) studied the effect of adding rubber crumb on different properties of concrete. Rubber crumb is used as a substitute for raw materials in the concrete mixture. Rubber crumb is prepared from waste tires. The raw materials are replaced by rubber crumbs at 0%, 30%, 40%, 60%, and 100%. Rubber concrete is tested in terms of flexural and compressive strength. The researchers found that the failure of rubber concrete increases first, but with the increase in the amount of rubber, the flexural strength decreases. It was observed that the compressive strength of rubber concrete decreased significantly. Rubber crumb (<5 mm) ground from used tires was introduced to replace fine natural raw materials in concrete and effectively solve the consumption challenge. The researchers found that the performance of concrete with rubber crumbs as fine raw materials is improved, providing evidence for the design and application of Crumbled Rubber Concrete (CRC)

materials. Crumbled rubber has a low specific gravity, hydrophobicity, and air entrainment compared to natural soft aggregates, which greatly reduces the workability of fresh CRC and shows poor bonding performance with the cementitious matrix.

2.2.3 The stress-strain relationship for rubberized concrete

Rubberized concrete's mechanical characteristics and stress-strain curve alter when rubber particles replace mineral aggregate. Nevertheless, rubberized concrete cannot be used with the current constitutive stress-strain models for normal concrete (Abbara *et al.*, 2022). Plastic energy refers to the energy absorbed by rubber until the rubberized concrete sample experiences its first crack. This characteristic enhances the ductility of rubberized concrete, allowing it to absorb more energy and exhibit greater resistance after cracking. Increasing the rubber replacement ratio further boosts these properties. As a result, rubberized concrete is suitable for applications such as jersey barriers and foundation pads in railroad stations, where improved blast or impact resistance and vibration damping are essential. (Batayneh, Marie and Asi, 2008) studied the stress-strain behaviors of specimens with up to 40% rubber (replacement by volume) exhibited a similar trend to the control specimen, with a smaller peak. The specimens behave like brittle materials, with elastic energy as the total energy generated upon fracture. However, specimens with 60% and 80% rubber exhibit nonlinear behavior, yielding after reaching peak stress. This behavior is similar to tough materials, which generate most of their energy as plastic energy upon fracture. Concrete with a higher percentage of crumb rubber has higher toughness, as the generated energy is mainly plastic, as shown in Figure 2-1.

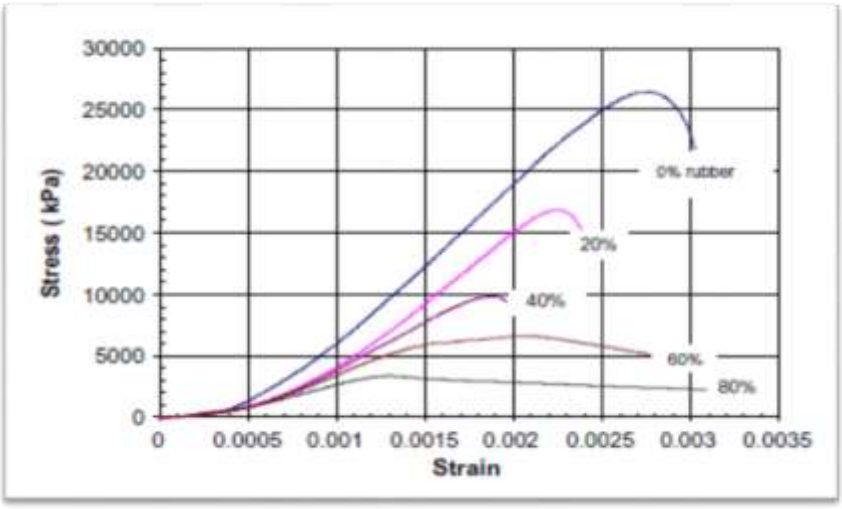

Figure 2-1: Stress-strain curves at different volumetric rubber replacement ratios range from (0%-80%) (Batayneh, Marie, and Asi, 2008).

(Strukar *et al.*, 2018) studied uniaxial compression tests on concrete with volumetric rubber replacement by 10%, 20%, 30%, and 40% of the total; it was possible to study and evaluate the effect of rubber content on its mechanical behavior. The entire stress-strain curve was investigated, including compressive strength, elastic modulus, strains at large stress levels, and failure modes. The experimental results (Figure 2-2)indicated that increasing the rubber content linearly reduces the compressive strength and elastic modulus but increases the ductility. By comparing the experimental stress-strain curves with those drawn using available constitutive stress-strain models, it was concluded that they are insufficient for rubberized concrete with high rubber content. Based on the identified deviations, an improvement of the existing model was proposed, which provides better agreement with the experimental curves. The obtained research results enabled important insights into the relationships between rubber content and stress-strain curve variations required when using nonlinear material properties.

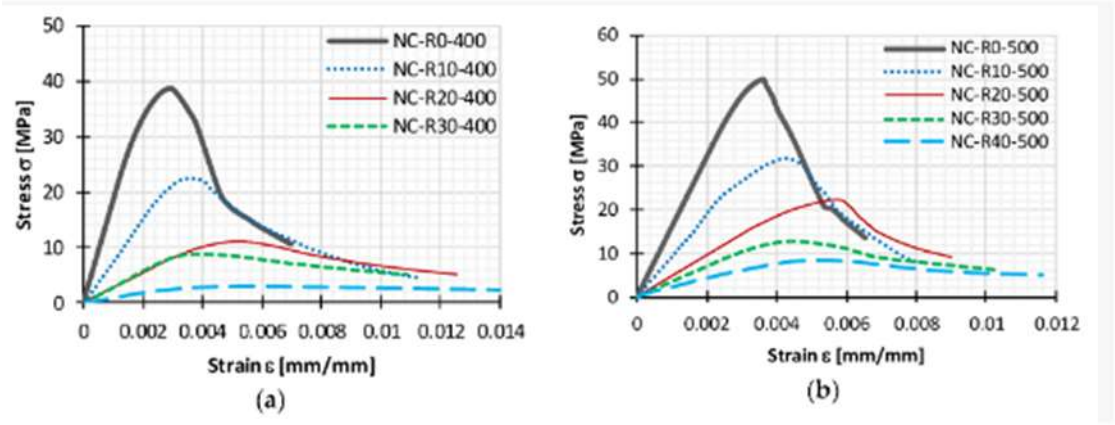

Figure 2-2: Compressive stress-strain curves for reference normal concrete (NC) and rubberized concrete (RC) with 10%, 20%, 30%, and 40% crumb rubber from (a) Series I and (b) Series II (Strukar *et al.*, 2018)

2.3 Structural behavior of Rubberized concrete beams.

Al-azzawi, Shakir, and Saad (2018) investigated the addition of waste rubber from scrap tires as fibers to a concrete mixture containing 0.5% superplasticizer. They studied the workability of concrete mixtures, the mechanical properties of concrete, and the flexural behavior of concrete beams. Rubber fibers with 2-4 mm diameters were added at 0.5% and 1% by weight of cement. The results showed that adding rubber fibers to natural aggregate concrete improved its ductility, compressive strength, and tensile strength compared with normal concrete. It was found that the behavior of the tested beams was significantly affected by the amount of rubber fibers. The maximum load increased by 21%, and the cracking load increased by 60% if the fiber content was increased from 0% to 0.5%. For rubber concrete, the maximum load increased by 4%, and the cracking load decreased by 7% with the increase in fiber content from 0.5 to 1.0%.

Eisa, Elshazli and Nawar, (2020) studied the effect of crumb rubber and steel fiber mixture on the behavior of reinforced concrete beams under static loads. The crumb rubber, with a size ranging from 2 mm to 3 mm, was

produced from used tires. It was then incorporated into normal concrete (PC) and steel fiber concrete (SFC) mixes by partial replacement of fine aggregates at different weight ratios (5%, 10%, 15%, and 20%). The volume fraction of steel fiber was kept constant at 1%. An extensive experimental program was conducted on 130 specimens in two phases. The first phase included compressive testing, splitting tensile testing, and flexural testing to investigate the mechanical properties of the designed concrete mixtures. The second phase was carried out to investigate the static behavior of reinforced concrete beams, using the designed concrete mixtures, under four-point flexural testing. The test results showed that the use of crumb rubber as a partial replacement for fine aggregate at 5% and 10% showed acceptable performance for reinforced concrete beams, and the use of steel fibres with rubber concrete at a rubber content of more than 10% improved the performance and durability of these mixtures.

AL-Hajjar and AL-Khafaji, 2024 Conducted a recent experimental study on the structural performance of rubberized concrete beams under impact loads, focusing on their mid-span displacement and maximum impact load. An automated drop weight testing machine was used to perform impact tests, and two main variables were examined: the volumetric replacement ratio of rubber (0%, 15%, 25%, and 35%) and the falling height of the impacting mass (1.5 m, 2.0 m, and 2.4 m). The results showed that increasing the rubber content in the concrete reduced the maximum impact strength. For example, at a falling height of 2.4 m, the impact strength decreased by 2.93%, 13.16%, and 17.53% for rubber contents of 15%, 25%, and 35%, respectively, compared to conventional concrete without rubber. In terms of mid-span displacement, the beams containing 15% and 25% rubber showed decreases of 8.44% and 6.26%, respectively, at a drop height of 2.4 m. However, at the

same height, the beam containing 35% rubber showed a 17.26% increase in displacement compared to the control beam. These results indicate that while rubberized concrete can effectively mitigate impact forces, a higher rubber content may negatively affect the deformation properties under impact load.

2.4 Behavior of reinforced concrete beams under repeated load

Certain constructions are repeatedly subjected to loads that change in direction and amplitude. The members may fail from fatigue at a stress lower than the material's yield point if the ensuing stresses are high enough and occur frequently.

Khalaf and Al-Ahmed, (2021) investigated the behavior of the presence of big gaps in continuous deep beams made of reinforced concrete by applying repeated loads. The repeated loading ranged from 30% to 70% of the final load applied to the beam under static load.

Zhu *et al.*,(2022b) examined under four-point cyclic loading (Figure 2-3) high-strength concrete beams reinforced with steel fibers and BFRP bars. manufactured and tested five concrete beams measuring 150 x 300 x 2100 mm. One conventional steel-reinforced concrete beam and four BFRP-reinforced concrete beams with varying reinforcement ratios (ρs)—0.56%, 0.77%, 1.15%, and 1.65%—were tested. Cracking, failure mechanisms, residual deformation, load deflection, and stiffness deterioration were examined. An increase in ρs lead to increase the flexural carrying capacity of beams while limiting fracture widths, deflections, and residual deformation. Compared to the first displacement cycle, the bearing capacity decreased by 10% in the third cycle. Before failing, stiffness quickly deteriorated. Relative stiffnesses of greater ρs beams are higher. Five loading and unloading cycles

were used to apply incremental loads incrementally up to 75% of the control specimen's ultimate load level before gradually releasing the load to zero.

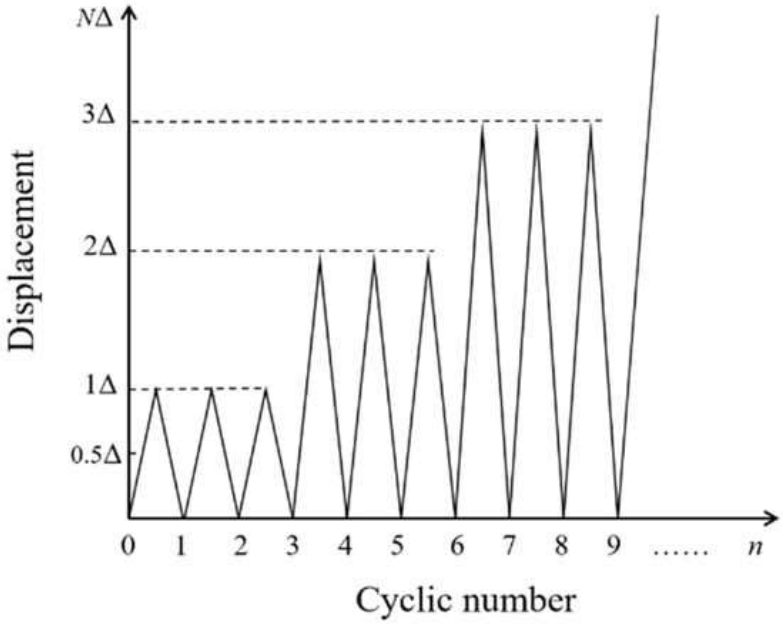

Figure 2-3: Scheme of loading (Zhu *et al.*, 2022b).

Hussein, Al-Abbas and Al-Khafaji, 2024 investigated the behavior of composite notched beams under repeated loading conditions, by combining experimental tests and numerical simulations. The researchers focused on evaluating the structural response to variations in opening shapes (circular, square, and hexagonal) and shear connector spacing (150 mm and 300 mm) using finite element analysis in Abaqus. Six models were developed to evaluate the effect of these parameters while maintaining consistent structural properties. The results showed that the numerical model provided reliable predictions of maximum load, deflection, and slip values, with an average difference of 9.41% for maximum load and 11.99% for maximum deflection compared to the experimental results. However, the slip predictions showed a greater discrepancy, with an average difference of 21.39%. The results highlight the potential of numerical modeling for the design of composite

beams under repeated loading, while emphasizing the need for rigorous validation and further research in diverse loading conditions and material properties.

Al-khafaji, Muhammed and Jadooe, (2024) studied the loading range for the 30 cycles in the current investigation was set between 25% and 75% of the maximum load obtained from the monotonic loading test (Pu). Three steps of the repeated loading procedure were performed, with 10 loading and unloading cycles in each stage. The first stage loads were 25% of Pu, the second stage loads were 50% of Pu, and the third stage loads were 75% of Pu. The specimen was loaded to failure after completing three stages of repeated loading test comprising loading and unloading cycles as shown in Figure 2-4 .

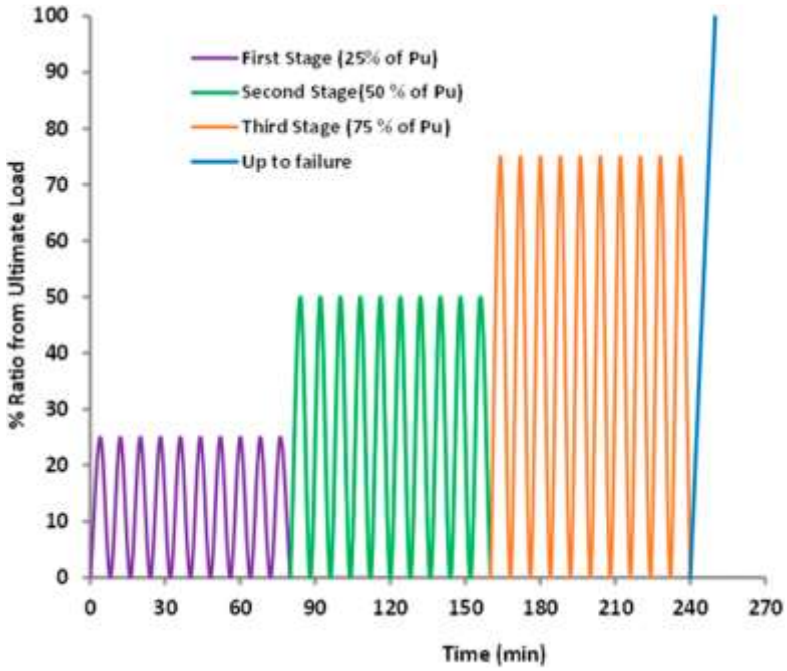

Figure 2-4: Protocol of repeated load (Al-khafaji, Muhammed and Jadooe, 2024).

2.5 Experiments on the strengthed by NSM-CFRP bar

Sharaky *et al.*,(2014) investigated how reinforced RC beams with NSM FRP bars behaved. Four point bending tests were conducted on eight

beams. The impacts of bar size, quantity of NSM bars, epoxy characteristics, and material type were investigated. The tested beams could only be cut difficultly up to the faces of the supporting columns, thus they were strengthened with a limited bond length to mimic as much as possible work-place conditions. Analysis was done on the tested beams' load capacity, deflection, mode of failure, FRP strain, concrete strain, free end slip, and transverse strain in both epoxy and concrete. When stronger and control beams were compared, the yielding loads of the strengthened beams increased by 155.8% and 129.8%, respectively. The ultimate loads increased by 166.3% and 159.4% for beams strengthened with carbon fiber reinforced polymer (CFRP) and glass fiber reinforced polymer (GFRP), respectively. Compared to the similar beams reinforced using GFRP bars, the CFRP-stiffeninged beams exhibited greater stiffness. The load capacity of the reinforced beams was not significantly affected by the size, number, or characteristics of the epoxy; instead, failures were primarily caused by the separation of the concrete cover or by defects in the epoxy.

(Al-Abbas *et al.*, 2016) conducted an experimental work to investigate the first cracking load, failure load, maximum deflection and failure modes of five full-size specimens of reinforced concrete T-beams. The control beam, B0, was the initial beam specimen without reinforcement. (CFRP) bars from (NSM) were used to reinforce the other beam specimens, B1, B2, B3 and B4. The beams had a total length of 3200 mm and an effective span of 3000 mm. The beams reinforced with varying numbers of 6 mm diameter CFRP bars were subjected to a four-point bending load. The bottom surface of the concrete beams was drilled with grooves with a cross-section of 12 mm and a depth of 14 mm. According to the data, the maximum load and stiffness of the reinforced beams were significantly increased, reaching twice that of the

control beam. The measured crack widths in the strengthened beams were approximately the same as those observed in the original control beam. However, the ultimate load capacity of the strengthened beams was up to twice that of the control beam with corroded steel reinforcement. This demonstrates the effectiveness of the Near-Surface Mounted (NSM) technique in reducing crack widths and, consequently, minimizing the risk of failure. These findings confirm the efficiency of the NSM method in enhancing the structural performance of reinforced concrete beams. Furthermore, the NSM approach was found to effectively reduce the fracture width while minimizing the possibility of corrosion of the reinforcing steel.

Al-Obaidi, Saeed and Rad, (2020) studied the use of near-surface-mounted (NSM) technique for flexural strengthening of reinforced concrete beams using fiber reinforced polymer (FRP) materials. It found that mechanical interlocking grooves can enhance bonding capacity and prevent premature bonding failure. The technique was applied to nine RC beams, with results showing more effectiveness for specimens with lower steel reinforcement ratios.

2.6 Experiments on the strengthed by NSM-CFRP strip

Pomeroy, (1993) studied used (CFRP) strips in concrete cracks, which is a new technology for adding reinforcement to concrete structures in need of renovation. The concrete structure has cracks carved into it that extend deep into the concrete cover. These cracks are filled with (CFRP) strips. Tests of links and packages Experiments were conducted to characterize the mechanical behavior. The ability to install "CFRP in concrete cracks" is higher than that of CFRP strips glued to the surface of a concrete structure.

The mechanical behavior is softer but stiffer under service loads at the limit state. In order to maximize the utilization of (CFRP) content.

Jadooe, Al-Mahaidi, and Abdouka (2017) reached reports on an experimental and numerical investigation of eight reinforced concrete beams. Six of the experiment's beams were heated using the ISO-834 standard fire curve, while the other two beams were kept at room temperature. The geometrical dimensions, reinforcement, loading, and support configurations were all the same for every beam. Following two hours of exposure to 600 and 700 °C, the flexural behavior was examined. Four beams were strengthened using carbon fiber-reinforced polymer (CFRP) strips after being heated, while the other two beams were un-strengthened control beams that had been destroyed by fire. The findings demonstrated a decrease in the heat-damaged beams' mid-span ultimate load, stiffness, and ductility when compared to the control beam at room temperature. While ultimate load and stiffness declined, near-surface mounted (NSM) repair

(Barris *et al.*, 2020) stuedied the flexural behavior of glass fiber reinforced polymer (GFRP) reinforced concrete beams reinforced with FRP carbon strips utilizing the near surface mounting (NSM) technique is examined in this paper through the results of an experimental program. By analyzing the crack section, its theoretical load-carrying capacity is determined. Despite the high degrees of distortion of GFRP RC, NSM CFRP has been demonstrated to offer an effective solution for increasing the flexural capacity of RC beams internally reinforced with GFRP bars. Furthermore, an analytical investigation was carried out to assess the impact of different variables on the flexural strength of concrete beams internally reinforced with either (GFRP) or steel bars and reinforced with (CFRP NSM).

Al-zu'bi, Abdel-Jaber and Katkhuda, (2022) studied the near-surface mounted carbon-fiber-reinforced polymers (NSM-CFRPs) approach was used to strengthen the flexure of reinforced concrete (RC) beams in an experimental and analytical study. Eleven full-scale RC rectangular beams were tested up to failure using a monotonic three-point bending test. The primary test factors used in this investigation were the number of (CFRP) strips, the length of the strips, and the concrete's compressive strength (high, medium, and low). The findings showed that the load-carrying capacity of the strengthened RC beams was effectively boosted by applying NSM-CFRPs strips in various configurations. These beams also showed a higher moment resistance than the comparable un-strengthened beam. The flexural capacity of the examined specimens was successfully increased by all strengthening methods.

2.7 Summery of literature review

Previous studies have extensively investigated the use of rubber in concrete mixtures as a partial replacement for both coarse and fine aggregates. Additionally, several studies have focused on the Near-Surface Mounted (NSM) strengthening technique, with some examining the use of bars and others utilizing strips for strengthening beams. Moreover, a number of investigations have explored different variables under specific repeated loading protocols. However, the research gap lies in the integration of these three main aspects: the use of reinforced rubberized concrete, the application of the NSM strengthening technique, and the evaluation under repeated loading following a defined protocol. This study aims to address this gap by combining these elements into a comprehensive experimental investigation.

Chapter Three: Experimental work

3.1 Introduction :

This chapter outlines the laboratory investigation on rubberized reinforced concrete strengthened with NSM-CFRP bars under repeated loading conditions. An experimental program was designed to examine the performance of rubberized concrete strengthened with CFRP bars and to assess how varying the proportion and amount of rubber replacing natural aggregates affects the structural behavior of the concrete. Additionally, the chapter details the properties of the materials used in the study, the characteristics of the cast samples, the testing methods, and the required tools for the experiments.

The effect of a number of variables was taken into account, such as: replacement ratios for coarse and fine aggregate, and NSM-CFRP.

The laboratory work program includes experimenting with six types of structural concrete mixtures. To understand the hardening properties, tests were studied (compressive strength test, splitting tensile strength test, modulus of rupture) and to understand the fresh properties, tests were studied (slump test).

3.2 Mix description

Seven design mixes were examined, as shown in Table 3.1 and Figure 3-1. One of the main objectives of this research is to study the effect of the size and quantity of rubber used to replace it with natural aggregate on the behavior of the concrete mixture to produce rubber structural concrete. The first mixture includes normal concrete. The second and third mixtures (F10,

F20) include normal concrete with 10% and 20% of the total volume of fine aggregate replaced with fine rubber, respectively.

The fourth and fifth mixtures (C10, C20) include normal concrete, replacing 10% and 20% of the total volume of coarse aggregate with chip rubber, respectively.

The sixth and seventh mixtures (C5F5, C10F10) include normal concrete, replacing 5% and 10% of the total volume of coarse aggregate with chip rubber and 5% and 10% of the total volume of fine aggregate with fine rubber, respectively.

Table 3-1 : Designation and description of the mixes

NO	Mixture symbols	Chip rubber content as a volumetric replacement with coarse aggregate (%)	Crumb rubber content as a volumetric replacement with fine aggregate (%)
1	N	0	0
2	F10	0	10
3	F20	0	20
4	C10	10	0
5	C20	20	0
6	F5C5	5	5
7	F10C10	10	10

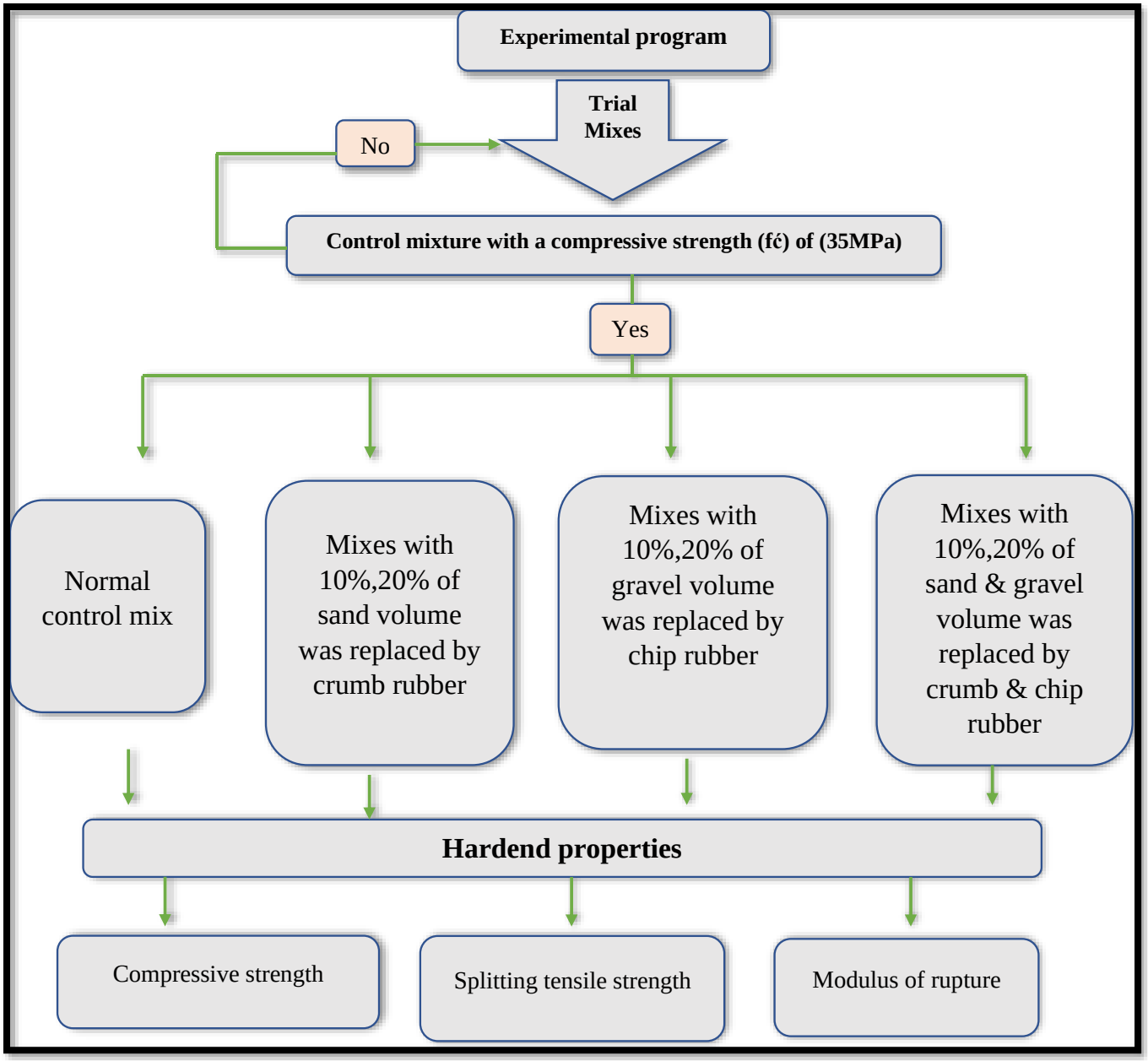

Figure 3-1: Flowchart for the specified mix design in the laboratory

3.3 Description of test RC beam specimens

To ascertain whether the built repeated testing machine was suitable, one reference beam was examined before initiating the first experimental activity. In the test program, fourteen simply supported reinforced concrete beams were used; 12 of them were constructed using rubberized reinforced concrete and the other two used ordinary reinforced concrete as a reference.

The geometric measurements of all beam test specimens are the same: the depth (h) and width (b) are 250 mm and 150 mm, respectively, and the overall length (L) is 1600 mm with a clear span of 1500 mm.

All of the beams were reinforced with two longitudinal 12 mm diameter reinforcement steel bottom bars and two 8 mm diameter top bars; shear reinforcement was provided by an 8 mm diameter bar spaced 100 mm apart on the side and bottom of the beams. The clear cover is 25 mm from the stirrup face to the concrete face. Figure 3-2 displays the beam's cross-section as well as specifics about the reinforcement.

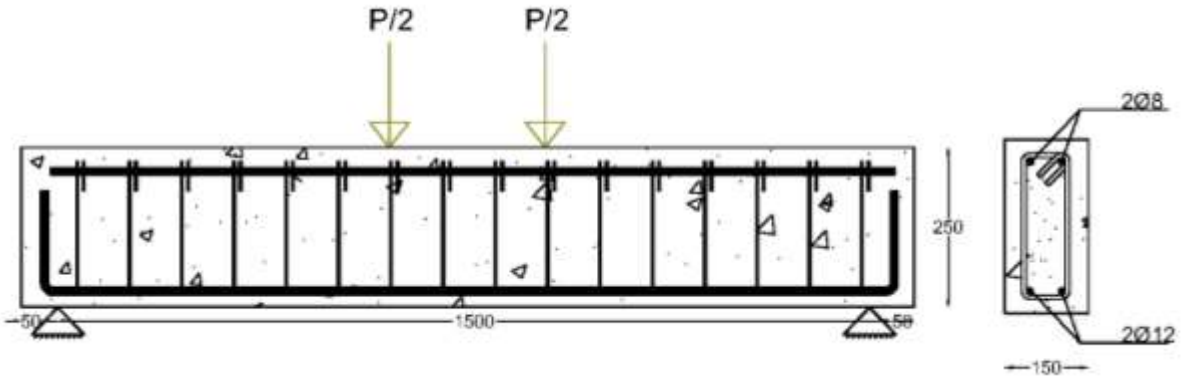

Figure 3-2: Product details for the test: Dimensions and reinforcing details (all dimensions in mm) .

3.1 Description of strengthening

The strengthening of rubberized concrete beams using CFRP bars and CFRP strip is another key aspect of the study (see Table 3-2 and Figure 3-3). A total of twelve reinforced concrete beams made from rubberized concrete were strengthened and tested. These beams are categorized into two groups based on coarse and fine rubber content.

The first group was strengthened with CFRP bars (Figure 3-5) and consisted of six beams with a coarse rubber content of 10% and 20%, fine rubber content of 10% and 20%, and coarse and fine rubber content in the

same mixture of 10% and 20%. The second group was strengthened with CFRP strip (Figure 3-6) and consisted of six beams with a rubber content. Coarse 10% and 20%, fine rubber content 10% and 20%, and coarse and fine rubber content in the same mixture 10% and 20%.

Table 3-2: Description of test specimens.

Symbols	Type of loading	Percentage of replacement		Type of strengthening	
		Coarse agg.	Fine agg.	CFRP bar	CFRP strip
B1	monotonic load	0	0	0	0
B2	repeated load	0	0	0	0
B3-F10-b		0	10%	2bar	0
B4-F20-b		0	20%	2bar	0
B5-C10-b		10%	0	2bar	0
B6-C20-b		20%	0	2bar	0
B7-C5F5-b		5%	5%	2bar	0
B8-C10F10-b		10%	10%	2bar	0
B9-F10-S		0	10%	0	2 strips
B10-F20-S		0	20%	0	2 strips
B11-C10-S		10%	0	0	2 strips
B12-C20-S		20%	0	0	2 strips
B13-F5C5-S		5%	5%	0	2 strips
B14-F10C10-S		10%	10%	0	2 strips

*

B :- Beam /Number:- number of beam b:- bar NSM-CFRP

F:- Fine aggregate , S:- Strip NSM-CFRP

C:- Corse aggregate , 10:- replace 10% , 20:- replace 20%

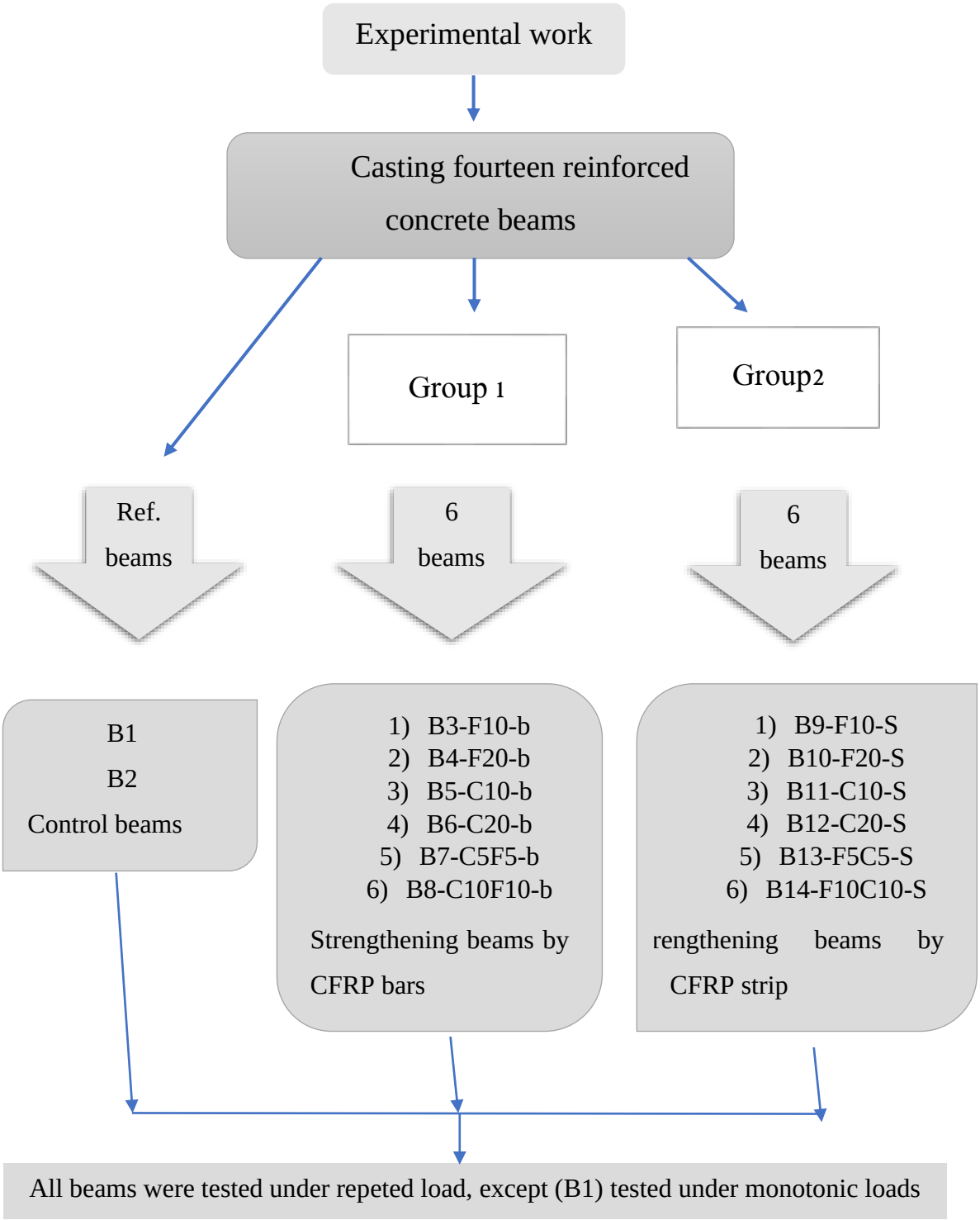

Figure 3-3: Flowchart for the test specimens.

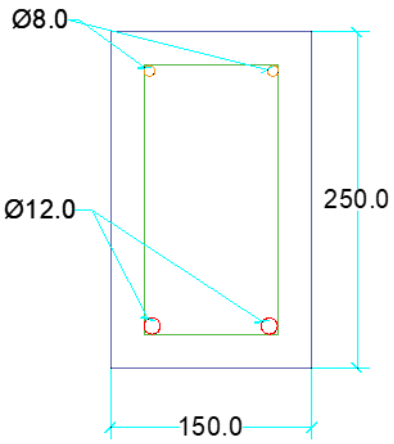

Figure 3-4: Detail of cross-section on normal beam (all dimensions in mm).

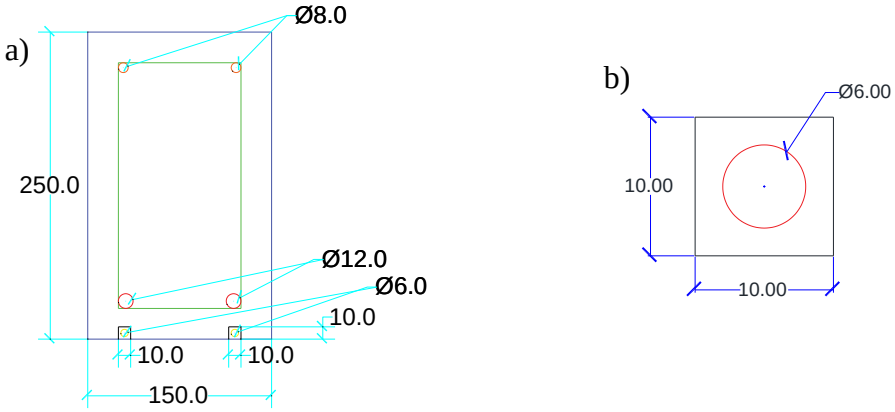

Figure 3-5: Detail of cross-section and groove for a beam with NSM-CFRP bar (all dimensions in mm).

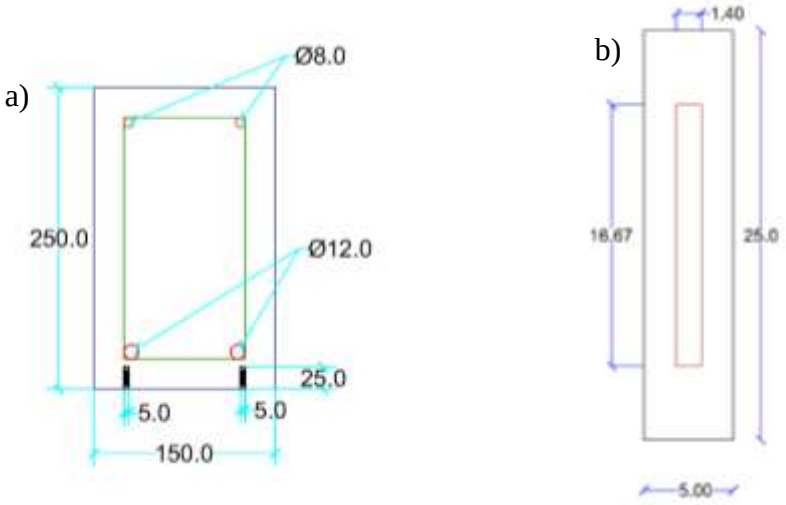

Figure 3-6: Detail of cross-section and groove for a beam with NSM-CFRP strip (all dimensions in mm).

3.2 Properties of the used material

3.2.1 Cement

In all experimental mixtures, Iraqi sulfate-resistant Portland cement produced by the "Lafarge Al-Jisr" company was used, and this type of cement conforms to Iraqi specifications (IQS No. 5/2019). This cement type's chemical makeup and physical characteristics are shown in Table 3-3and Table 3-4, respectively.

Table 3-3: The chemical make-up and main ingredients of the cement.

Composition of oxides	Abbreviation	% by weight	Limit of (IQS. No. 5/2019)
Lime	CaO	60.09	-
Silica	SiO2	17.61	-
Alumina	Al2O3	3.29	-
Iron oxide	Fe2O3	4.31	-
Sulfate	SO3	2.02	≤ 2.5%
Magnesia	MgO	1.75	≤ 5%
Loss on Ignition	L.O.I	3.97	≤ 4%
Lime saturation factor	L.S.F	0.87	0.66-1.02
Insoluble residue	I.R	0.56	≤ 1.5
Main compounds (Bouge's eq.)		% by weight of cement	
Tricalcium silicate (C3S)			-
Diacalcium siliccat (C2S)			-
Tricalcium aluminate (C3A)		1.48	≤ 3.5%

Table 3-4: The physical properties of the cement utilized.

Physical properties	Test result	Limit of (IQS. No. 5/2019)
Specific surface area method (Blaine method) (m^2/kg)	386	≥ 280
Setting time (vicats method) Initial setting (min) Final setting (hr)	 120 4:00	 ≥ 45 ≤ 10
Compressive strength (MPa) 2 days 28 days	 22.1 46.3	 ≥ 10 ≥32.5

3.2.2 Fine aggregate

A maximum particle size of 4.75 mm was employed in this investigation for the natural sand that was obtained from the Maqale Karbala factory. Both the Table 3-5, Table 3-6 and the Figure 3-7show the results of the sieve analysis and the grading curve of fine aggregate (sand) as per the Iraqi Standards (IQS. No. 45/1984). All three tables show chemical and physical characteristics that meet the same standard.

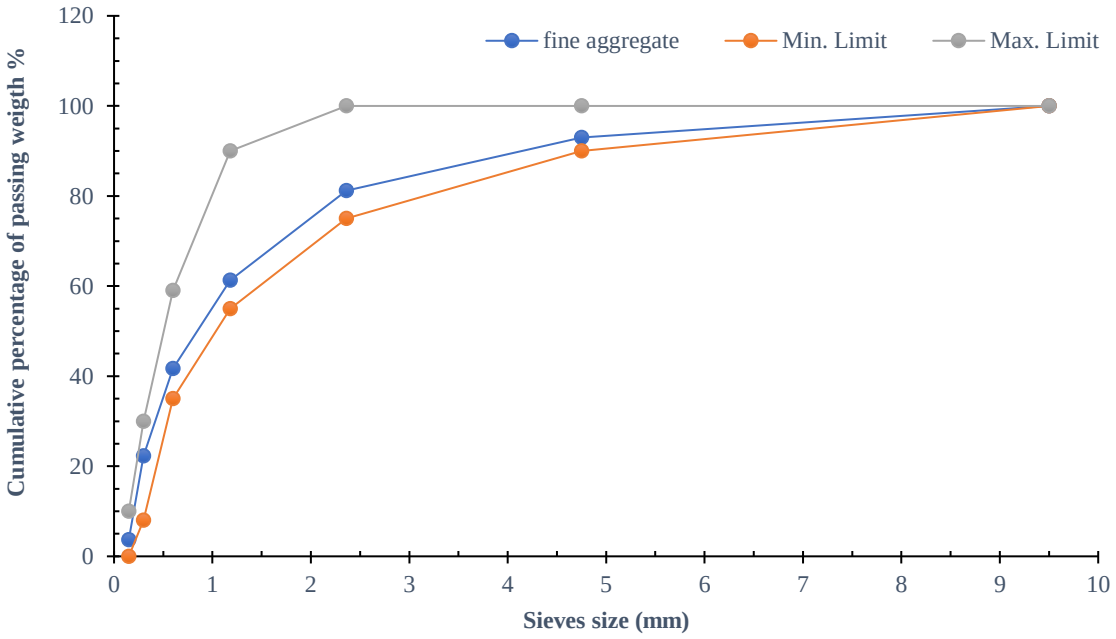

Figure 3-7: Grading curve for fine aggregate in accordance with Iraqi Specification (IQS No. 45/1984).

Table 3-5: The physical and chemical of the fine aggregate utilized.

Characteristics	Test results	Limits of (IQS. No. 45/1984
Sulfate content (SO3) %	0.322	0.5% (max.)
Material finer than 75 µm	1.8	5% (max.)
Specific gravity	2.68	-
Absorption %	0.8	-
Fineness modulus	1.99	-

Table 3-6: Grading of the of fine aggregate used .

Sieves size (mm)	The passing Percentage of fine aggregate	Limits of (IQS. No.45/1984) (Zone 2)	
		Min. Limit	Max. Limit
10	100	100	100
4.75	96	90	100
2.36	90	85	100
1.18	84	75	90
0.6	73	60	79
0.3	40	40	12
0.15	1.4	0	10

3.2.3 Coarse aggregate

For the experiments, we used 20 mm-sized pre-graded gravel from the Al-Niba'ai area. Following a thorough washing to eliminate any dust, the gravel was allowed to air-dry until it reached the desired saturated surface state. The gravel's grading curve and sieve analysis are displayed in Figure 3-8 in compliance with the Iraqi standard (IQS No. 45/1984) . The chemical and physical characteristics are listed in Table 3-7 , Table 3-8 respectively , which conform to the Iraqi standard (IQS No. 45/1984).

Table 3-7: Grading of the coarse aggregate used

Sieve size (mm)	Percentage passing of coarse aggregate (C.A)	Limits(IQS No. 45/1984)	
		Min. Limit	Max. Limit
37.5	100	100	100
20	97	95	100
9.5	36	30	60
5	2	0	10

Table 3-8: The physical and chemical of the coarse aggregate used .

Characteristics	Test results	Limits of (IQS. No. 45/1984
Sulfate content (SO3) %	0.043	0.1% (max.)
Material finer than 75 µm	0.06	3% (max.)
Specific gravity	2.65	-
Absorption %	0.8	-

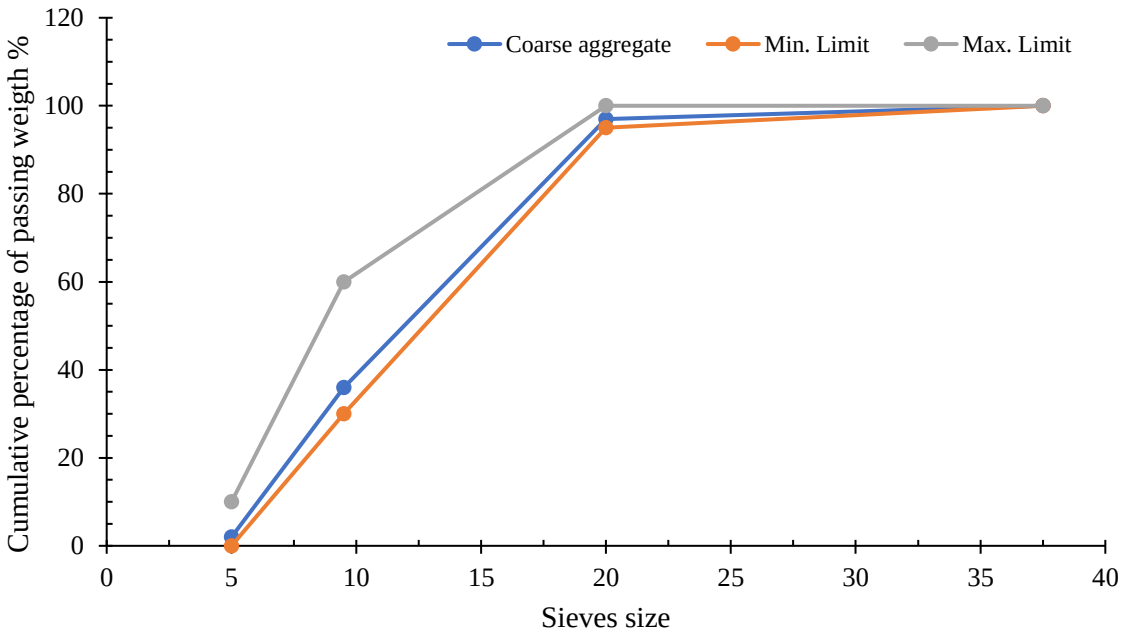

Figure 3-8: Grading curves for coarse aggregate in (IQS No. 45/1984)

3.2.4 Waste tires rubber

The General Company for Rubber Industries and Tires in Al-Najaf provided the waste tire rubber (Plate 3-1) that was devoid of steel wires and rubber fibers for this study. The rubber was used in different sizes, specifically (0.15-1.18), (1.18-2.36), (2.36-4.75), and (4.75-10). Volumetric proportions (10% and 20%) of the crumb rubber graded from 0.15mm to 4.75 mm was used instead of fine aggregate(Figure 3-9 and Table 3-10), while chip rubber graded from 4.75mm to 10mm were used instead of coarse aggregate(Figure 3-10 and Table 3-11) . The chemical composition and physical characteristics are illustrated in Table 3-9.

Plate 3-1: Iraq's waste tire rubber crose and fine production

Table 3-9: The physical and chemical characteristics of used tire rubber

Chemical composition		Physical characteristics	
Rubber components major	Results%	characteristics	Results
Extract of acetone	10	Finesse modulus	3.14
Rubber hydrocarbon	25	Specific gravity	1.78
Content of carbon black	30	Water absorption	2%
Content of natural rubber	31		
Content of ash	4		
The physical and chemical testing was carried out by the General Company for Rubber Industries and Tires/Al-Najaf.			

Table 3-10: Grading of the crumb rubber.

Sieves size (mm)	The passing Percentage of crumb rubber	Limits of (IQS. No. 45/1984) (Zone 1)	
		Min. Limit	Max. Limit
10	100	100	100
4.75	100	90	100
2.36	88	60	95
1.18	49	30	70
0.6	27	15	34
0.3	10	5	20
0.15	2	0	10

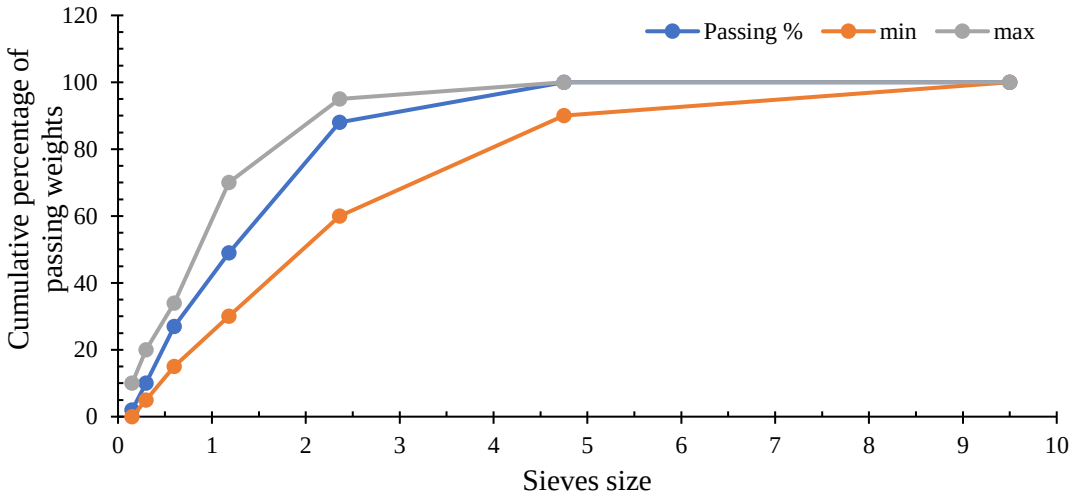

Figure 3-9: Crumb rubber grading curves according to (IQS.No.45/1984).

Table 3-11: Grading of the chip rubber.

Sieve size (mm)	Chip rubber Percentage passing	Limits(IQS No. 45/1984)	
		Min. Limit	Max. Limit
37.5	100	100	100
20	97	95	100
9.5	30	30	60
5	10	0	10

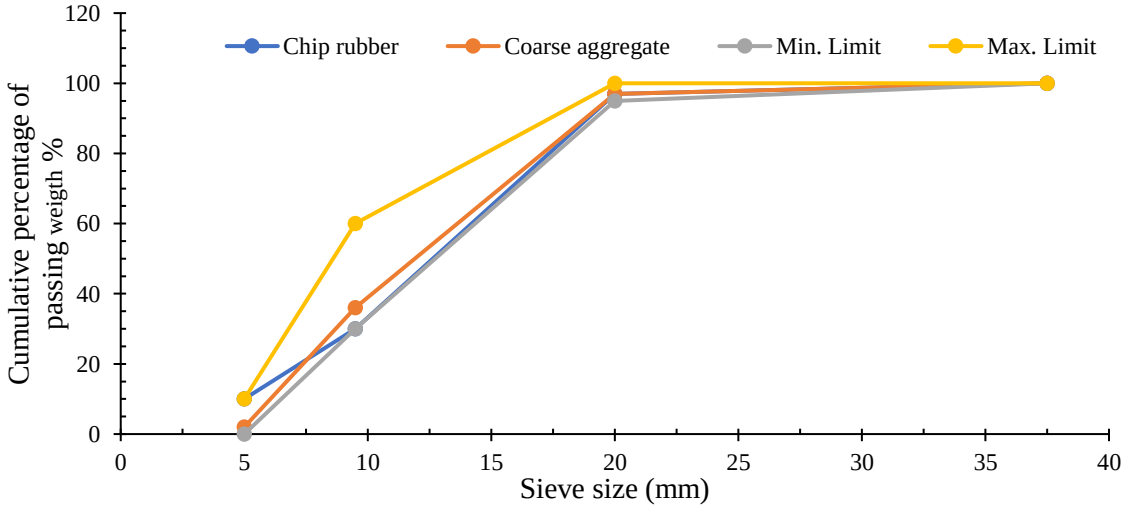

Figure 3-10: Coarse aggregates and chip rubber grading curves according to (IQS No. 45/1984)

3.2.5 Water

Ordinary clean tap water was used for handling rubber and coarse aggregate samples and for casting and processing concrete samples.

3.2.6 Steel reinforcement properties

Two diameters of deformed rebar, Ø12 mm and Ø8 mm, were used to reinforce the beams, as illustrated in Plate 3-2. The primary longitudinal reinforcement at the base had a diameter of 12 mm, while the steel reinforcement at the top had a diameter of 8 mm. Shear reinforcement tests on the steel bars were conducted in the laboratory of the Mechanical Engineering at the University of Karbala using a computerized testing machine, as shown in Plate 3-3. The samples were tested following ASTM A615M-05a. The 12 mm and 8 mm diameter rebar met the technical requirements for steel grades 60 and 40, respectively. The results of the steel reinforcement tests are summarized in Table 3-12.

Table 3-12: Steel reinforcement properties.

Properties	Results		Tensile requirement ASTM 615M – 05a (Minimum)	
Nominal diameter (mm)	Ø12	Ø 8	Grade 60	Grade 40
Yield stress, fy (MPa)	479.6	411.8	420	280
Ultimate stress, fu (MPa)	634.6	640.9	620	420
Elongation %	17.6	23.9	7-9	11-12
We conducted all of our experiments at Kerbala University's laboratory.				

Plate 3-2: Steel reinforcement details.

Plate 3-3: Steel reinforcement testing machine.

3.2.7 Super-plasticizer (SP)

Superplasticizer Structuro 502 (Fosroc) is a high-performance concrete hyperplasticiser based on polycarboxylate technology. The normal dosage range is between 0.2 to 3.0 litres/100 kg of cementitious material.

Structure 502 is differentiated from conventional superplasticizers in that it is based on a unique carboxylic ether polymer with long lateral chains. This greatly improves cement dispersion. At the start of the mixing process, an electrostatic dispersion occurs, but the presence of the lateral chains linked to the polymer backbone generates a steric hindrance that stabilizes the

cement particle's capacity to separate and disperse. This mechanism considerably reduces the water demand in flowable concrete.

Structure 502 combines the properties of water reduction and workability retention. It allows the production of high-performance concrete and/or concrete with high workability. Table 3-13 shows the technical characteristics of this superplasticizer.

Table 3-13: Structure 502 (Fosroc) technical data*.

Properties	Value or Description
Appearance	Light brown coloured liquid
PH value	6.5
S.G. @ 20-C	1.06 ± 0.02
Chloride content	Nil
Alkali content	Typically, less then 1.5 gm Na2O equivalent per litre of admixture
*The manufacturer provides this info.	

3.2.8 Strip made of carbon fiber reinforced polymer (CFRP):-

Six rubberized reinforced concrete beams were strengthened with carbon fiber-reinforced polymer strip (Plate 3-4). The carbon fiber reinforced polymer strip was placed on the lower face of the beam with a near-surface mounted (NSM). The carbon fiber reinforced polymer strip's dimensions were 1.4 mm in thickness and 16.67 mm in width. The technical characteristics of the carbon fiber reinforced polymer strip provided by the manufacturer are as shown in the Table 3-14.

Plate 3-4: Sika carbon fiber reinforced polymer (CFRP) strip.

Table 3-14: Properties of sika carbon fiber reinforced polymer (CFRP) strip*.

Thickness	1.4mm
Tensile strength	2400-2800 MPa
Tensile modulus	≥ 200 GPa
Elongation	≥1.6 %
Width	5 cm
Length	50M
* This information comes from the source.	

3.2.9 Bar made of carbon fiber reinforced polymer (CFRP)

Two rubber-reinforced concrete beams were strengthened with carbon fiber-reinforced polymer bars (Plate 3-5). The carbon fiber-reinforced polymer bars were placed on the lower face of the beam with a near-surface mounted (NSM). The diameter of the carbon fiber-reinforced polymer bars used was 6 mm. The technical characteristics of the carbon fiber-reinforced polymer bars provided by the manufacturer are shown in Table 3-15.

Plate 3-5: Sika carbon fiber reinforced polymer (CFRP) bar.

Table 3-15: Properties of sika carbon fiber reinforced polymer (CFRP) bar*.

Diameter	6mm
Tensile strength	1800-2200 MPa
Elastic modulus	140-155 GPa
Elongation	1.3-1.5%
Density	1.3-1.8 g/m3
Cofficint of thermal expanion	(*10-6/C)
*The manufacturer provides this data.	

3.2.10 Epoxy Resin

The type of epoxy (Plate 3-6) used for the strengthening technique is Sikadur®-30 LP, a two-component structural adhesive based on a mixture of epoxy resins. It is specially designed for use at higher temperatures ranging from +25°C to +55°C and is suitable for use in hot and tropical climates.

The technical characteristics of the epoxy are shown in Table 3-16. The grooves were filled with a layer of epoxy mixture, and then the CFRP strip and CFRP bar were inserted into the grooves. The surface was wiped and cleaned. Before being tested, the samples were left to make sure that the carbon fibers (bar and strip) would stick better to the concrete surface.

Plate 3-6: The epoxy Sikadur®-30 LP.

Table 3-16: Properties of Sikadur®-30 LP Epoxy Resin) *.

Color	Component A: white Component B: black Component A + B: light grey
Density	~1.8 kg/l (+23 °C) (components A + B)
Mixing ratio	Component A: Component B = 3:1 (by weight or volume) Only mix complete pre-batched units of Sikadur®-30 LP.
Application temperature	+25 °C min. / +55 °C max.
Tensile strength	~17 N/mm2 at +25 °C ~28 N/mm2 at +55 °C
Modulus of elasticity in compression	~10 000 N/mm2 (+25 °C)
Modulus of elasticity in tension	~10 000 N/mm2 (+25 °C)
Flexural Strength	> 25 N/mm2 at +25 °C ~28 N/mm2 at +55 °C
* This information comes from the source.	

3.3 Concrete mixes

The NC master reference mix. As a minimum requirement, the cylinder compressive strength target of 21 MPa (fc') was suggested for rubberized concrete due to its widespread usage in building applications. The final design mix was selected after numerous laboratory trial mixtures of ordinary and rubberized concrete. Cement, sand, and gravel were the final proportions, with a water-cement ratio of 0.21. The ACI 318M-19 guidelines were used in the creation of these mixes. The creation of six rubberized mixtures was carried out with consistent material proportions as shown in Table 3-17.

Table 3-17: Concrete mixtures details.

Mix No.	Specimens	Replace rubber with	Mix materials quantities (Kg for each cubic meter)				
			Coarse aggregates	Fine aggregates	Chip rubber	Crumb rubber	FOSROC Structuro 502
1	B1 B2		808.5	768.5	0	0	4.5
2	B3-F10-b B9-F10-S	10% fine agg.	808.5	691.65	0	22.35	6.7
3	B4-F20-b B10-F20-S	20% fine agg.	808.5	614.819	0	44.71	8
4	B5-C10-b B11-C10-S	10% coarse agg.	727.65	768.5	24.5	0	4.5
5	B6-C20-b B12-C20-S	20% coarse agg.	646.8	768.5	49	0	4.8
6	B7-C5F5-b B13-F5C5-S	(5%fine +5% coarse)10%	768.075	730.079	12.25	11.176	5
7	B8-C10F10-b B14-F10C10-S	(10% fine +10%coarse)20%	727.65	691.65	24.5	22.356	6.4
Density of materials (kg/m3)			1650	1650	500	480	
	Cement and water content are constant with values of (536.72,110) kg/m3						

3.4 Procedure for mixing, preparing, and casting beams

Rectangular hardwood planks 20 mm thick served as the formwork for casting the concrete beams. Fourteen shapes measuring 1600 × 150 × 250 mm were made of hardwood and fastened to the bed with four sides fastened with screws and nails. A concrete mixer with a capacity of 0.25 m^3 was used to cast the samples as shown in Plate 3-7. The capacity of each beam was 0.06 m^3. In each mix, the required capacity was 0.280 to cast 2 beams, and the remaining samples were for the fresh and hardened tests explained in heading 3.8.

Plate 3-7: Laboratory concrete mixer.

Before starting to place the reinforcing steel cage inside the wooden forms, the inner sides of the plywood form were lubricated to ensure easy disassembly of the formwork (Plate 3-8).

Plate 3-8:Preparation of plywood formwork and reinforcement

The concrete mixing process was carried out in detail in the following steps (Plate 3-9):-

1) The concrete mixing ingredients were metered out and put into separate, clean bags. Then mixed for 1.5 minutes without water, the rubber, gravel, sand, and cement were mixed using an electric concrete mixer.

2)Water mixed with superplasticizer was gradually added to the mixer, and the mixing continued for an additional 1.5 minutes.

3) With great care, the concrete mixture was poured vertically into a plywood mold. The surface was leveled with a shovel. Burlap sheets were placed over each RCB specimen to stop the water from evaporating.

4) Once the 72 hours had passed, the specimens were taken out of their molds. The beams were stacked once the molds were taken out, covered with a layer of burlap, and watered every day for a maximum of 28 days. It was necessary to apply a thin coat of paint to both the plain and rubber-reinforced concrete beams (without strengthening) after the water curing phase in order to detect any gaps.

Testing for hardness During the casting process, samples of six cubics of 15 * 15 *15 cm, six cylinders with diameters of 10 cm and lengths of 20 cm, and four prisms with dimensions of 10 x 10 x 40 cm were cast for each type of mixture. Conditions similar to those encountered during the casting of beam samples were used to create the concrete in conventional test molds. After that, the samples were and covered with nylon sheets to stop water from evaporating (Plate 3-10A). After a day, they were taken out of their mold and kept submerged in water tanks for 7 and 28 days, depending on the test's age. After the treatment period, the samples were taken out of the water and processed for testing in accordance with the test requirements (Plate 3-10B).

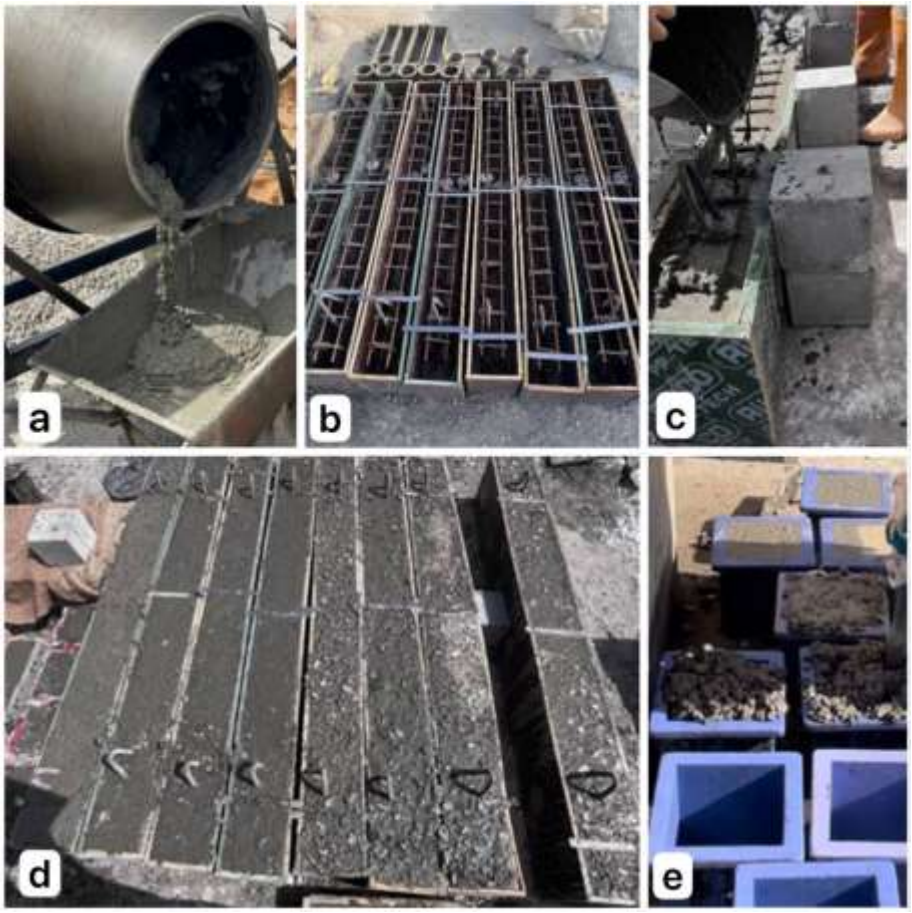

Plate 3-9: (a) Casting of concrete ,(b) Preparing the molds ,(c) Pouring concrete mix into molds (d) The shape of the molds after casting,(e) Cube modeling.

Plate 3-10: (a) Curing of RCBs , (b) Curing of hardening tests samples.

3.5 Fresh and cured testes

3.5.1 Workability (slump flow test)

The following test was carried out immediately after mixing to determine the workability of normal and rubberized concrete (Plate 3-11). Undertaking the slump test was a truncated cone that measured 100 mm in top diameter, 200 mm in bottom diameter, and 300 mm in height. The cone was filled three times with the concrete mixture, and then the mixture was progressively removed. Measurements were taken of the slamp test diameter of both NC and rubberized concrete.

Plate 3-11: Slump flow test.

3.5.2 Compressive strength test

According to (BS 1981: part 116), the test was conducted using cubic blocks with dimensions of 15 * 15 * 15 cm for each mixture at ages 7 and 28 days. The experiment was carried out using a compressor with a 2000 kN capacity, as seen in Plate 3-12.

Plate 3-12: Compression hydraulic machine.

3.5.3 Splitting tensile strength test

This test was done in accordance with (ASTM C496) at 7 and 28 days via cylinder (200x100) mm. As shown in Plate 3-13, the cylinder was placed horizontally between two plates of wood to distribute loads of the compressive machine uniformly on the upper and lower sides of the cylinder. The average of three cylinders samples is used to evaluate the splitting tensile resistance and was calculated by using the equation below (ASTM C496):

$ft = 2P/\pi hD$

Where:

ft = tensile stress (MPa).

P = total failure load (N).

D = section diameter (mm).

h = section height (mm).

Plate 3-13: Tensile strength splitting test

3.5.4 Modulus of rupture

Modulus of rupturetests were performed on prisms measuring (100 x 100 x 400) mm, as illustrated in Plate 3-14, in accordance with the ASTM C78-02 standard [56] at 7 and 28 days. three-point load tests were conducted a flexural testing machine with a capacity of 150 kN. The modulus of rupture was ascertained by averaging the results from two specimens, computed using the equation outlined in ASTM C78.

fr = PL / bd^2

fr = Flexural stress (MPa).

P = Total failure load, (N).

L = supports distance (mm).

b = width of the prism section, (mm).

d = depth of the prism section, (mm).

Plate 3-14: Flexural strength test.

3.6 CFRP bar and CFRP strip installation

To improve the flexural capacity and compare it with controlled specimens, the Near-Surface Mounted system was used once using CFRP bars and once using CFRP strip before starting the testing of the beams under repetitive loads. This procedure was completed over a period of four days.

Grooves preparation is the most important aspect in the application process of CFRP bar and CFRP strip . Several operations are required to prepare the grooves. The grooves should be intact and clear, and dust, silt and other foreign particles should be removed from inside.

The groove dimensions were marked on the beams and then an electric hand grinder was used to drill grooves into the underside of the beams, as shown Plate 3-15. Air pressure and a brush were used to remove any remaining dust inside the grooves. The CFRP strip and CFRP bar installation process consists of the following steps:

Step 1: Clean the grooves from the inside and remove any dust and any obstacles between the concrete and the epoxy using air pressure and a brush.

Step 2: The components A (white) and B (black) of the adhesive (Sikadur®-30 LP) were individually prepared in accordance with the manufacturer's specifications and subsequently blended in a ratio of 3A:1B until a uniform gray color was achieved.

Step 3: The grooves were filled with the epoxy mixture material

Step 4: Both CFRP bar and CFRP strip were inserted inside the grooves and the surface was cleared and polished well

Plate 3-15: Stages of installation CFRP bar and CFRP strip, (a)Clean the grooves by air pressure, (b) Clean the grooves by brush, (c) grooves were filled with the epoxy, (d) Insert the bar into the grooves, (d) Surface leveling.

3.7 Protocol of repeated loads

The repetitive loading protocol was developed according to a protocol previously described by the researchers (Al-khafaji, Muhammed and Jadooe, 2024). Although with a slight modification, the current study adopted 30 cycles with a loading range between 30% and 80% of the ultimate load

resulting from the monotonous loading test (Pu). The repetitive loading process was implemented in three stages (Figure 3-11):

The first stage: - 30% of Pu with ten loading and unloading cycles, and the loading in each cycle is on ten divisions of the load.

The second stage: - 60% of Pu with ten loading and unloading cycles, and the loading in each cycle is on ten divisions of the load.

The third stage: - 80% of Pu with ten loading and unloading cycles, and the loading in each cycle is on ten divisions of the load.

The last stage: -The loading is done gradually until the beam reaches failure.

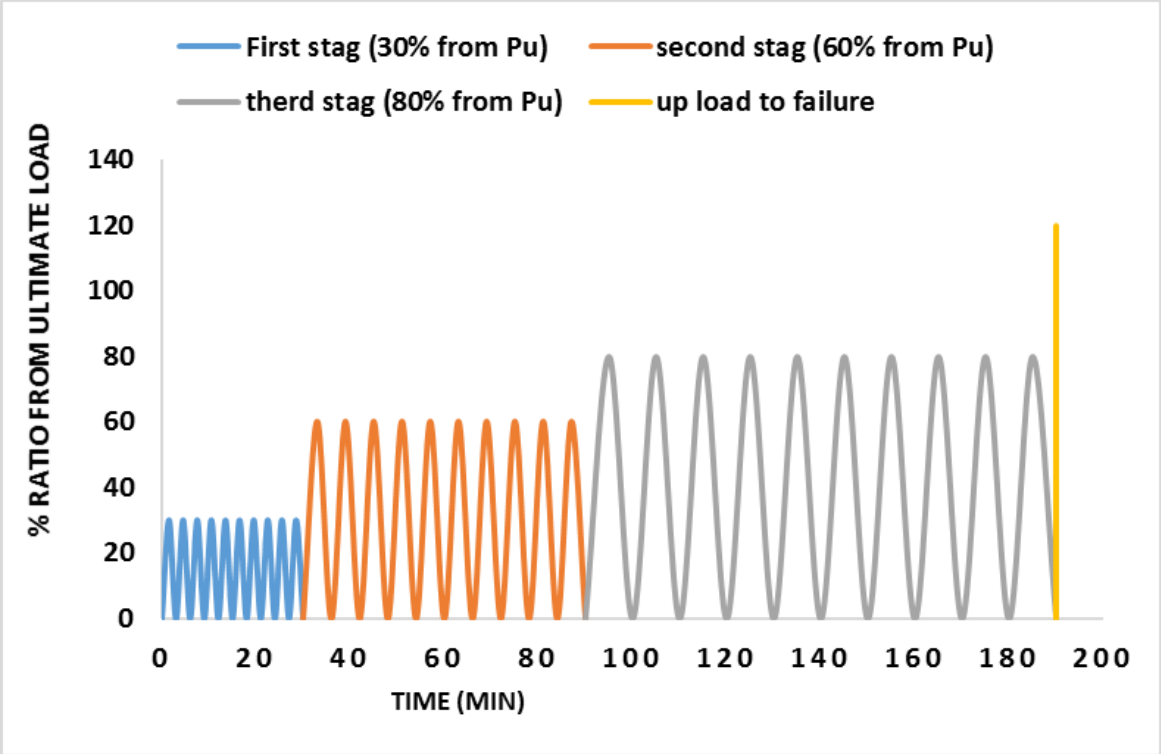

Figure 3-11: :Protocol of repeted load.

3.8 Procedure for tests

An experimental repeted test was conducted on a single reinforced concrete beam for regulatory purposes in the testing apparatus. The test procedure can be summarized in the following steps:

1. Every piece of apparatus and sensor had been precisely positioned.

2. Plate 3-16 shows the selection of the pin support and roller support for the steel support frame, which was used to fix the specimen.

3. The load cell was located in the middle of the upper face of the beam (Plate 3-17a).

4. The LVDT sensor was installed below the middle of the beam (Plate 3-17b).

5. The load distributor was placed above the beam.

6. The device was turned on and put on the electronic system to allow the load to be entered electronically via the program.

7. The load cell measures the impact load once any load is entered, while the LVDT sensor measures the displacement.

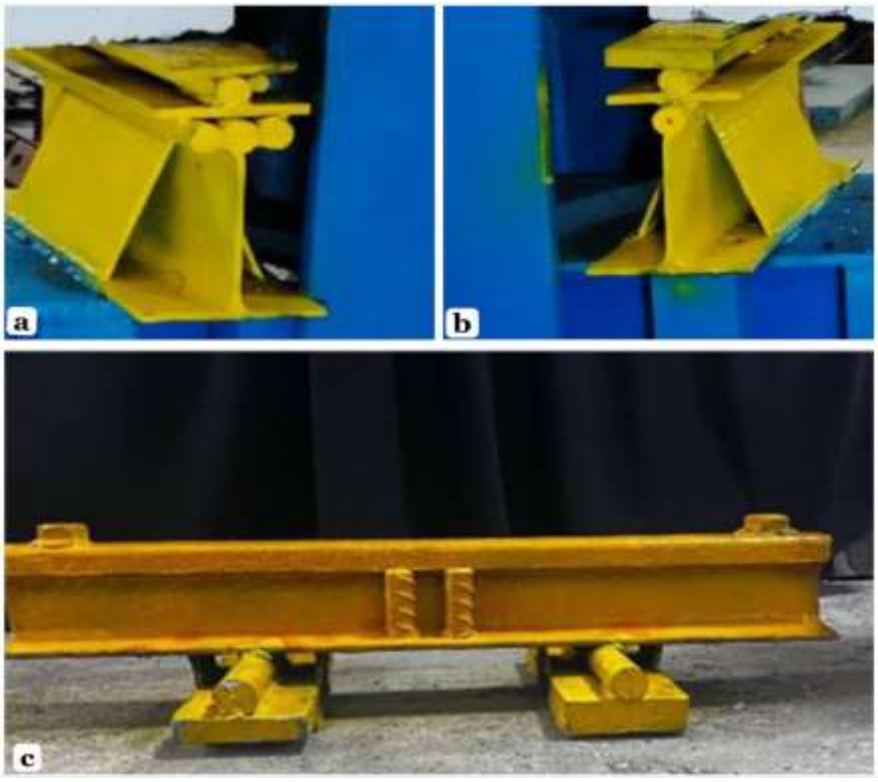

Plate 3-16: (a) Pin support ,(b) Roller support , (c) Load distributor.

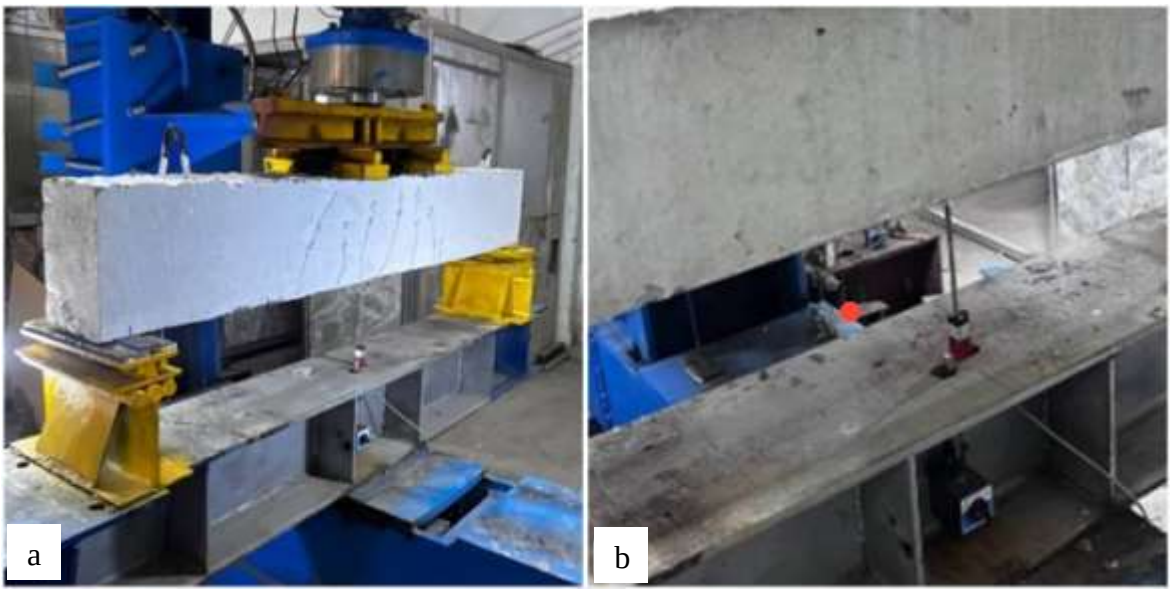

Plate 3-17: (a) Preparing the load cell in the middle of the sample , (b) Loading initiated by load cell.

Chapter Four: Results and Discussion

4.1 Introduction

This chapter presents the experimental results of tests conducted on normal and rubberized reinforced concrete beams incorporating varying proportions of recycled tire rubber. The investigation is divided into two main parts. The first part focuses on the experimental evaluation of fresh and hardened properties of rubberized concrete mixtures, including density, workability, compressive strength, tensile strength, and flexural strength. The second part analyzes the structural behavior of fourteen reinforced concrete beams—twelve rubberized and two conventional—subjected to repeated loading.

All beams had identical dimensions of 1600 mm in length, 150 mm in width, and 250 mm in depth. The specimens were divided into two groups based on the strengthening technique. The first group included six beams strengthened with two carbon fiber-reinforced plastic (CFRP) bars, replacing 10% and 20% of the crumb and chip rubber, as well as a combination of both. The second group consisted of six beams strengthened with two strip of carbon fiber-reinforced plastic (CFRP), using the same rubber replacement ratios. Two unreinforced beams containing conventional concrete were tested under monotonic and repetitive loads, respectively.

The chapter further discusses the failure modes, load-deflection behavior, and the influence of NSM-CFRP bars and laminates on the performance of rubberized beams under cyclic loading.

4.2 Fresh concrete properties

4.2.1 Fresh density

The density values of seven samples of the mixtures are tabulated in Table 4.1. These values decrease when rubber is added to the reference concrete mixtures as a partial volume replacement of natural aggregates , as shown in Figure 4-1. The density of the rubberized concrete mixtures is lower than the reference mixtures for two reasons:

1- The specific gravity values of the natural aggregates (sand and gravel) were higher than the specific gravity values of the partial rubberized aggregates (crumbs and chip).

2- As the hydrophobic feature of rubber particles keeps water away from their surfaces while trapping air on their rough surface, the air content in rubberized concrete can be increased by raising the volume replacement ratio of rubber.

When the volume replacement ratio of fine aggregates was changed from 10% to 20% (see Figure 4-1), the fresh density of the rubberized concrete decreased by 3.30%-6.44% compared to the concrete without rubber. As shown in Table 4-1, replacing 10%-20% of the volume of the coarse aggregate with chip rubber reduces the fresh density by 2.44%-4.57%, compared to the control mix containing 0% rubber. In addition, replacing 10%-20% of the volume of the coarse aggregate with chip rubber and crumb rubber in the same mix reduces the fresh density by percentage -2.78% and -5.55% compared to the control mix containing 0% rubber.

Table 4-1: density statistics for different combinations.

NO. mix	Mixture symbols	The fresh density of mixes (kg/m3	%Difference
1	N	2359.25	0
2	F10	2281.48	-3.30
3	F20	2207.41	-6.44
4	C10	2301.74	-2.44
5	C20	2251.48	-4.57
6	F5C5	2293.75	-2.78
7	F10C10	2228.25	-5.55

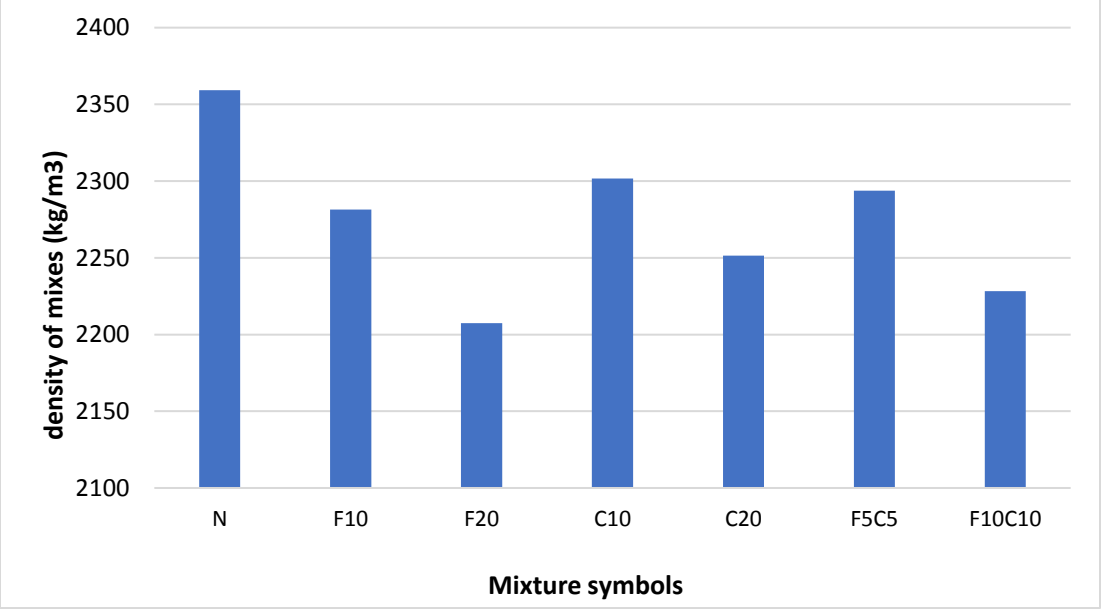

Figure 4-1: : Fresh density.

4.2.2 Workability (Slump flow test)

The test results for the seven concrete mixes given in the Table 4-1, and as followes:-

1) Natural mix (N):

This is the reference mix without rubber, and its slump flow value is 64 cm. This value will be used as a basis for comparison with the rest of the mixes.

2) Second mix (F10):

Replacing 10% of the fine aggregate with rubber. The slump value decreased to 53.5 cm, which represents a decrease of 16.406%. This can be explained by the fact that replacing the fine aggregate with rubber leads to a decrease in the flow of the mix due to the properties of rubber that hinder movement more compared to natural aggregate.

3) Third mix (F20):

Replacing 20% of the fine aggregate with rubber. The slump value increased slightly to 56.5 cm, with a decrease of 11.718% compared to the natural mix.

Despite the increased replacement ratio, the negative effect on flow is not as severe as in the second mixture. This may be due to the better distribution of rubber in the mixture with the increased ratio.

4) Fourth mixture (C10):

Replacing 10% of the coarse aggregate with rubber. The flow value here is 58 cm, with a decrease of 9.375%. It is noted that replacing the coarse aggregate with rubber has less effect on flow than replacing the fine aggregate, perhaps due to the larger particle size of the coarse aggregate.

5) Fifth mixture (C20):

Replacing 20% of the coarse aggregate with rubber. The flow value is close to the natural mixture, which is 62.5 cm, with a slight decrease of 2.343%. Replacing the coarse aggregate with a higher percentage did not significantly affect flow, which means that the effect of rubber is less when used as a substitute for the coarse aggregate.

6) Mixture 6 (F5C5):

Replacing 5% of fine aggregate and 5% of coarse aggregate with rubber. The flow value is equal to the natural mixture (64 cm), with a slight decrease of 0.781%.This shows that replacing a small percentage of both types of aggregate with rubber leads to maintaining the flow properties significantly.

7) Mixture 7 (F10C10):

Replacing 10% of fine aggregate and 10% of coarse aggregate with rubber. The flow value is 60 cm, with a decrease of 6.25%. Here it can be said that the effect is more pronounced with increasing the replacement ratio, but the effect is still moderate.

In general, replacing fine aggregate with rubber appears to have a greater effect on reducing flow than replacing coarse aggregate. Also, increasing the replacement ratio leads to reducing flow, but the effect is not completely linear, as shown in Table 4-2 and Figure 4-2 .

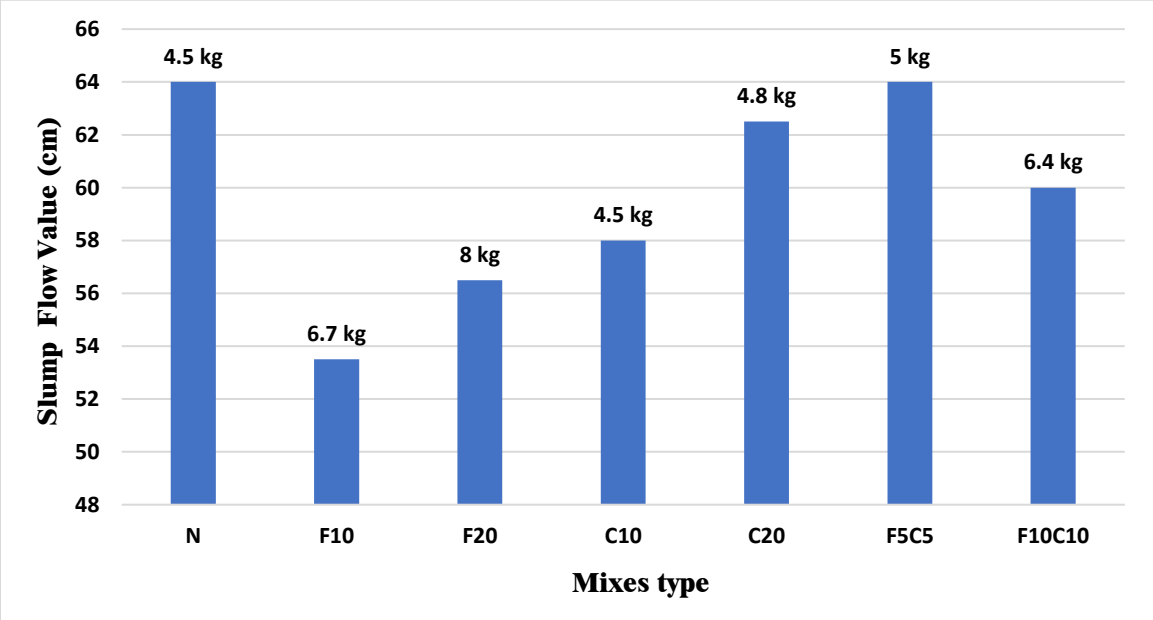

Figure 4-2: Slump flow test.

Table 4-2: Slump values for different combinations

NO. mix	Mixture symbols	Slump Flow Value (cm)	%Difference
1	N	64	0
2	F10	53.5	-16.406
3	F20	56.5	-11.718
4	C10	58	-9.375
5	C20	62.5	-2.343
6	F5C5	63.5	-0.781
7	F10C10	60	-6.25

4.3 Hardened concrete properties

The characteristics of curing concrete to comprehend the actions of rubberized concrete, one must be familiar with its mechanical characteristics. Hardened characteristics, including flexural, compression, and splitting tensile strength, have thus been evaluated.

4.3.1 Compressive strength

The results in Table 4-3 and Figure 4-3 show that the increase in the ratio of rubber replacement leads to a significant decrease in compression resistance values in rubberized concrete mixes, as the compression resistance values for samples containing 20% of chip rubber instead of coarse aggregates (C20) decreased by 29.23% than normal concrete mixtures (N) and this decrease is lower than rubber-containing mixtures instead of fine aggregates, as the result of(F20) samples showed a decrease in the compression resistance value of about 32.75%. These results are consistent with previous studies **(Ghoneim and Sharobim, 1997)** . Also, the adhesion between the cement paste and the rubber parts is not strong enough at the transition zone between the surfaces between them. A small amount of rubber particles tend to move to the upper surface of the molds

during the molding of samples due to the low specific weight of rubber particles. The compressive strength of rubber-containing mixtures instead of fine aggregates decreased slightly more than rubber-containing mixtures instead of coarse aggregates, due to the lower surface area of coarse aggregates compared to the surface area of fine aggregates.

Table 4-3: Results of the tested mixtures' cube's compressive strength after 7 and 28 days

NO.mix	Mixture symbols	Cube Compressive strength (*f*cu), MPa			
		At 7 Days	%Difference	At 28 Days	%Difference
1	N	66.47	0	67.29	0
2	F10	48.45	-27.11	55.97	-16.82
3	F20	44.09	-33.67	45.25	-32.75
4	C10	47.31	-28.83	48.75	-27.55
5	C20	43.97	-33.85	47.62	-29.23
6	F5C5	49.84	-25.0	57.29	-14.9
7	F10C10	41.14	-38.1	47.29	-29.9

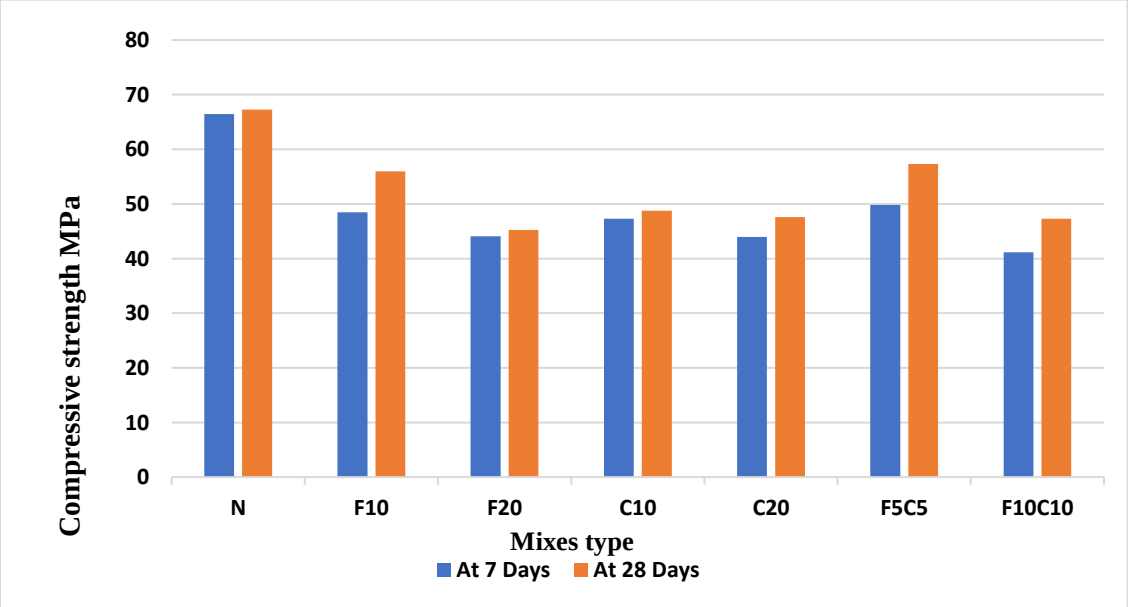

Figure 4-3: Compressive strength results of the mixes

4.3.2 Splitting tensile strength

In general, the results of seven different mixtures in Table 4-4 and Figure 4-4 showed that there was a decrease in tensile strength values with increasing rubber replacement ratio. The failure mode of the reference mixture (N) showed a true splitting of the specimen, where the cylinder splits into two halves (brittle failure) (Plate 4-1).

Plate 4-1: Failure patterns due to the splitting tensile strength test .

However, other mixtures containing rubber particles (crumbs or chip) did not show this failure mode. The failure mode of the rubber concrete mixtures was gradual rather than brittle. The tensile strength values of the samples containing 20% of chips rubber instead of coarse aggregate (C20) decreased by about 17.12% compared to the normal concrete mixtures (N) and this decrease is less than that of the mixtures containing rubber instead of fine aggregate, where the result of the F20 samples shows a decrease in tensile strength value by 22.95%. These results are in agreement with previous studies (Senouci and Member, 1994). In addition, the tensile strength values of the samples containing 10% chips rubber and crumb rubber in the same mixture were higher than the mixture containing 20% chips rubber and crumb rubber in the same mixture by 10.20% of the normal concrete mixtures, so replacing the chips is better

than replacing the crumbs, and replacing the chips and crumbs in the same mixture by 10% is better than replacing the 20%. The results also showed that the decrease in the split tensile strength values was less than the decrease in the compressive strength.

Table 4-4: Results of splitting Tensile strength at 7 and 28 days.

NO. mix	Mixture symbols	Splitting tensile stress (f_{sp}), MPa			
		At 7 Days	%Difference	At 28 Days	%Difference
1	N	4.84	0	5.49	0
2	F10	4.25	-12.19	4.88	-11.11
3	F20	4.02	-16.94	4.23	-22.95
4	C10	4.22	-12.81	4.67	-14.94
5	C20	3.94	-18.60	4.55	-17.12
6	F5C5	3.92	-19.01	4.93	-10.20
7	F10C10	3.55	-26.65	4.25	-22.59

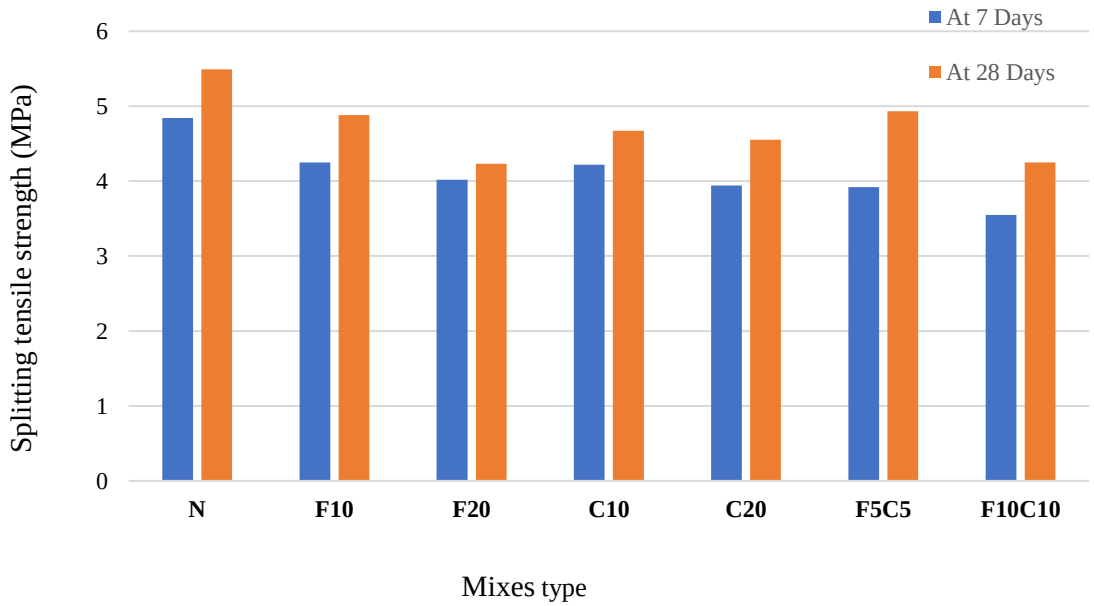

Figure 4-4: Tensile strength results.

4.3.3 Modulus of Rupture

This test was performed as described in ASTM C78, using a (100x100x400) mm prism (Plate 4-2).

a

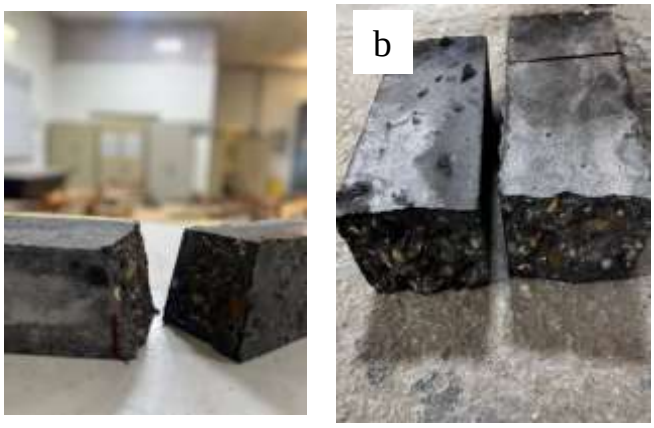

Plate 4-2: a) Failure mode NC; b) Failure mode C20.

The results of the flexural strength test for seven different concrete mixtures are shown in

Table 4-5 and Figure 4-5. The flexural strength was reduced by adding rubber particles. The failure mode of the reference mixture (N) shows that the failure of the prism occurred in the middle of the specimen. This is related to the homogeneity of the mixture. In mixtures containing rubber particles, the failure mode occurred not exactly in the middle of the specimen but still within the inner third due to the non-uniform distribution of rubber, especially in F20, C20 and F10C10. The flexural strength values of the samples containing 20% of chips rubber instead of coarse aggregate (C20) decreased by about 11.5% compared to the normal concrete mixes (N), and this decrease is less than the mixes containing rubber instead of fine aggregate, as the result of the F20 samples showed a decrease in the flexural strength value by about 35%, and these results are consistent with previous studies **(Senouci and Member, 1994)**. As for the samples containing replacement of coarse and fine aggregate in the same mix F5C5,

they showed a decrease in the flexural strength value by about 35.6% compared to the normal concrete mixes, and this decrease is less than the mixes containing replacement of coarse and fine by 20% F10C10, as the result of the F10C10 sample showed a decrease in the flexural strength by 38%.

Table 4-5: Seven- and twenty-eight-day Modulus of rupture findings

NO. mix	Mixture symbols	Modulus of rupture (*fr*), MPa			
		At 7 Days	%Difference	At 28 Days	%Difference
1	N	5.95	0	10	0
2	F10	5.6	-5.82	7.36	-26.4
3	F20	5	-15.96	6.5	-35
4	C10	7.45	25.21	8.9	-11
5	C20	7.1	19.32	8.85	-11.5
6	F5C5	7	17.64	8.63	-13.7
7	F10C10	4.71	-20.67	7.25	-27.5

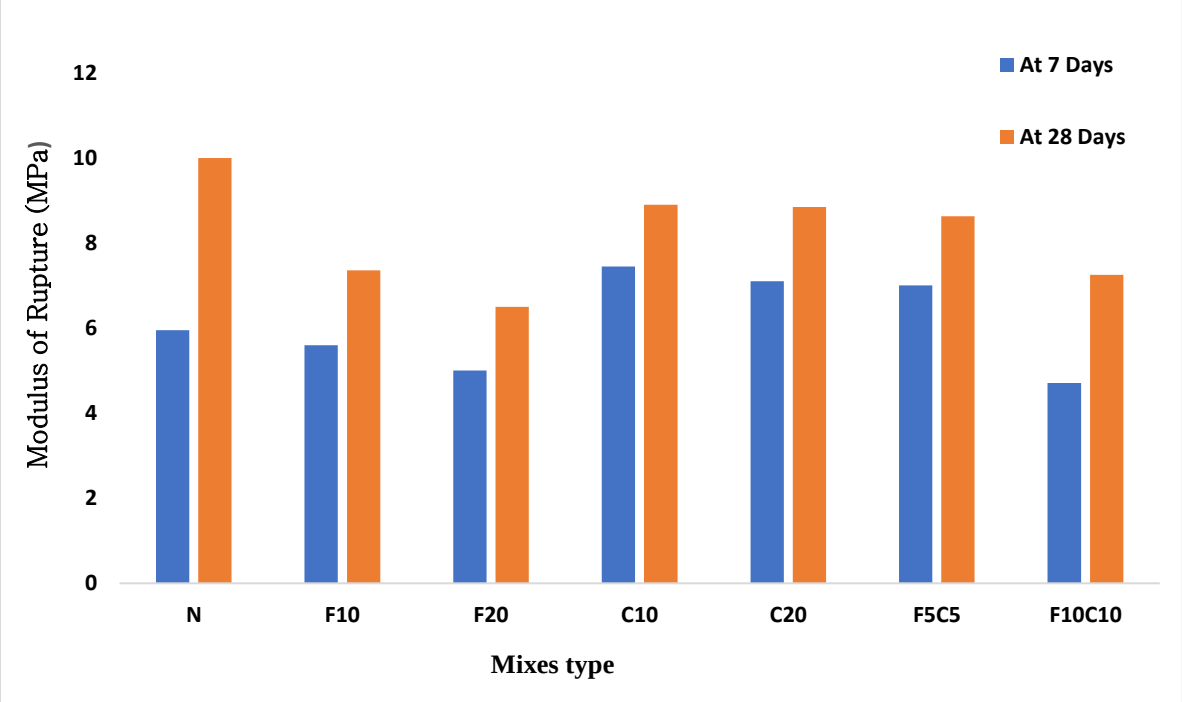

Figure 4-5: Modulus of rupture results.

4.4 Tested beam specimens

An essential consideration in building projects is a structure's ability to endure repeated loading. Lightweight, energy-absorbing, and easy to work with, rubberized reinforced concrete is another material utilized in construction. Fourteen reinforced concrete beams' responses to repetitive loading are detailed and discussed in this section. There are three sets of fourteen beams. In the first set, you'll find a pair of beams: one that withstands monotonic loading and another that does the same thing but with repeated loading. The second group consists of six beams with volume ratios of 10% and 20% of stripd rubber instead of coarse blocks, volume ratios of 10% and 20% of crumb rubber instead of fine blocks, and volume ratios of 10% and 20% of stripd rubber and crumb rubber instead of coarse and fine blocks, all reinforced with 2bars of CFRP. The third group is the same as the second group but reinforced with 2 strip of CFRP.

The repetitive load was simulated by a specific protocol as explained previously in Chapter 3, which are three percentages of the maximum load were chosen, which are 30%, 60%, and 80%, and each percentage has 10 cycles.The response of the mid-span displacement was evaluated using the LVDT sensor in the middle of the beam. The data was measured and then stored in an Excel sheet at a rate of about 125,000 readings per second.

Table 4-6 illustrate the results of the concrete beam samples the first appearance of cracks along with the corresponding deflection. Additionally, the ultimate load sustained by the beam is presented together with its associated deflection.

Table 4-6:Results of all beams tested.

No.	Spacimens	First crack (KN)	Deflection (mm)	Ultimate Load (KN)	Difference%	Deflection (mm)	Difference%
1	B1	15	1.13	87	0	29.5	0
2	B2	20	0.77	80	-8.05	27.3	-7.46
3	B3-F10-b	26	1.11	116	45	13.35	-51.10
4	B4-F20-b	30	0.95	108	35	9.84	-63.96
5	B5-C10-b	30	0.85	127	58.75	15.17	-44.43
6	B6-C20-b	35	0.35	120	50	10.75	-60.62
7	B7-C5F5-b	40	0.88	160	100	15.35	-43.77
8	B8-C10F10-b	52	1.26	127	58.75	13.18	-51.72
9	B9-F10-S	30	1.21	147	83.75	31.14	14.07
10	B10-F20-S	35	0.88	143	78.75	12.83	-53.00
11	B11-C10-S	40	1.04	165	106.25	31.31	14.69
12	B12-C20-S	49	0.85	128	60	20.15	-26.19
13	B13-F5C5-S	45	1.27	168	110	20.46	-25.05
14	B14-F10C10-S	52	2.44	148	85	24.27	-11.10

4.1 Load-deflection relationship

Interpreting the load-displacement curves of rubberized concrete beams when subjected to repeated loading and containing different proportions of coarse and fine aggregate replacement by rubber, requires a careful understanding of the effect of these variables on the behavior of the beam. The following is an explanation of how these variables affect the curves (Figure 4-6 to Figure 4-19):

1- Elastic Response in all replacement rates:

In the initial stages of frequent loading, the response of the beam is within the flexible stage. This stage determines the initial stiffness . Replacing the aggregate with rubber significantly affects this stiffness . The higher level of rubber, the less stiffness . When replacing 10% of the fine or coarse aggregate, the effect of rubber on stifness will be less compared to the replacement by 20%.

2- Plastic region:

After exceeding the elastic limit stage, the plastic deformation stage begins and the curve becomes nonlinear. Here, rubber plays a major role in improving the ductility, as it allows the material to absorb more abnormalities before failure. When replacing 10% of the fine or coarse aggregate, the plasticity remains relatively limited but is better than regular concrete. In the event that 20% of the fine rubber is replaced, a greater increase in the plasticity appears. But that comes with a clear reduction in stiffness. When the replacement is 10% or 20% for both types (fine and coarse aggregate), stiffness is further affected and the curve becomes more prone to large deformations.

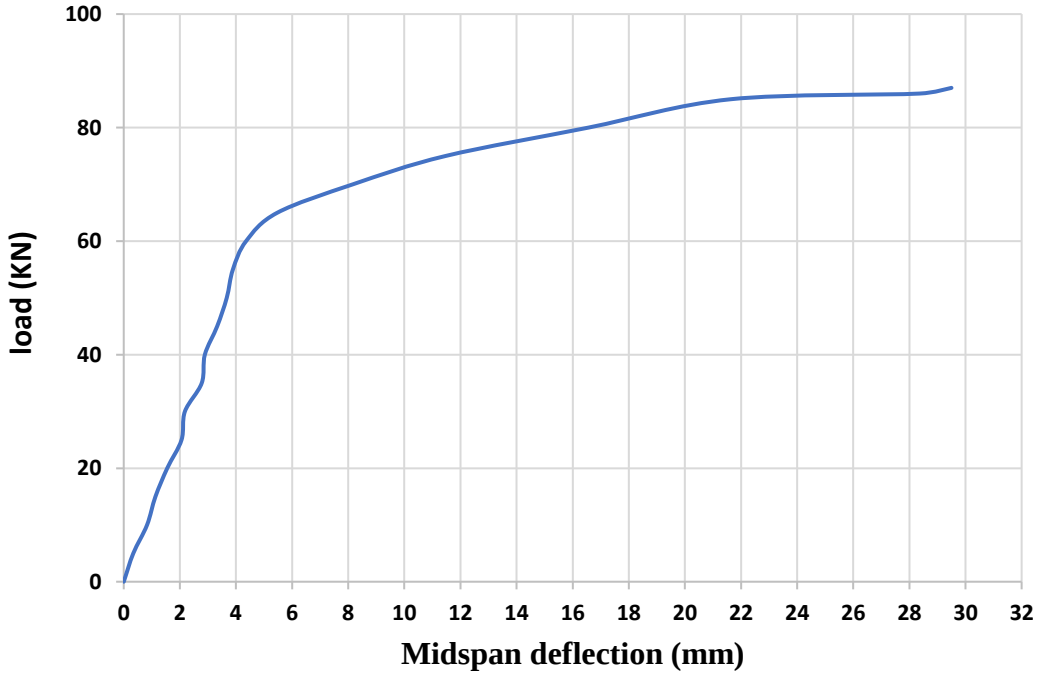

Figure 4-6: Load-deflection of beam B1 under monotonic.

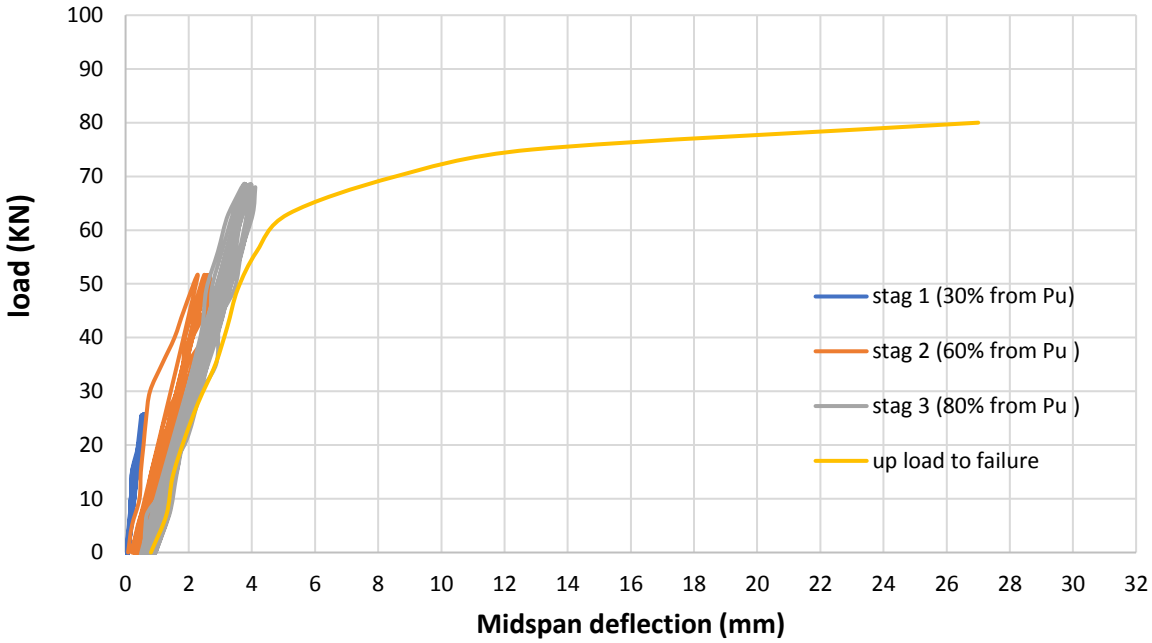

Figure 4-7: Load-deflection of beam B2 under repeted load.

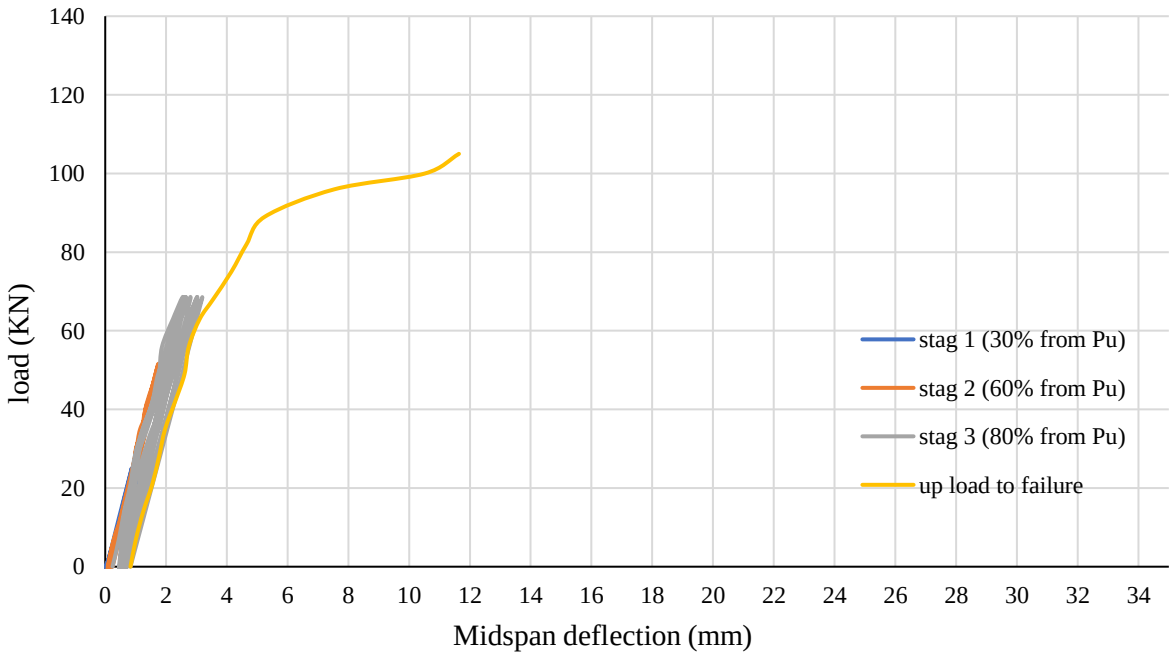

Figure 4-8: Load-deflection of beam B3-F10-b under repeted load.

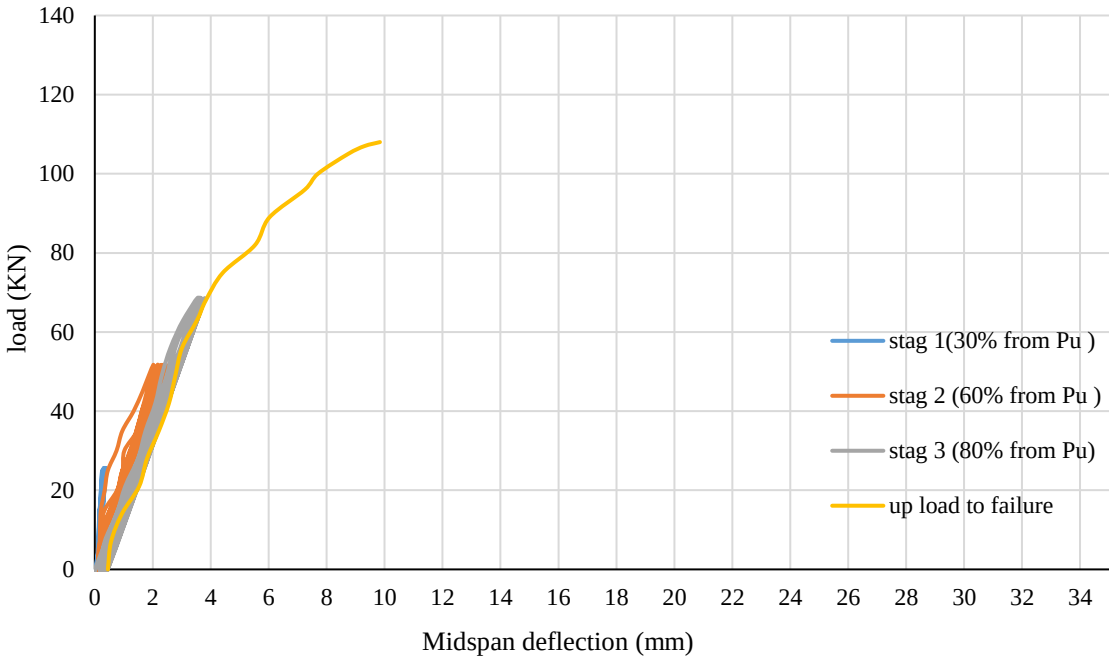

Figure 4-9: Load-deflection of beam B4-F20-b under repeted load.

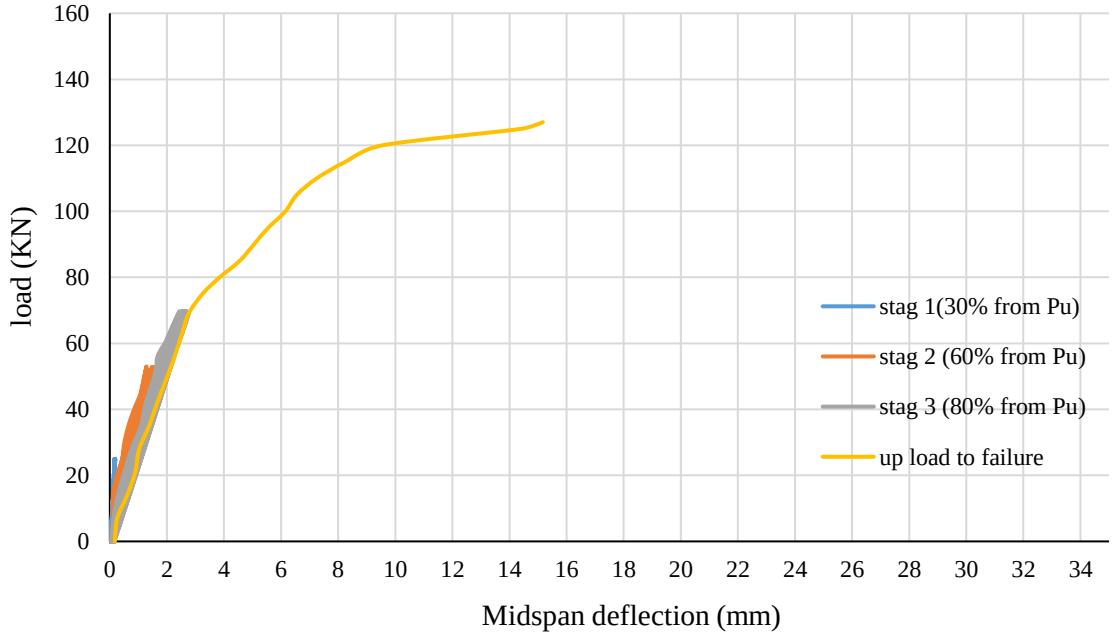

Figure 4-10: Load-deflection of beam B5-C10-b under repeated load

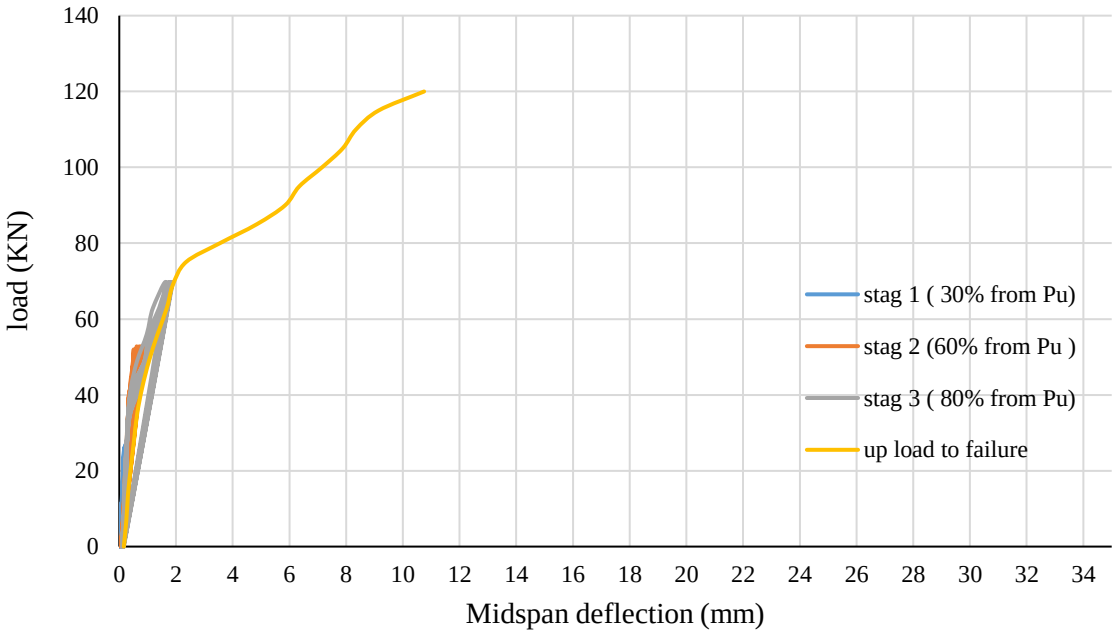

Figure 4-11: Load-deflection of beam B6-C20-b under repeated load

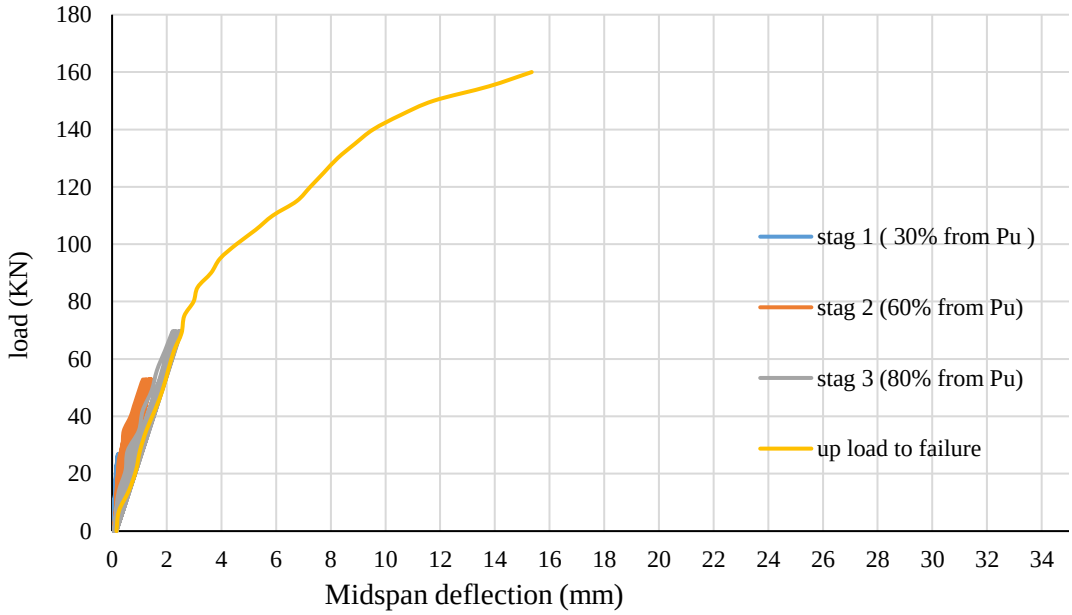

Figure 4-12: Load-deflection of beam B7-C5F5-b under repeated load

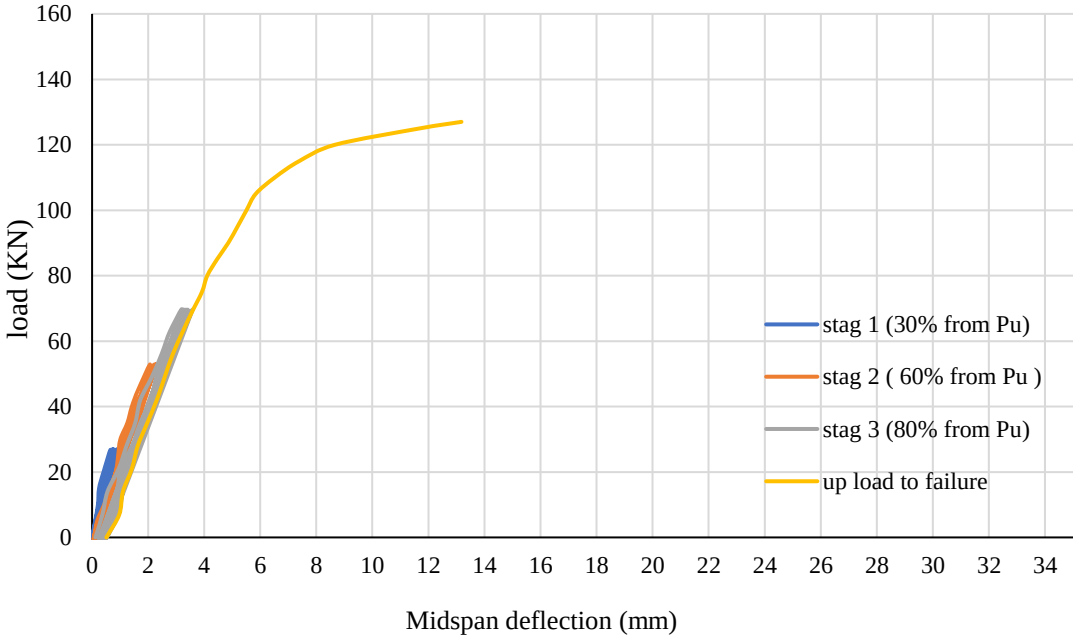

Figure 4-13: Load-deflection of beam B8-C10F10-b under repeated load

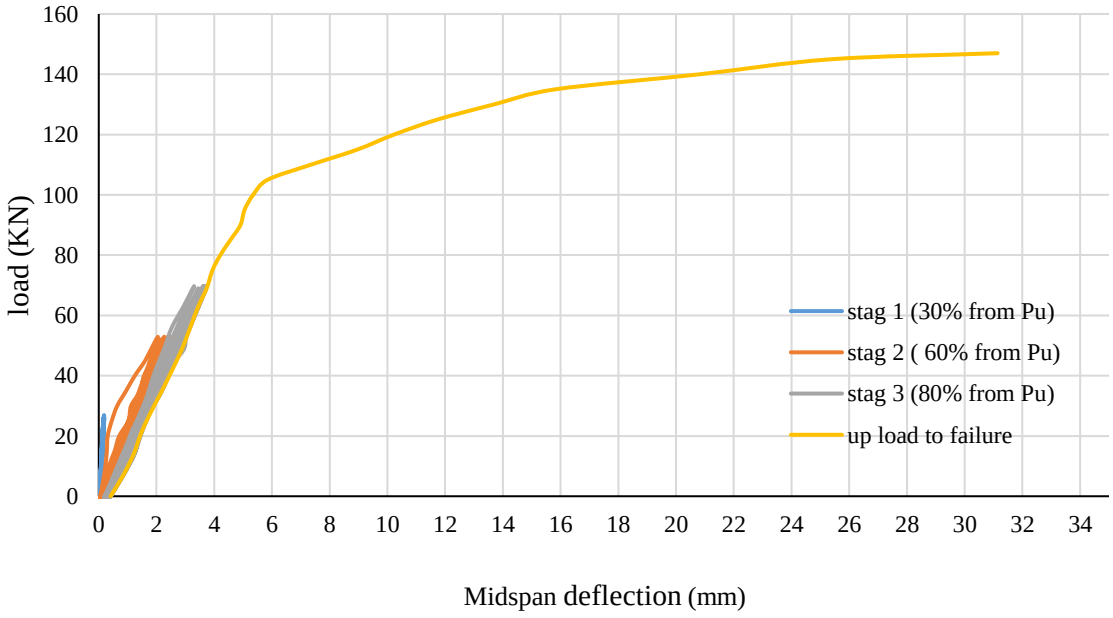

Figure 4-14:Load-deflection of beam B9-C10-S under repeted load.

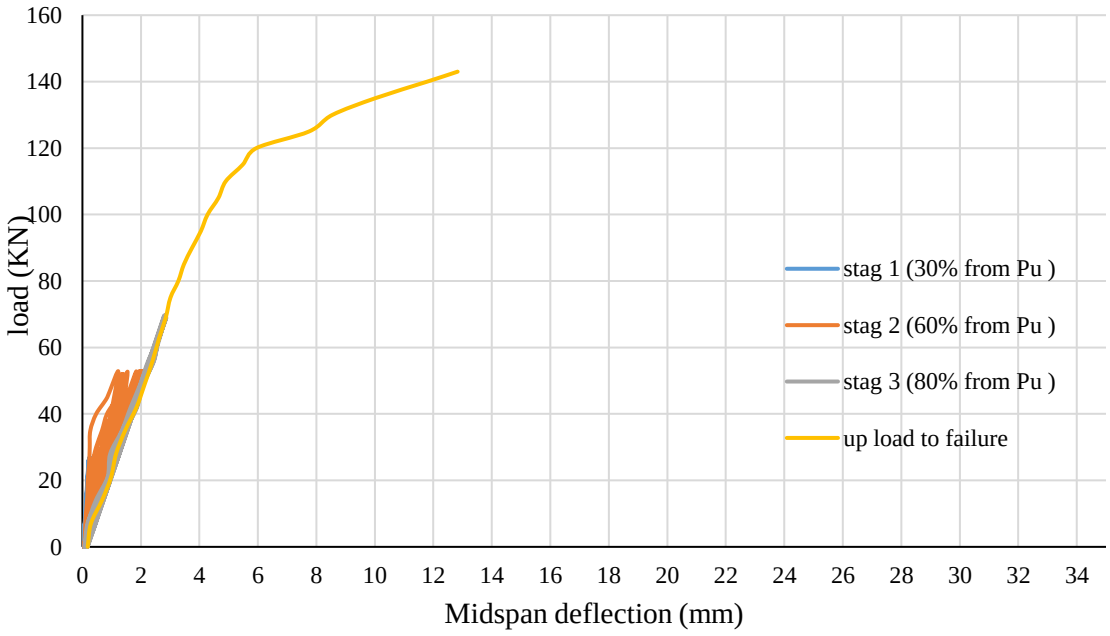

Figure 4-15:Load-deflection of beam B10-F20-S under repeted load

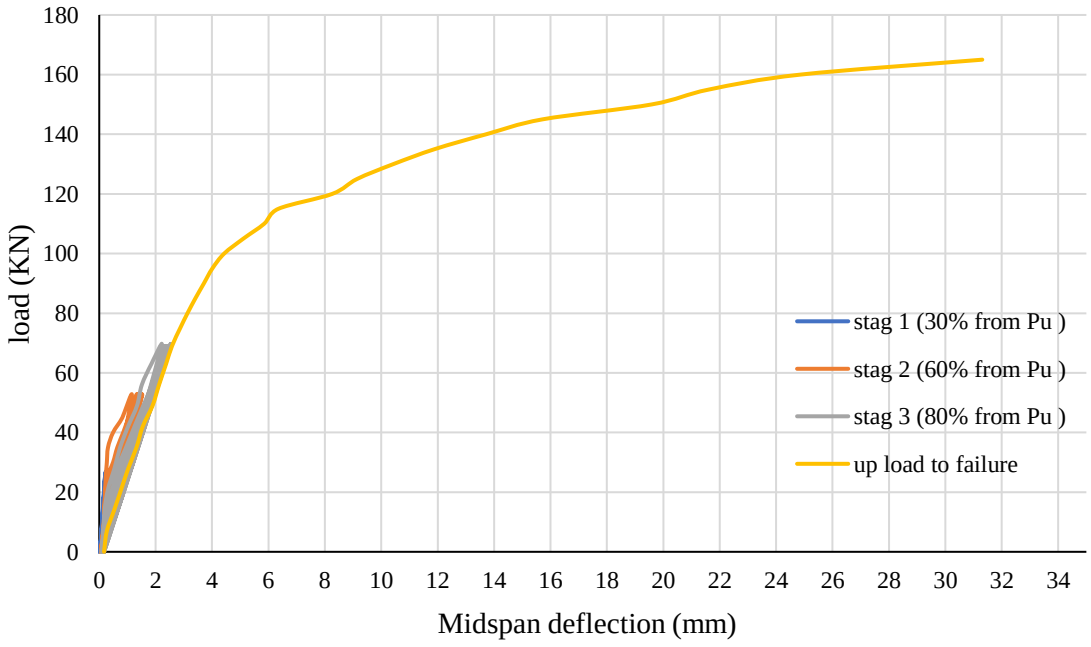

Figure 4-16:Load-deflection of beam B11-C10-S under repeted load

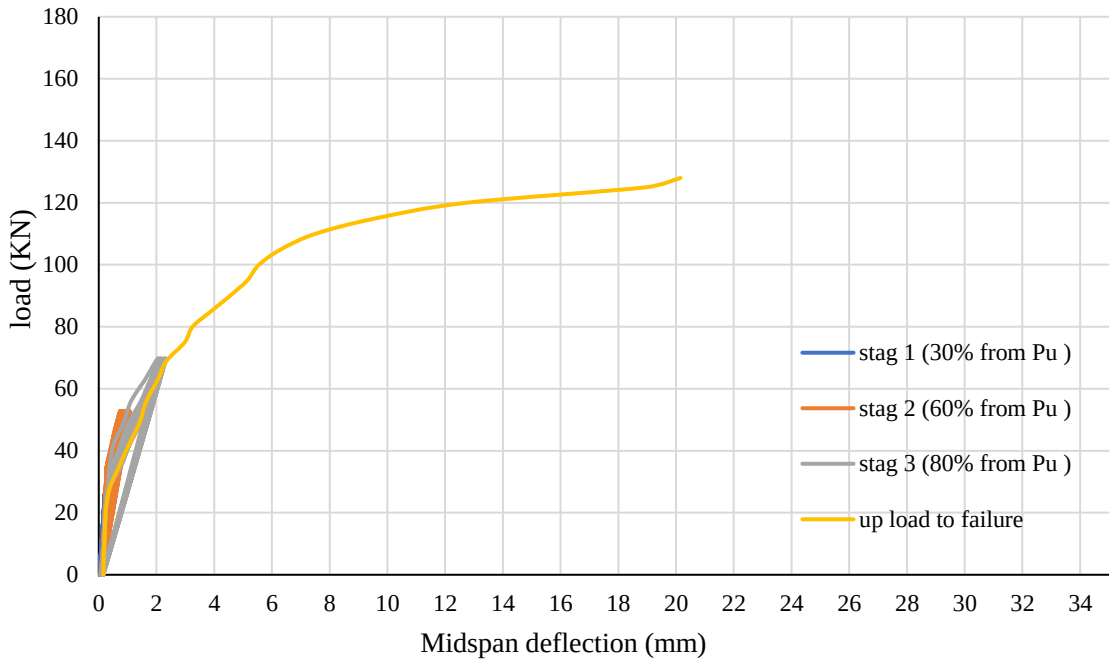

Figure 4-17:Load-deflection of beam B12-C20-S under repeted load

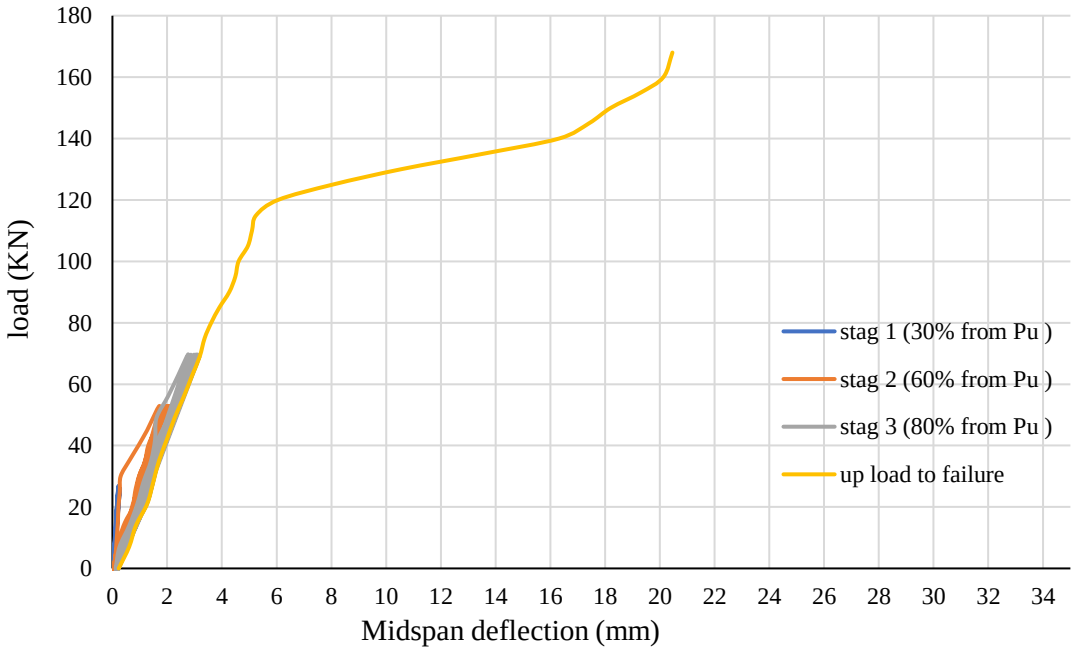

Figure 4-18:Load-deflection of beam B13-C5F5-S under repeted load.

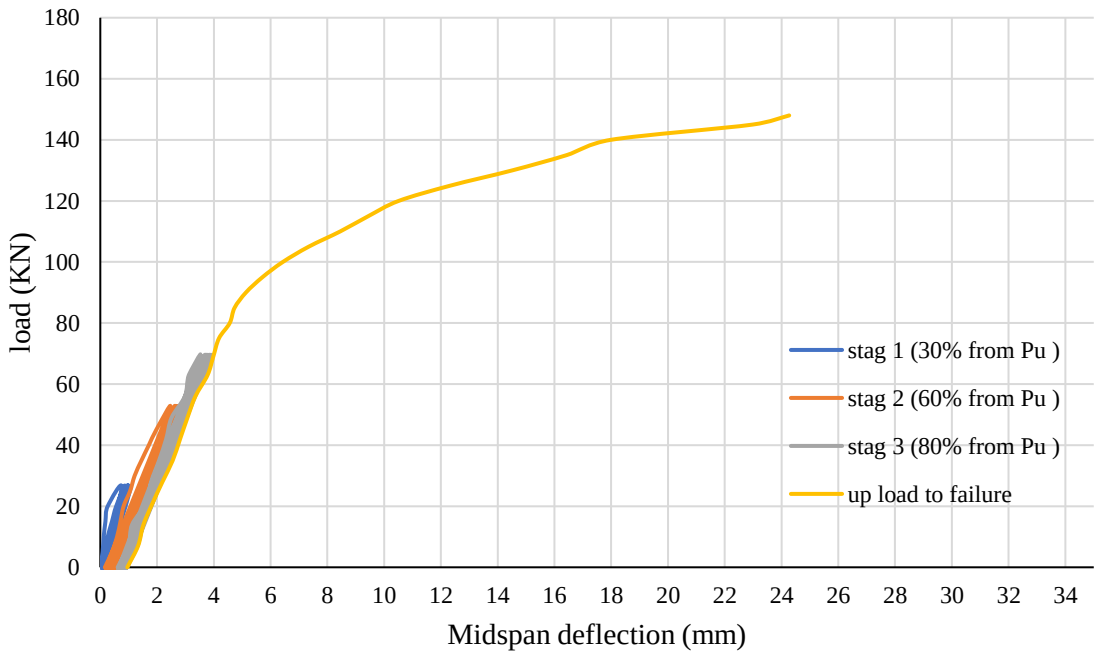

Figure 4-19:Load-deflection of beam B14-C10F10-S under repeted load.

4.2 Parameters effecting on the RC beams.

4.2.1 The effect of repeated load

From observing Table 4-6, the test results demonstrated that applying repeated loading has a significant impact on the structural behavior of reinforced concrete beams. Compared to specimen B1, which was tested under monotonic loading, specimen B2—having the same concrete mix but subjected to repeated loading—showed a reduction in ultimate load by 8.05% and a slight decrease in maximum deflection by 7.46%. This indicates that repeated loading can reduce the load-carrying capacity of conventional concrete even without any modifications to the mix or additional strengthening. However, when modified mixes incorporating recycled rubber as a partial replacement for fine or coarse aggregates—or both—were used, with or without near-surface mounted (NSM) CFRP strengthening systems, some specimens not only resisted the negative

effects of repeated loading but also demonstrated enhanced performance. This suggests that the detrimental impact of repeated loading can be mitigated, or even reversed, through improved concrete mix design or the application of effective strengthening techniques..

4.2.2 The effect of using different percentages of rubber particles in RC beams

The test results demonstrated that incorporating recycled rubber as a partial replacement for natural aggregates—either fine (F) or coarse (C)—significantly affects the structural behavior of concrete beams. The influence of rubber varies depending on both the type of aggregate replaced and the replacement ratio.

For instance, replacing 10% of fine aggregate with rubber (as in specimen B3) increased the ultimate load to 116 kN, which is a 45% improvement compared to the control specimen B2 (80 kN). Similarly, B5, which included a 10% replacement of coarse aggregate, achieved 127 kN, indicating a 58.75% increase. These results suggest that moderate rubber inclusion can enhance load-bearing capacity under repeated loading conditions.

However, when the replacement ratio was increased to 20%, a reduction in performance was observed. Specimen B4, with 20% fine rubber, had an ultimate load of 108 kN, which is lower than B3. Similarly, B6, with 20% coarse rubber, recorded 120 kN, showing reduced gains compared to B5. This trend indicates that high rubber content may negatively affect strength due to reduced bond and stiffness within the concrete matrix.

In conclusion, the use of recycled rubber in concrete can improve structural performance under repeated loading when optimized at moderate replacement levels. However, excessive rubber content may lead to diminished strength, emphasizing the importance of carefully selecting the replacement ratio.

4.2.3 CFRP configuration effect

From Table 4-6 , Experimental results demonstrated that strengthening rubberized concrete beams using the Near-Surface Mounted Carbon Fiber Reinforced Polymer (NSM-CFRP) technique, whether in the form of bars or strips, significantly enhanced their structural performance under repeated loading. The specimens were divided into two groups: specimens B3 to B8 were strengthened using two CFRP bars, while specimens B9 to B14 were strengthened using CFRP strips.

In the group strengthened with bars, the beams exhibited clear improvement compared to the unstrengthen control specimen B2, which reached a maximum load of 80 kN. For example, specimen B3 (10% fine rubber + 2 bars) achieved 116 kN, B5 (10% coarse rubber) reached 127 kN, and B7 (10% fine + 10% coarse rubber) recorded the highest load in this group with 160 kN, effectively doubling the load capacity of the control.

In the strip-strengthened group, the performance was even higher in some cases. Specimen B9 reached 147 kN, B11 achieved 165 kN, and specimen B13 (with the highest combined rubber replacement) recorded the maximum load capacity of 168 kN among all tested beams. This indicates that the use of CFRP strips significantly enhanced the load-bearing capacity, even for mixes with high rubber content.

Based on these findings, the main differences between the two strengthening methods can be summarized as follows:

- CFRP strips demonstrated superior performance over bars in terms of ultimate load capacity, attributed to their higher tensile strength, elastic modulus, and greater moment of inertia, which contributed to increased stiffness under repeated loading.
- At the onset of first cracking, deflection values were lower in bar-strengthened specimens, suggesting better control of early-stage deformations. However, strip-strengthened beams showed greater enhancement in overall strength.
- Considering the percentage increase in peak load, CFRP strips yielded a more significant improvement under repeated loading, especially in specimens with higher rubber content.
- In terms of endurance and failure behaviour, strip-strengthened beams exhibited prolonged resistance and delayed failure, as reflected in their load-deflection curves. This performance suggests that CFRP strips provide better long-term durability under repeated stress compared to CFRP bars.

In conclusion, both CFRP bars and strips are effective in strengthening rubberized concrete beams. However, CFRP strips proved to deliver superior performance in terms of load capacity, stiffness, and long-term resistance, while CFRP bars were more effective in controlling initial deflections..

4.3 Stiffness of tested beams

The ability of a member to withstand applied loads that attempt to bend it is known as stiffness (Muthuswamy and Thirugnanam, 2014). The stiffness is calculated by dividing the service load, which equals 70% of the ultimate load on a deflection at the same service load (Russell, 2003).

$$\text{Stiffness (k)} = \frac{FS}{\Delta y}$$

Where:-

FS= load before plastic region in load-deflection curve

Δy= deflection at FS

Table 4-7: Stiffness of tested specimens

No.	Specimens	load before plastic region FS	Deflection Δy mm	Stiffness (k)
1	B1	65	4.8	13.54
2	B2	65	4.7	13.83
3	B3-F10-b	65	3	21.67
4	B4-F20-b	70	4	17.50
5	B5-C10-b	71	3.2	22.19
6	B6-C20-b	75	2.5	30.00
7	B7-C5F5-b	80	2.9	27.59
8	B8-C10F10-b	113	6	18.83
9	B9-F10-L	111	5.8	19.14
10	B10-F20-L	119	5.9	20.17
11	B11-C10-L	117	6	19.50
12	B12-C20-L	105	6	17.50
13	B13-F5C5-L	117	5.5	21.27
14	B14-F10C10-L	88	4.9	17.96

Different variables affect the stiffness of specimens under repeated loading. Reference specimen B1 is subjected to monotonic loading and shows a relatively high stiffness (13.54). B2 is subjected to repeated loading and shows similar stiffness with a slight decrease (13.83).

Samples B3 to B8 have an aggregate replacement with rubber and a strengthening CFRP bar. The samples show an overall improvement in stiffness compared to B2, but they vary with the rubber percentages. B3 and B4 show stiffness values of 21.67 and 17.5, while B5 and B6 show stiffness values of 22.18 and 30. Substitution in the same mixture of coarse and fine

rubber gives stiffness values between coarse and fine rubber, with B7 and B8 giving stiffness values of 27.58 and 18.83, respectively.

B9 to B14 has the same rubber ratios but with strengthening CFRP strip, showing slightly different performance, as shown in Table 4-7.

4.4 Ductility of tested beams

A material's ductility, its capacity to withstand plastic deformation under tensile strain while the load is still applied (Russell, 2003). Table 4-8 displays the ductility index of the specimens.

Ductility index= $\frac{\Delta u}{\Delta y}$

Where:

Δu: Maximum Deflection

Δy: Deflection at service load

Table 4-8: Ductility index of tested specimens

No.	Specimens	Deflection Δy mm	Maximum Deflection Δu mm	Ductility index Δu/ Δy
1	B1	4.8	29.5	6.15
2	B2	4.7	27.3	5.81
3	B3-F10-b	3	13.35	4.45
4	B4-F20-b	4	9.84	2.46
5	B5-C10-b	3.2	15.17	4.74
6	B6-C20-b	2.5	10.75	4.30
7	B7-C5F5-b	2.9	15.35	5.29
8	B8-C10F10-b	6	13.18	2.20
9	B9-F10-L	5.8	31.14	5.37
10	B10-F20-L	5.9	12.83	2.17
11	B11-C10-L	6	31.31	5.22
12	B12-C20-L	6	20.15	3.36
13	B13-F5C5-L	5.5	20.46	3.72
14	B14-F10C10-L	4.9	24.27	4.95

As shown in Table 4-8, reference specimen B1 under monotonic loading shows a Ductility Index value of 6.14, as this specimen shows the highest ductility index because it was tested under monotonic loading. High ductility index values indicate the specimen's ability to deform significantly before failure. Reference specimen B2 under repetitive loading shows a Ductility Index value of 5.81.

Specimens B3 to B8 with strengthening NSM-CFRP bar show varying values of ductility index depending on the proportion and type of aggregate replaced. B5 (10% coarse replacement) and B6 (20% fine replacement) show slight improvement compared to B3 and B4. B8 with double replacement (coarse and fine) show lower ductility values due to the double effect of rubber.

Specimens B9 to B14 strengthening with NSM-CFRP strip show relatively different ductility index values than those with CFRP bar specimens. B11 (with 10% coarse replacement) show better deformation capacity due to better stress distribution. B13 and B14 (double replacement) show slightly lower ductility index due to reduced overall stiffness.

The NSM-CFRP near-surface reinforcement enhanced the deflection ductility index value compared with the reference specimen. The CFRP bar and strip's ability to distribute stresses during the loading process allows the specimen to resist more applied stresses.

4.5 Failure modes

Understanding the failure mechanism is important because it helps evaluate the response of reinforced elements and select the best strengthening techniques. The repeated loading protocol was applied to each beam except for B1 under monotonic loading. Repeated loading

generates longitudinal compressive stress waves that propagate along the beams. Concrete peeling was found on both the top and sides of the beam around the loading location on B1 (Plate 4-3). Reference specimen B2 (Plate 4-4) exhibited cracks at 26 kN during the first ten repeated loading cycles, and during the second ten loading cycles, the number of cracks increased, and they propagated into the tension zone. During the last ten cycles, cracks from the previous cycles developed and extended from the tension zone towards the compression zone. As the load was increased to failure, the cracks developed further until failure occurred in the tension zone below the loading location. Under repeated and monotonic loading conditions, flexural was identified as the failure mode for B1 and B2.

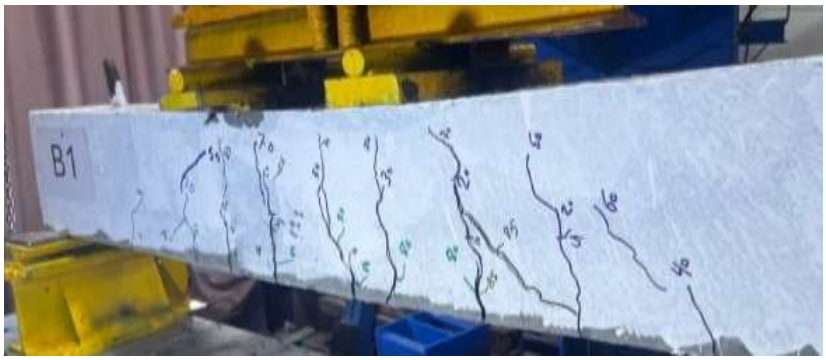

Plate 4-3: Failure mode for B1 under monotonic

Plate 4-4: Failure mode for B2 under repeated load

A smaller number of cracks appear in the samples containing 10 and 20% fine rubber B3-F10-b and B4-F0-b, but they continue to develop at every ten loading cycles. Whereas the sample B3-F10-b shows few hairline cracks at the first ten loading cycles, and then these cracks develop in the subsequent cycles, and when the load is increased to failure, the development of cracks increases, especially the crack at the tension zone under the loading point, and thus the beam reaches failure. As for sample B4-F0-b has very simple hairline cracks at the first ten cycles, and at the subsequent loading cycles, these cracks develop gradually until they reach the final failure point near the middle of the span in the tension zone. Some peeling occurs at the load application zone, as shown in Plate 4-6 and Plate 4-6.

Plate 4-5: Failure mode for B3-F10-b under repeated load

Plate 4-6: Failure mode for B4-F20-b under repeated load

In the samples containing 10 and 20% coarse rubber B5-C10-b and B6-C20-b. Whereas sample B5-C10-b did not show cracks in the first ten loading cycles, and hairline cracks started to appear in the twelfth loading cycle; then these cracks developed in the subsequent cycles, and when the load was increased to failure, the development of cracks increased, especially the crack in the tension zone under the loading point, and thus the beam reached failure near the middle of the span. As for sample B6-C20-b, very simple hairline cracks appeared in the first ten cycles, and in the subsequent loading cycles, these cracks gradually developed until they reached the final failure point near the middle of the span in the tension zone, and some peeling occurred in the load application area, as shown in Plate 4-7 and Plate 4-8.

Plate 4-7: Failure mode for B5-C10-b under repeated load

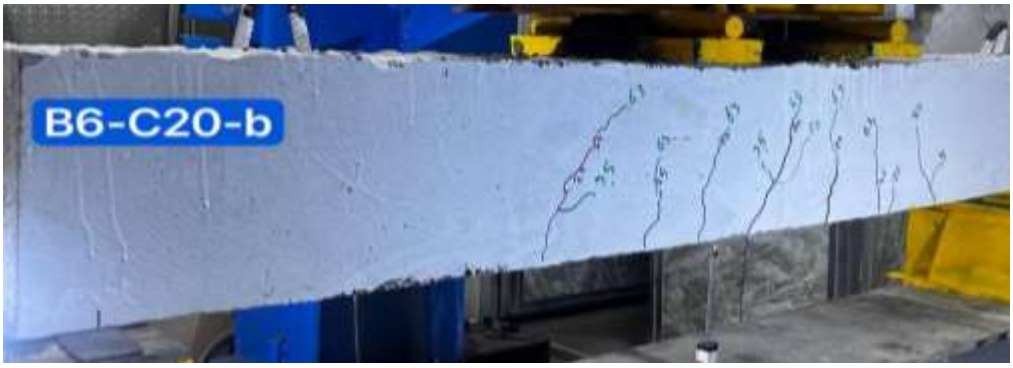

Plate 4-8: Failure mode for B6-C20-b under repeated load.

In the samples containing 10 and 20% coarse and fine rubber B7-C5F5-b and B8-C10F10-b, the crack propagation was less than in the previous samples. Whereas sample B7-C5F5-b did not show cracks in the first ten loading cycles, and hairline cracks began to appear in the twelfth loading cycle, then these cracks developed in the subsequent cycles. When the load was increased to failure, the crack development increased, especially the crack in the tension zone under the loading point. Thus, the beam reached failure near the middle of the span with peeling at the loading points in the compression zone and also in the tension zone from below during the failure of the beam. As for sample B8-C10F10-b, cracks did not appear in the first ten cycles, and very simple hairline cracks began in the twelfth cycle. In the subsequent loading cycles, these cracks gradually developed until they reached the final failure point near the middle of the span in the tension zone, and no crack appeared in the compression zone. As a result, the failure modes of B7-C5F5-b and B8-C10F10-b were flexure, as shown in Plate 4-9 and Plate 4-10.

Plate 4-9: Failure mode for B7-F5C5-b under repeated load

Plate 4-10: Failure mode for B8-F10C10-b under repeated load

The crack propagation behavior of specimens incorporating fine and coarse rubber and strengthened with NSM-CFRP strip was examined under cyclic loading. In specimens containing 10% (Plate 4-11) and 20% (Plate 4-12) fine rubber (B9-F10-L and B10-F20-L), crack initiation was delayed, with no visible cracks in the first ten loading cycles. Hairline cracks began to appear at the twelfth cycle and progressively developed in subsequent cycles. Upon reaching failure, cracks intensified near the mid-span of the beam, predominantly in the tension region, with no cracks observed in the compression zone. Both specimens exhibited a flexural failure mode. Similarly, specimens incorporating 10% and 20% coarse rubber (B11-C10-L and B12-C20-L) showed no cracks within the first ten cycles, with minor hairline cracks emerging at the twelfth cycle and gradually propagating until failure. The failure occurred near the mid-span in the tension zone, accompanied by minor peeling at the loading area. The failure mode of these specimens was also classified as flexural (see Plate 4-13 and Plate 4-14). Furthermore, crack propagation followed a similar trend in specimens containing fine and coarse rubber in the same mixture at 10%

and 20% replacement levels (B13-F5C5-L and B14-F10C10-L). No cracks appeared in the first ten cycles, while hairline cracks initiated in the twelfth cycle and expanded progressively. The failure of B13-F5C5-L (Plate 4-15) occurred in the tension zone near the loading point, with some peeling observed, whereas B14-F10C10-L (Plate 4-16) failed near the mid-span in the tension zone. The failure mode for these specimens was identified as bending. Overall, the results indicate that including rubber aggregates, whether fine, coarse or a combination of both, affects crack propagation patterns, delaying crack initiation and influencing failure characteristics, with all specimens exhibiting Similar to previous models.

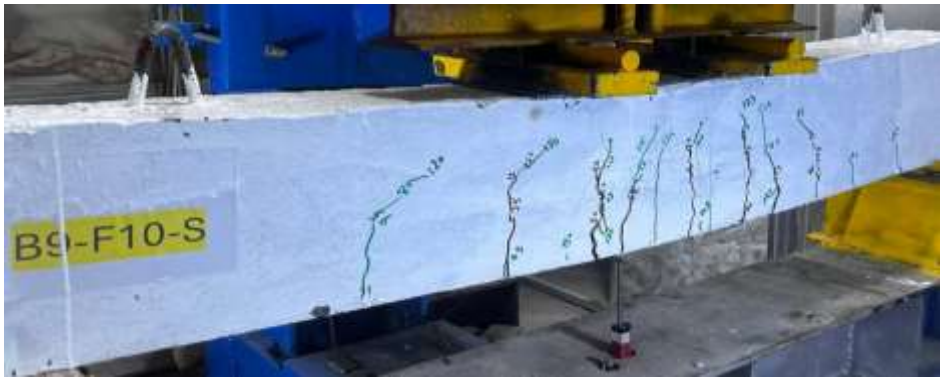

Plate 4-11: Failure mode for B9-F10-S under repeated load.

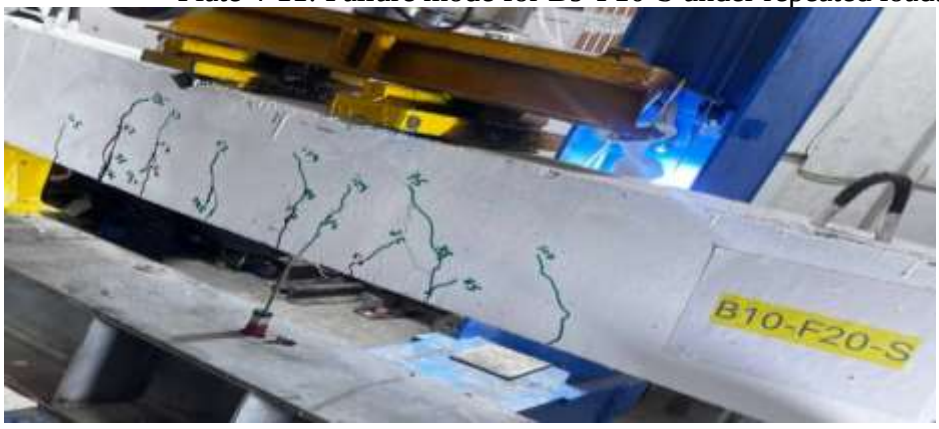

Plate 4-12: Failure mode for B10-F20-S under repeated load.

Plate 4-13: Failure mode for B11-C10-S under repeated load

Plate 4-14: Failure mode for B12-C20-S under repeated load

Plate 4-15: Failure mode for B13-F5C5-S under repeated load

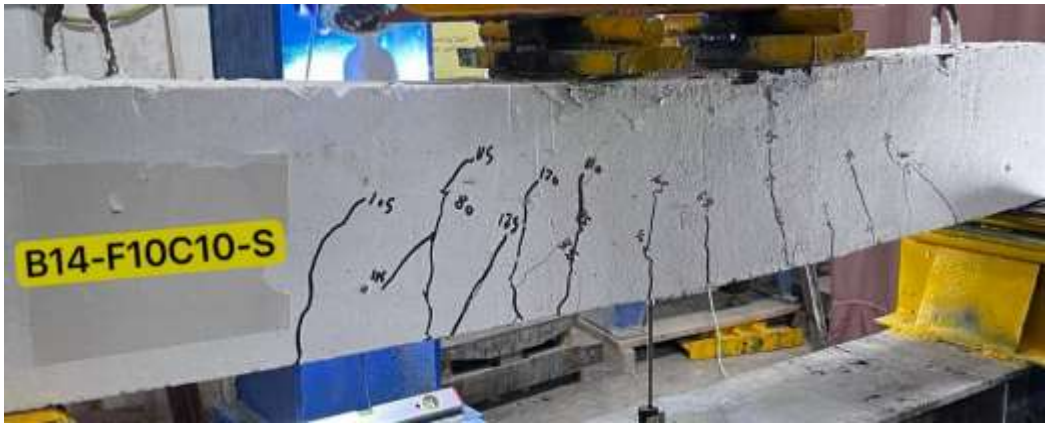

Plate 4-16: Failure mode for B14-F10C10-S under repeated load

Chapter Five: Finite Elements Analysis

5.1 Introduction

The finite element analysis process divides complicated issues or domains into discrete, straightforward parts or finite elements, whose behavior may be explained by simpler equations using approximation techniques. It was developed to examine a range of engineering issues in several domains, such as civil and mechanical engineering.

This study included numerical modeling for rubberized concrete beams with the near-surface strengthening system and varying replacement ratios of coarse and fine aggregates.

For this aim, rubberized concrete beams under repeated load were examined using ABAQUS software version 2021. Therefore, this chapter's goal is to offer practical guidelines that are represented on rubberized reinforced concrete beams using various variables, including the strengthening system and concrete characteristics. Additionally, the experimental and numerical results were compared. Other parameters' structural behavior on rubberized beams was examined by the model that was adopted using the finite element approach.

5.2 Finite element modeling

The finite element modeling of the rubberized concrete beams used the same physical properties, loading conditions, and boundary constraints as those used in the experimental study. The beams had the same shape and length. The modeling process consisted of six distinct components, each contributing to the representation of the fourteen rubberized concrete beams. These components included the part beam, reinforcement bar, plate load,

stirrups, plate at support, plate load, epoxy, and CFRP bar&strip (Figure 5-1, Figure 5-2, Figure 5-3). Each component was carefully specified individually and subsequently combined to construct the overall specimen model.

5.2.1 Geometry

The study analyzes rubberized concrete beams using 3D nonlinear finite element analysis. The beams have spans and dimensions similar to concrete beams.

Table 5-1: Finite element types for rubberized concrete beam model

No	Part	Types of Elements
1	beam	C3D8R
2	reinforcement	T3D2
3	Stirrups	T3D2
4	plate at support	C3D8R
5	plate load	C3D8R
6	CFRB plate	S4R
7	CFRB bar	T3D2
8	epoxy	C3D8R

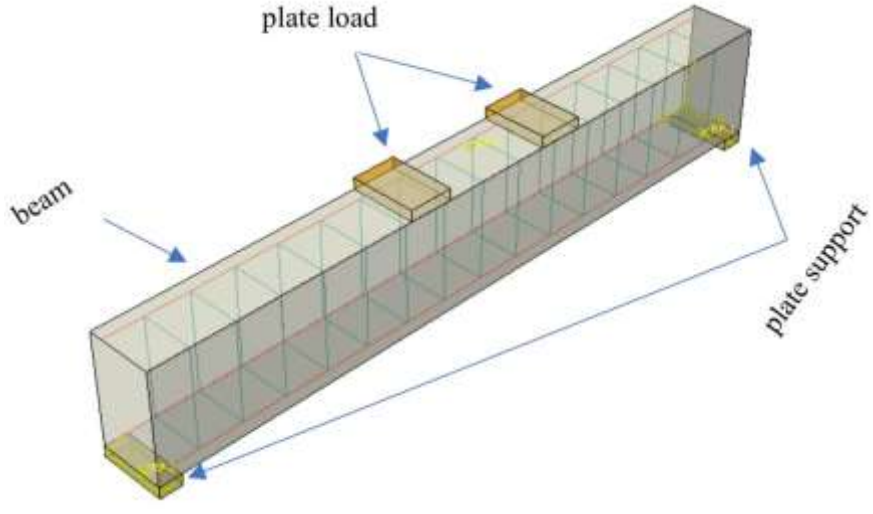

Figure 5-1: Geometry of the Numerical Model.

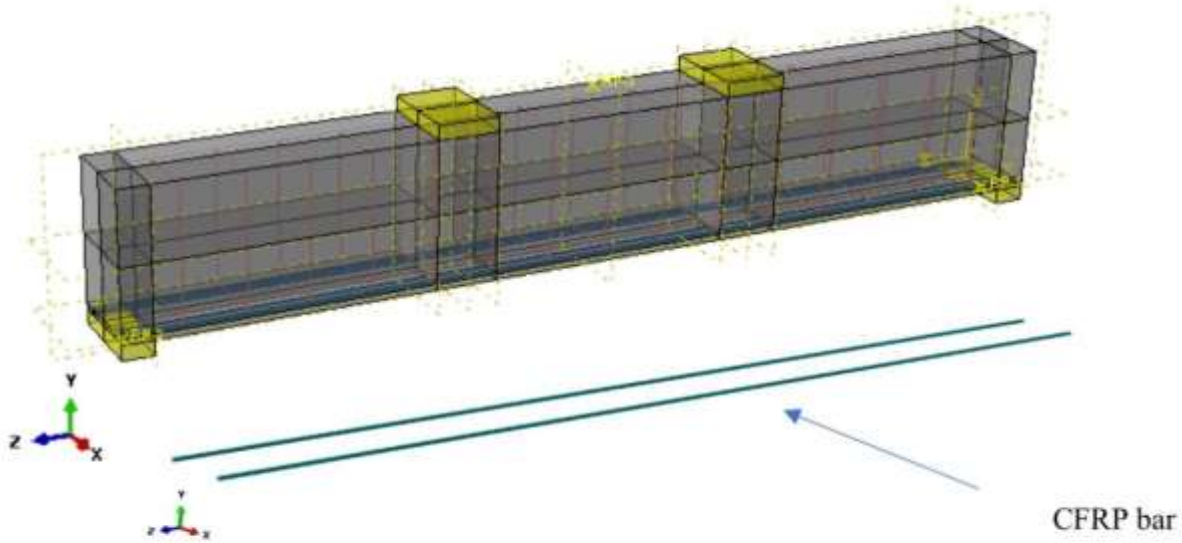

Figure 5-2: Geometry of the beam contain CFRP bar.

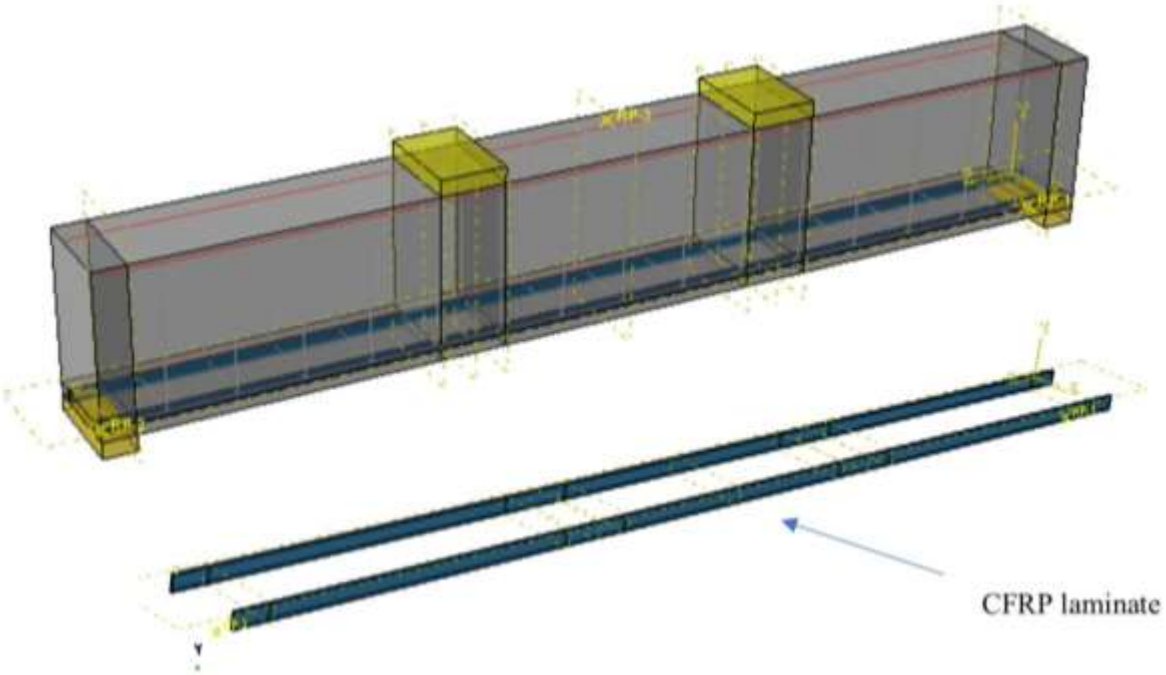

Figure 5-3: Geometry of the beam contain CFRP strip.

5.2.1.1 Types of elements

C3D8R, this element refers to an 8-node 3D continuum element used for modeling solid structures in finite element analysis.

- C: Indicates a continuum (solid) element.
- 3D: Specifies that the element is three-dimensional.
- 8: Denotes the number of nodes (8-node hexahedral element).
- R: Stands for "Reduced Integration," which improves computational efficiency and reduces locking effects in near-incompressible materials.

It is particularly suitable for modeling solid structures with large deformation or complex geometries.

T3D2, this element is a 2-node truss element used for modeling one-dimensional structures subjected to axial loads.

- T: Indicates a truss element.
- 3D: Specifies that the element operates in three-dimensional space.
- 2: Denotes the number of nodes (2-node linear truss element).

It is commonly used in structures like cables, wires, and struts, where axial force is the dominant load.

S4R, this element represents a 4-node shell element designed for analyzing thin-walled structures.

- S: Indicates a shell element.
- 4: Denotes the number of nodes (4-node quadrilateral element).
- R: Refers to "Reduced Integration," which enhances computational efficiency.

This element is ideal for simulating thin plates, shells, and structures where bending is significant.

5.2.2 Modeling of the material

It is important that the material modelling approach you choose can track how the material's inelastic flow develops and spreads until it fails. It is also important that the material's behaviour be clearly understood. This section includes the finite element modelling and thoroughly details the stress-strain curves of the two main components. Included in the modelling of the material properties of the concrete are the rubber particles.

5.2.2.1 Concrete material modeling

Concrete Damaged Plasticity (CDP), initially predicted by Lubiner et al. (1989), is the most famous ABAQUS material model for concrete. Following that, the model was revised by (Jeeho Lee and Gregory L. Fenves, 1998). The concrete damage plasticity (CDP) model was used to introduce concrete behaviour for both normal and rubberised concrete due to its ability to forecast concrete behaviour up to failure. Figure 5-4 shows that CDP follows the two main failure criteria of compressive crushing and tension stiffening, which form the basis of the continuous plasticity damage theory. Two primary metrics that can be utilised to characterise yield surface hardening are compressive and tensile stresses.

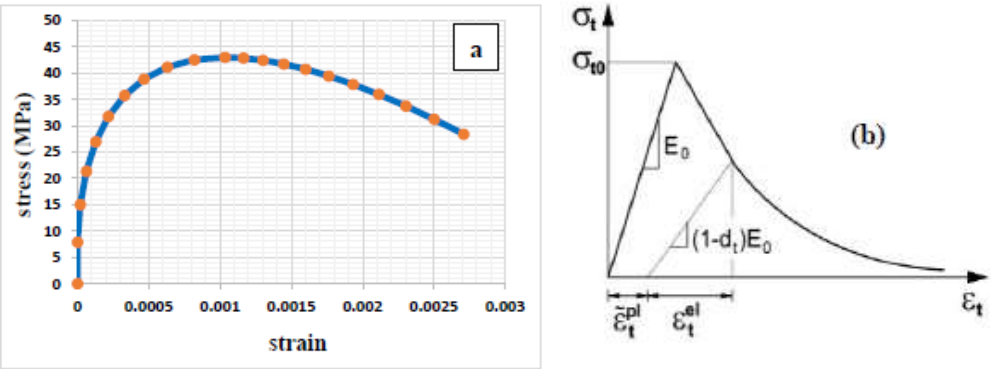

Figure 5-4: Stress-strain relation of concrete: a- compression b- tension.

There were two steps to accomplish concrete modelling in CDP. Step one involved determining the elastic modulus and Poisson's ratio. In the second step, the nonlinear portion of the stress-strain curve for the concrete was defined using the damage plasticity model.

Concrete damage plasticity was one of the coefficients included in the ABAQUS software suite. Typically, the dilation angle (ψ) should be utilised at the maximum value when dealing with ductile concrete. Zero is the minimum, and 56.3 is the maximum value of the angle. In this investigation, a 30° angle was used. This figure was chosen in accordance with models based on repeated trials.

The flow potential eccentricity (Δ), which was set to 0.1, is another component of the CDP model that needs to be properly calculated. Then there's the (fb0/fc0) ratio, which is 1.16 ABAQUS by default and is the ratio of the initial uniaxial compressive yield stress to the first equibiaxial compressive yield stress. Furthermore, the ratio of the second stress invariant in the tensile meridian to the compressive meridian is defined for any initial yield pressure value. Approximately (0.5 to1) in length, it was developed to characterise the multi-axial behaviour of concrete. The value of 2/3 is the default in ABAQUS. Lastly, the viscosity parameter (μ) was used at 0.001 when compared to a low characteristic time increment. The factors utilized in determining the damaged plasticity of both regular and rubberized concrete are displayed in Table 5-2.

Table 5-2: Concrete damage plasticity parameters

	Ψ (Dilation angle)	∈(Eccentricity)	fbo / fco	K	M (viscosity parameter)
1	30	0.1	1.16	2/3	0.001

5.2.2.2 Steel reinforcement material modeling

The numerical model assumes that the steel acts in an elastoplastic manner. Reinforced steel has a Young's module of 200,000 MPa and a Poisson ratio of 0.3. The model used by the finite element method assumes these numbers (Table 5-3).

Table 5-3: Steel properties used in FEA modeling.

Property	Value		Unit
	Ø 8	Ø 12	
Density	7.8*E-9	7.8*E-9	Ton/mm^3
E	200000	200000	N/mm^2
Fty	411	480	N/mm^2
Ftu	640	634	N/mm^2

5.2.2.3 CFRP material modeling

In order to find the elastic moduli, one-way shear moduli, and Poisson's ratio for reinforcing rubber beams, the bar and strip model must be used to establish the linear elastic response of CFRP. Since no failure of CFRP has been observed in the experimental work, its inelastic behaviour remains undefined. Table 5-4 lists the CFRP values found in the elastic behaviour.

Table 5-4: The CFRP bar and strip material properties used in the model.

Property bar	Value	Property strip	Value
Density	1.7*E-9 Ton/mm3		
Young’s modulus	145000 N/mm2	Young’s modulus	200000 N/mm2
Poisson ratio	0.3	Poisson ratio	0.3
Yield stress	2200	Yield stress	2500

5.2.2.4 Epoxy material modeling

Epoxy was defined to BAQUS as a high resistance material, and data was entered based on information provided by the company. The parameters utilized in the concrete damage plasticity test for epoxy are displayed in Table 5-5.

Table 5-5: Concrete damage plasticity parameters

	Ψ (Dilation angle)	∈(Eccentricity)	fbo / fco	K	μ(viscosity parameter)
1	30	0.1	1.16	2/3	0.001

5.2.2.5 Load and support modeling

The boundary condition and load cell base were represented by the plate material, which is modelled as a linear elastic isotropic material. Table 5-6 lists the values of the steel plates as defined in the elastic behaviour.

Table 5-6: The model's use of the material properties of steel plates

Property	Value
Density	7.8*E-9
Young’s modulus	200000
Poisson ratio	0.3
Yield stress	640
Plastic strain	0.0023

5.2.3 Convergence study

The selection of the appropriate mesh size is of paramount importance in finite element modeling. A comprehensive preliminary analysis, considering several mesh densities, was performed to determine the optimum density to achieve the desired accuracy level. Successful convergence of the

results occurs when the beam is appropriately divided into a sufficient number of distinct elements. This phenomenon becomes evident in cases where reducing the mesh size has only a modest effect on the resulting data. To achieve this goal, convergence analysis was performed as a key component of the ongoing finite element analysis (FEA) to determine the most appropriate mesh size. The present investigation entailed deliberately selecting the discrete element dimensions for the B1 model, namely 40, 35, 30, and 25 mm, as visually shown in Figure 5-6.

Moreover, comparing the obtained values with the experimental data (Figure 5-5) for the control beam may show a noticeable improvement in the precision of deflection measurements. As a result, an ax mesh size of 30 mm was chosen for all the beams that underwent testing.

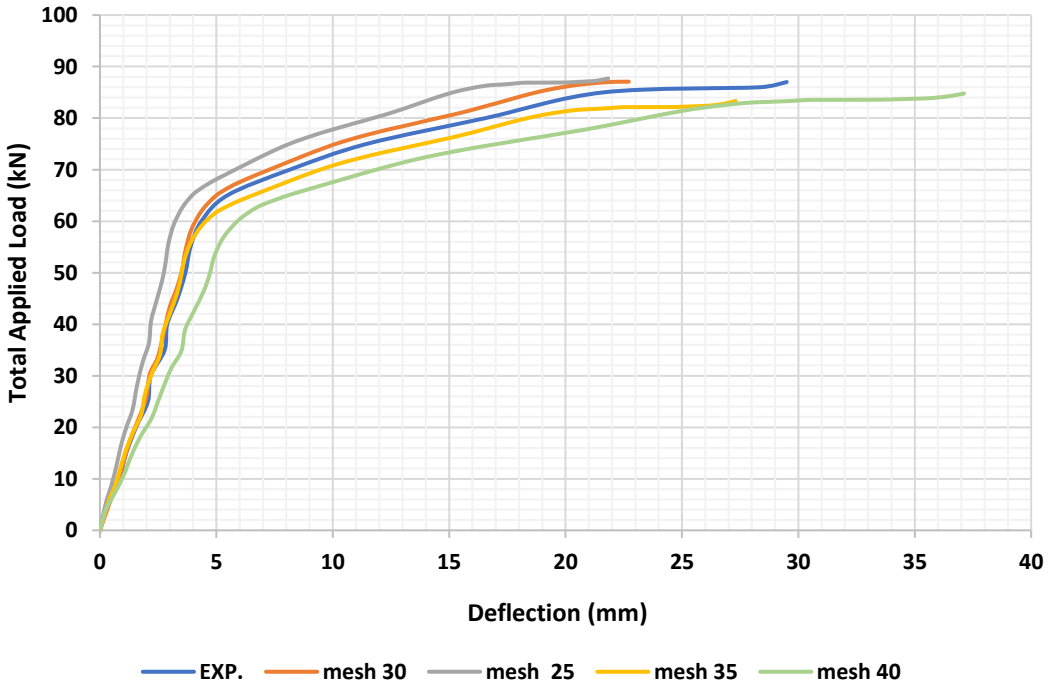

Figure 5-5: Mesh Size effect on mid-span load-deflection curve.

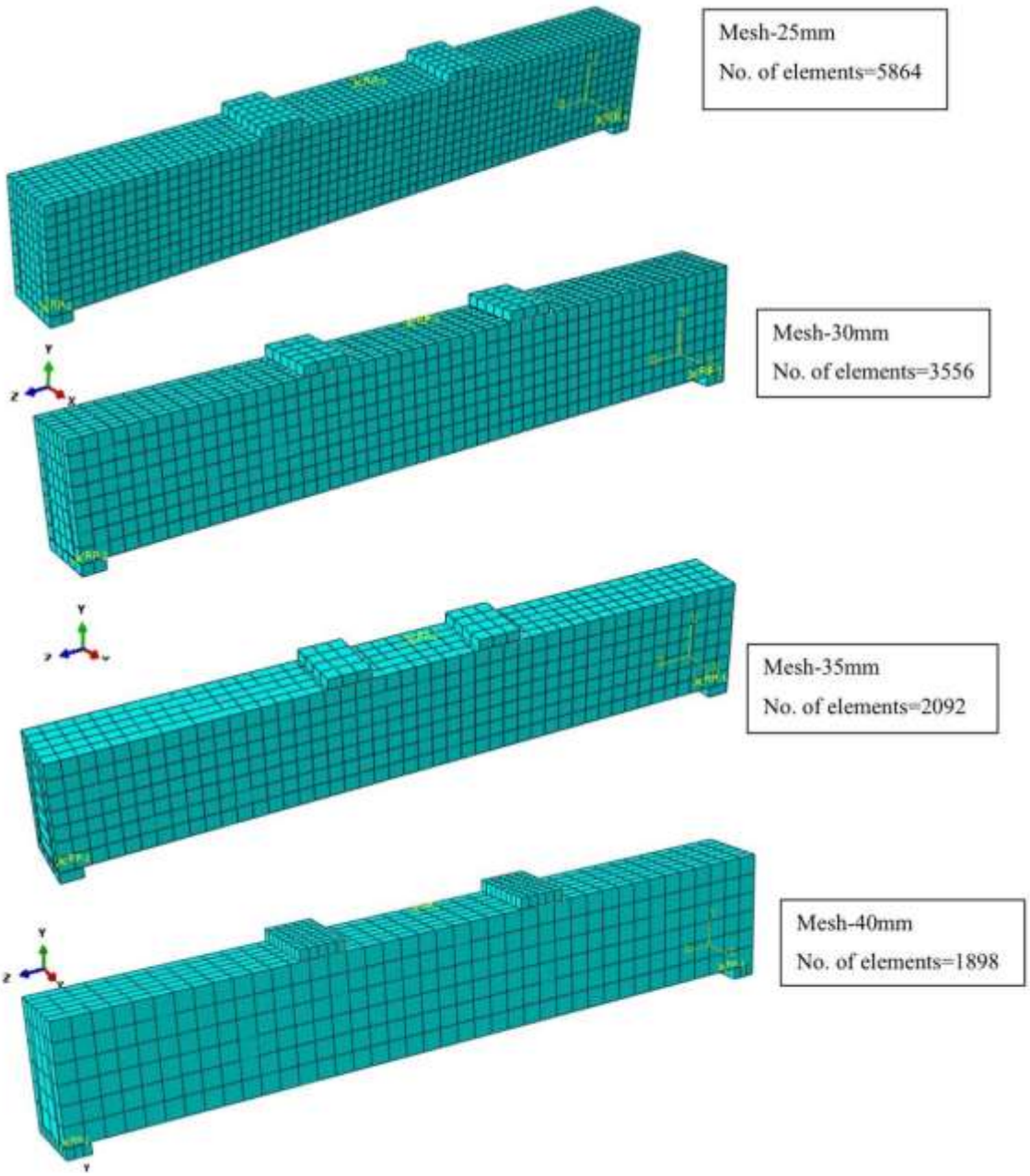

Figure 5-6: Finite element mesh density.

5.2.4 Interaction between different elements

After the assembly process, several components are assembled together, such as concrete beams, steel reinforcement, bearing plates, support plates, CFRP, and epoxy. The relationships between them are facilitated by

using several types of constraints consistent with experimental observations to build a coherent composite system (Table 5-7).

Table 5-7: Finite element interactions for beam model.

No	Part	Type of interaction	Master	Slave
1	Concrete beam and reinforcement	Embedded region	Reinforcement	concrete
2	CFRP plate and epoxy	Embedded region	CFRP plate	epoxy
3	CFRP bar and epoxy	Embedded region	CFRP bar	epoxy
4	Top surface-plate load and point load	Coupling	Top surface-plate load	point load
5	Bottom surface-plate support and point BC	Coupling	Bottom surface-plate BC	point BC

The interaction between the concrete beam and the longitudinal and transverse reinforcement components (Figure 5-7) uses the embedded zone approach, allowing for a detailed representation of the interlocking behavior and load transfer mechanisms. The interaction between the CFRP bar or strip and the epoxy is represented by the embedded zone approach, also allowing for a detailed representation of the interlocking behavior and load transfer mechanisms. The interaction between the point load and the top surface of the load plate is characterized by a "coupling" interaction, accurately simulating the mechanical bonding of the load transfer on the surfaces of the load plate. The interaction between the bottom surface plate BC and the point BC is also achieved by a "coupling" interaction so that the support is transferred evenly on the surface of the plate.

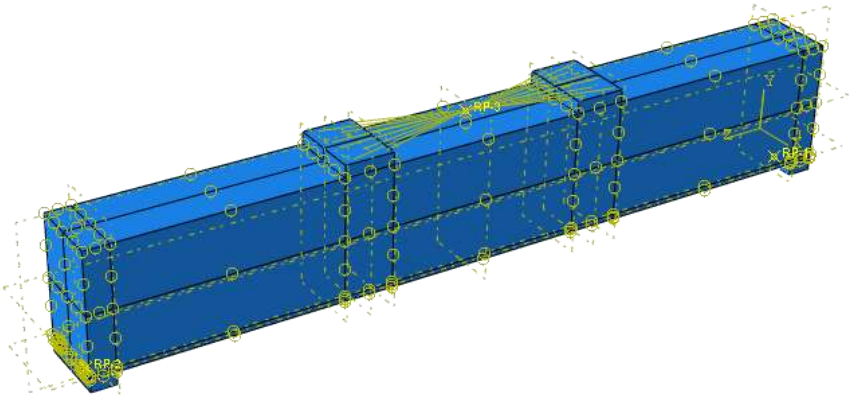

Figure 5-7: Interactions for beam model.

5.2.5 Loading and boundary conditions

Loads were applied to each tested beam at the loading point in the experimental work. The loading point distributes the loads to the two steel plates that perform these loads. The loading plates with dimensions of 100 × 25 × 150 mm, located on the upper face to transfer the loads to the tested beam. The displacements at the boundaries were used to constrain all the reinforced concrete specimens to obtain the appropriate solution. All specimens were constrained in the z-direction and y-direction (Uz=Uy=Ux=0) at the hinge support while they were constrained in the y-direction and x-direction (Uy=Ux=0) at the roller support, as shown in Figure 5-8.

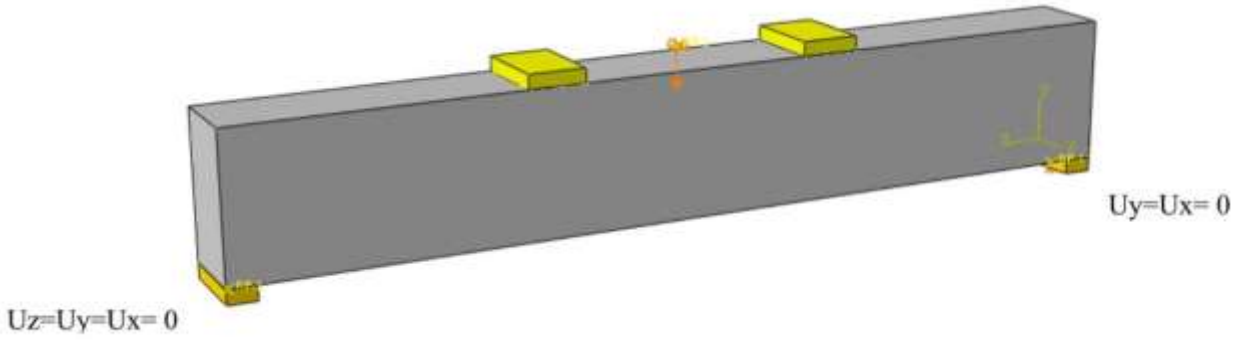

Figure 5-8: Boundary conditions that used in test of models.

5.3 Numerical results

This study compared the ultimate load values and deflections determined by finite-element analysis with experimental test results (Table

5-8). This comparative investigation aimed to confirm that the numerical model was accurate.

Table 5-8: Comparison of the ultimate load and ultimate deflection for beams.

Sample	Ultimate load Pu (kN)			Ultimate deflection (mm)		
	Exp.	Num.	Difference* %	Exp.	Num.	Difference* %
B1	87	88.91	2.20	29.5	27.71	-6.07
B2	80	85.21	6.51	14.55	12.3	-15.46
B4	108	126.71	17.32	9.84	15.99	62.50
B14	148	152.13	2.79	24.27	20.13	-17.06

*Difference = $\frac{Num-Exp.}{Exp.}$*100%

5.4 Comparison between experimental and finite element results

The finite element analysis results from ABAQUS software were compared with experimental beams' ultimate load, ultimate deflection, load-deflection curve, and failure pattern for various samples.

5.4.1 Control beam under monotonic load (B1)

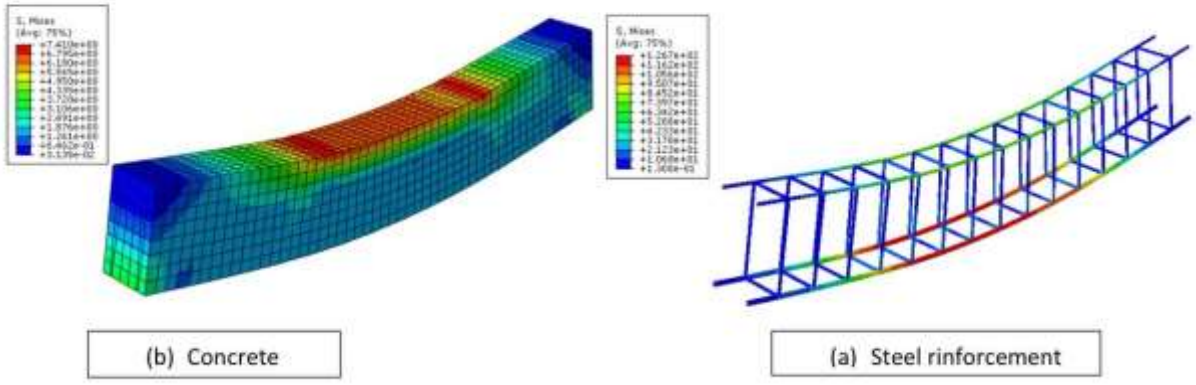

Figure 5-9: Distribution of von mises stresses of B1.

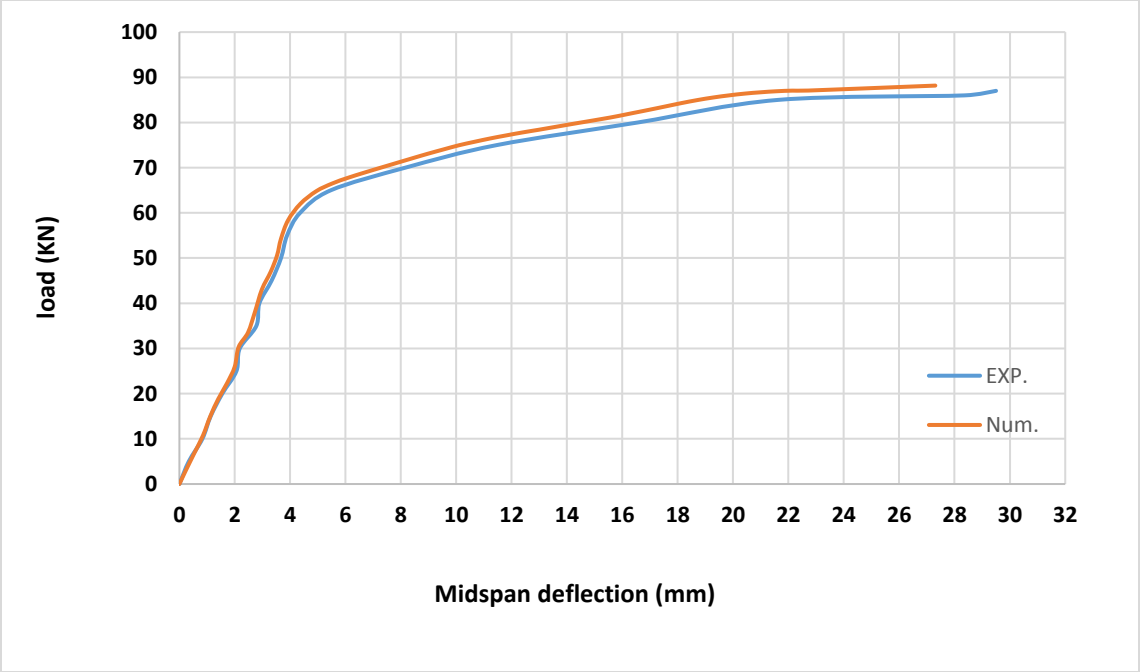

Figure 5-10: Load-Deflection Curves for beam B1.

5.4.2 Control beam under repeted load (B2)

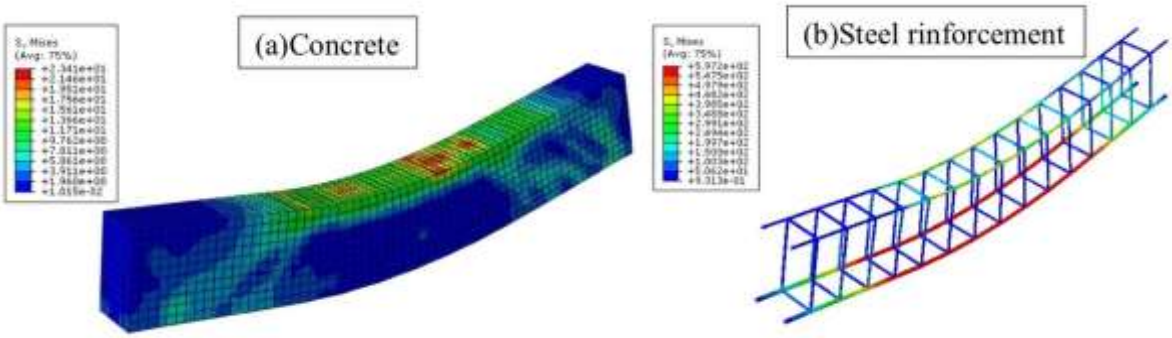

Figure 5-11: Distribution of von mises stresses of beam B2.

a)

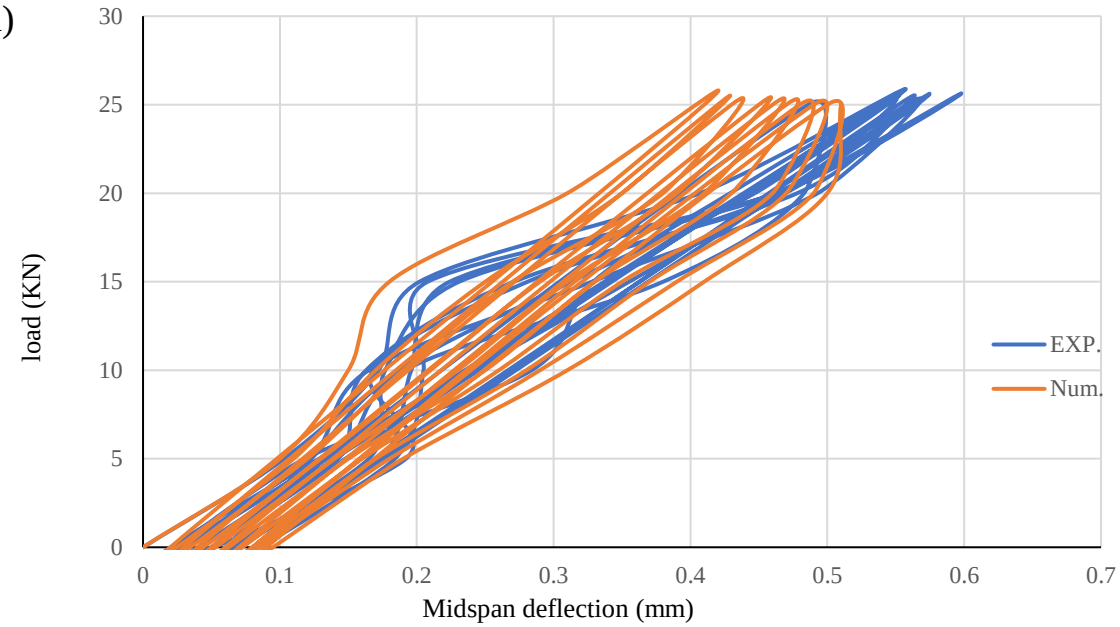
load (KN)
Midspan deflection (mm)
EXP.
Num.
0
5
10
15
20
25
30
0
0.1
0.2
0.3
0.4
0.5
0.6
0.7

b)

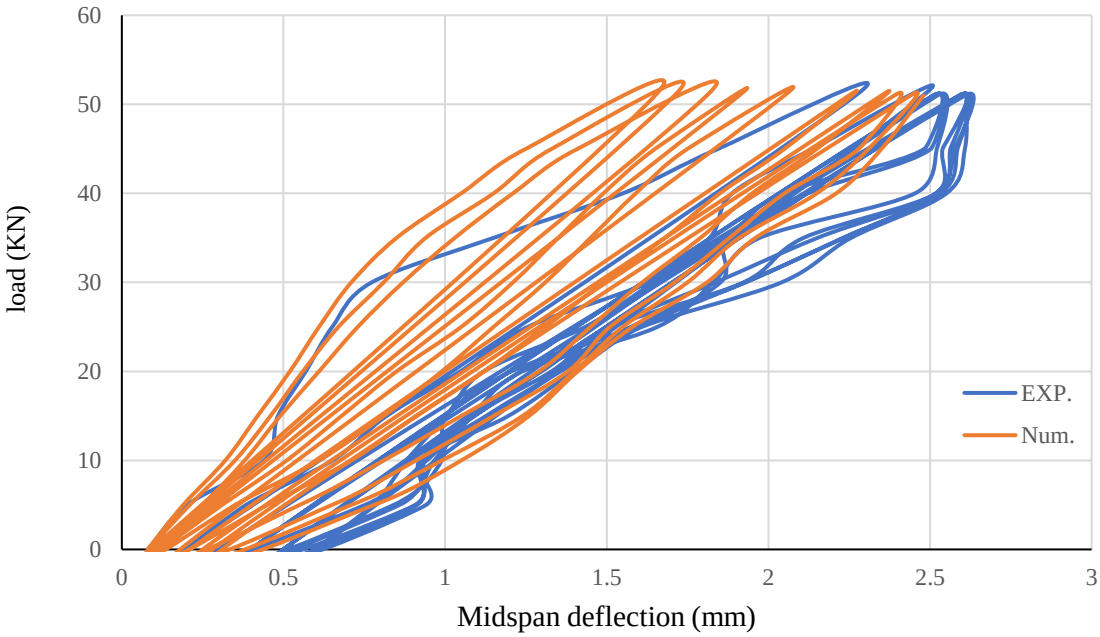
load (KN)
Midspan deflection (mm)
EXP.
Num.
0
10
20
30
40
50
60
0
0.5
1
1.5
2
2.5
3

c)

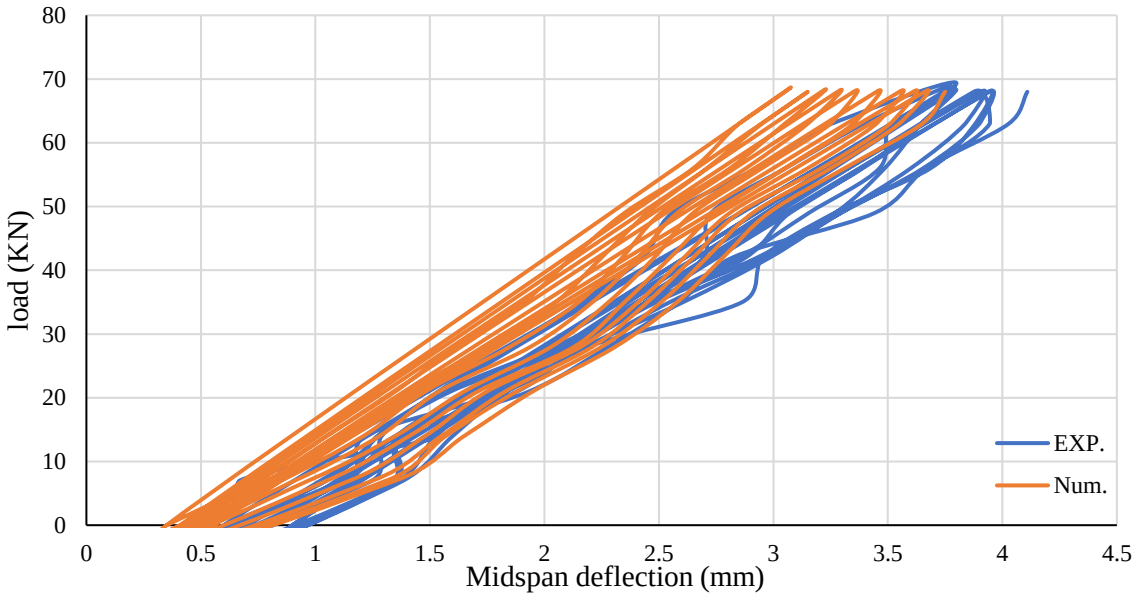

d)

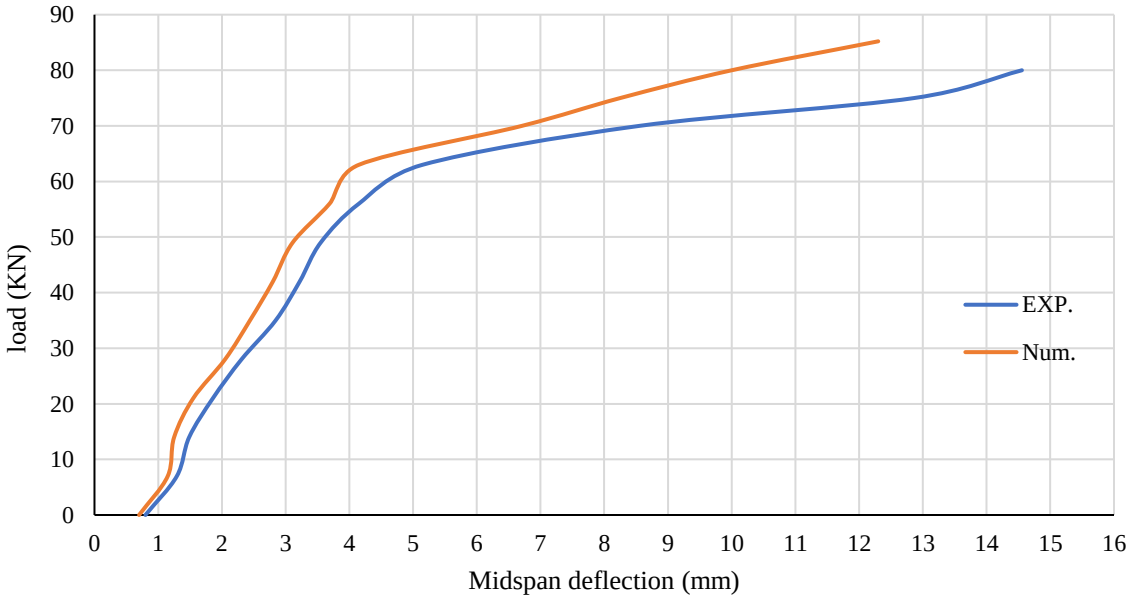

Figure 5-12: Load-Deflection Curves for beam B2 a) first 10 cycles from repeated load. B) second 10 cycles from repeated load c) third 10 cycles from repeated load d) up to failure load

5.4.3 Beam (B4F10b)

This beam have replacement 10% of fine aggregate with rubber and sterenthining CFRP bar under repeated load .

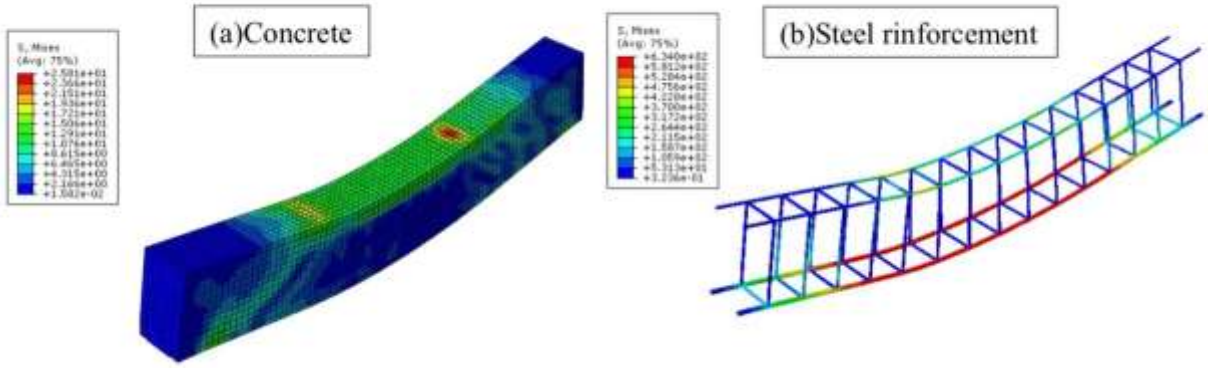

Figure 5-13: Distribution of von mises stresses of beam B2.

a)

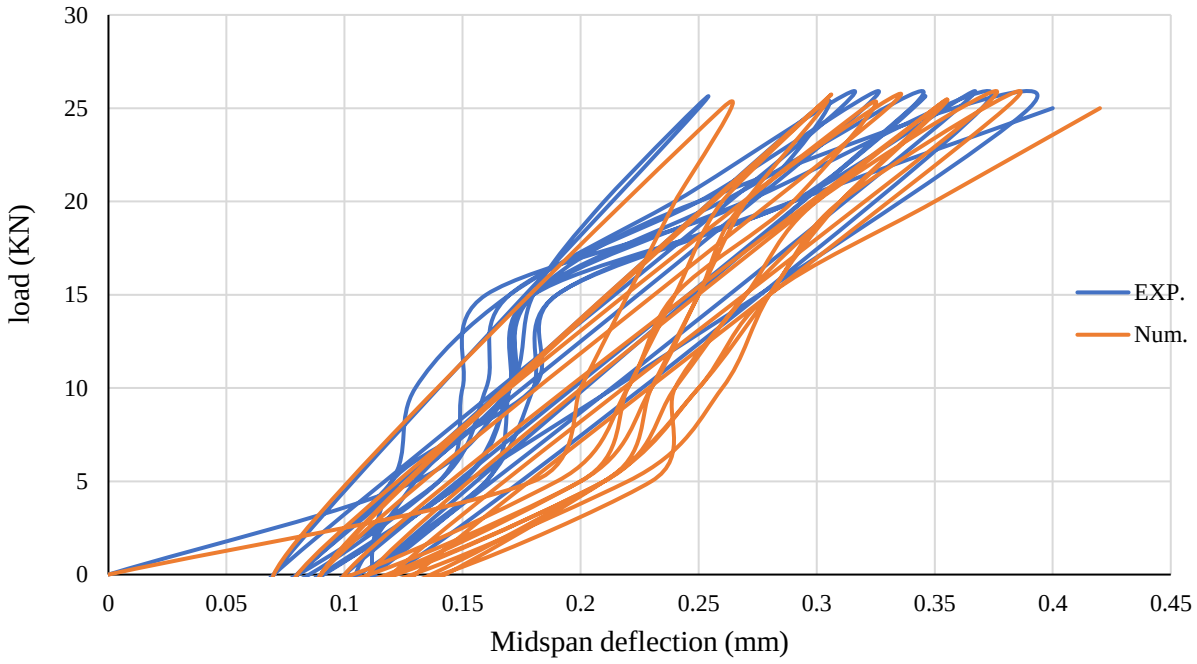

b)

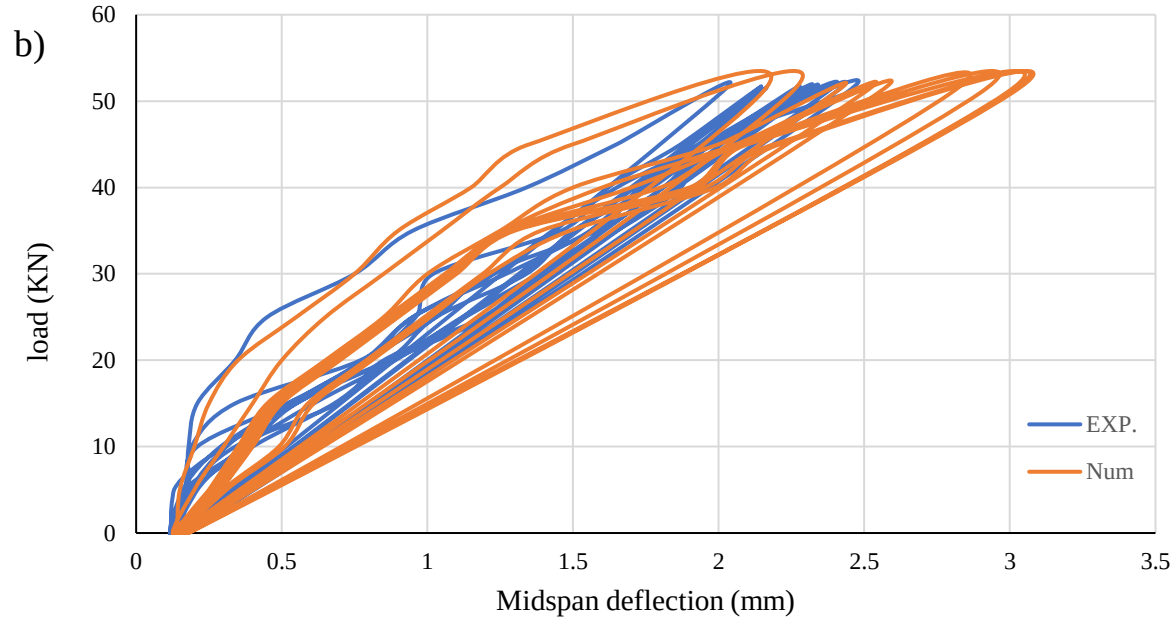
load (KN)
Midspan deflection (mm)
EXP.
Num
0
10
20
30
40
50
60
0
0.5
1
1.5
2
2.5
3
3.5

c)

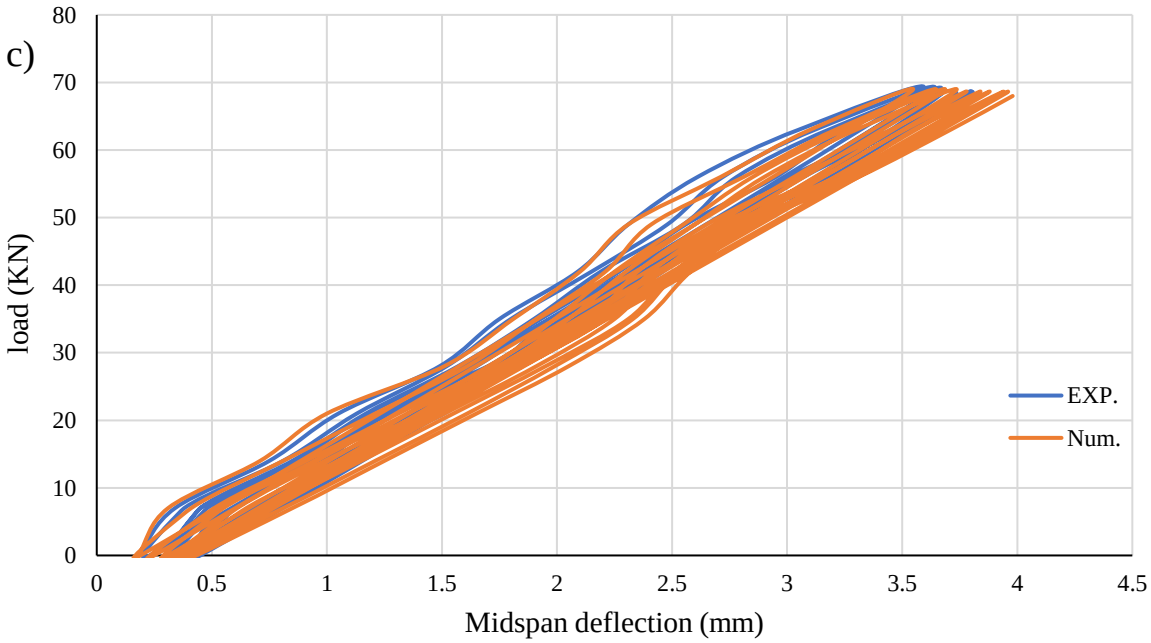
load (KN)
Midspan deflection (mm)
EXP.
Num.
0
10
20
30
40
50
60
70
80
0
0.5
1
1.5
2
2.5
3
3.5
4
4.5

d)

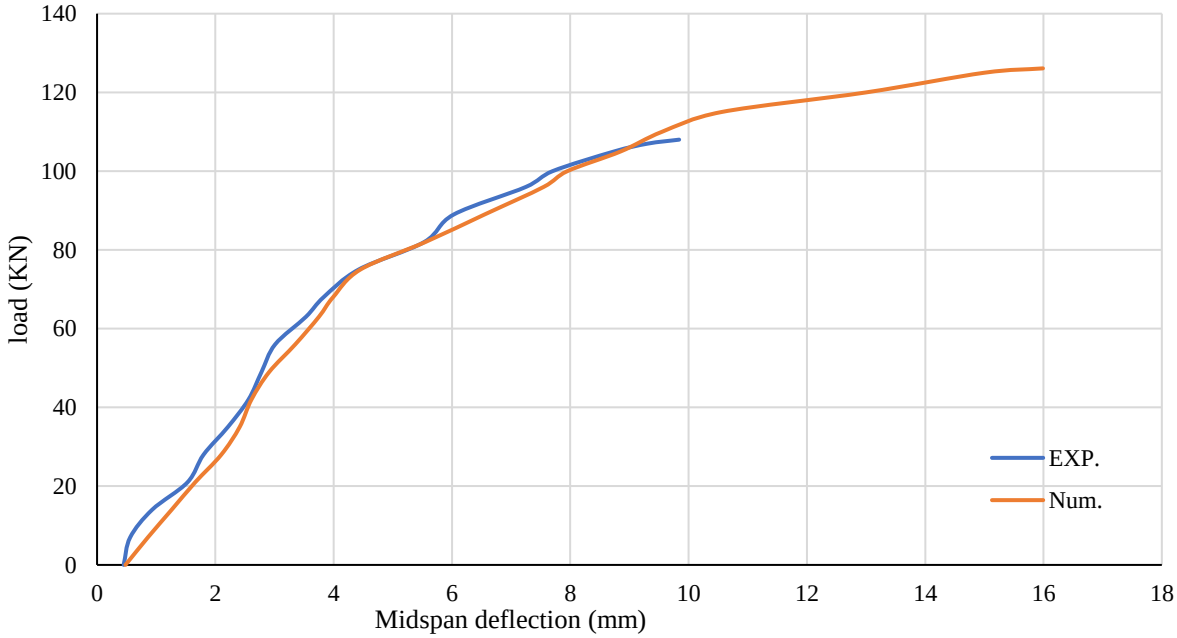

Figure 5-14: Load-Deflection Curves for beam B4F10b a) first 10 cycles from repeated load . b) second 10 cycles from 10 cycles from repeated load c) third 10 cycles from repeated load. d) up to failure load

5.4.4 Beam (B14F10C10L)

This beam have replacement 20% of fine and coarse aggregate with rubber and strengthening CFRP strip under repeated load.

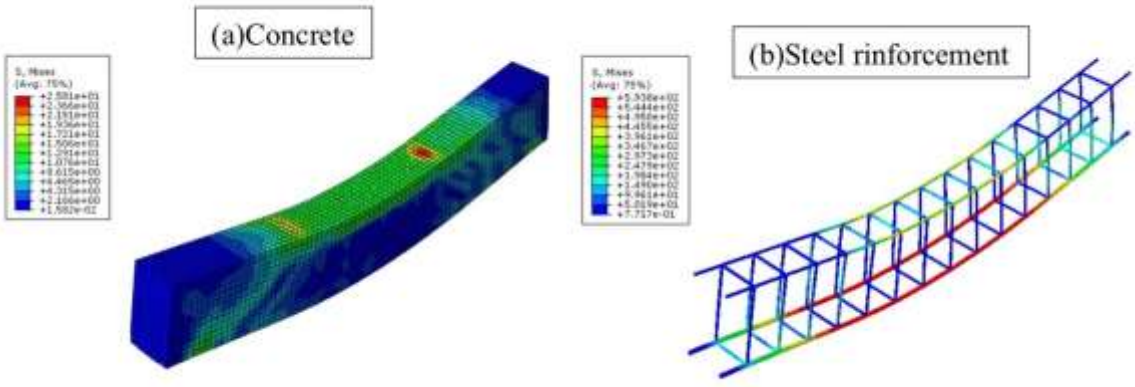

Figure 5-15: Distribution of von mises stresses of beam B14F10C10L.

a)

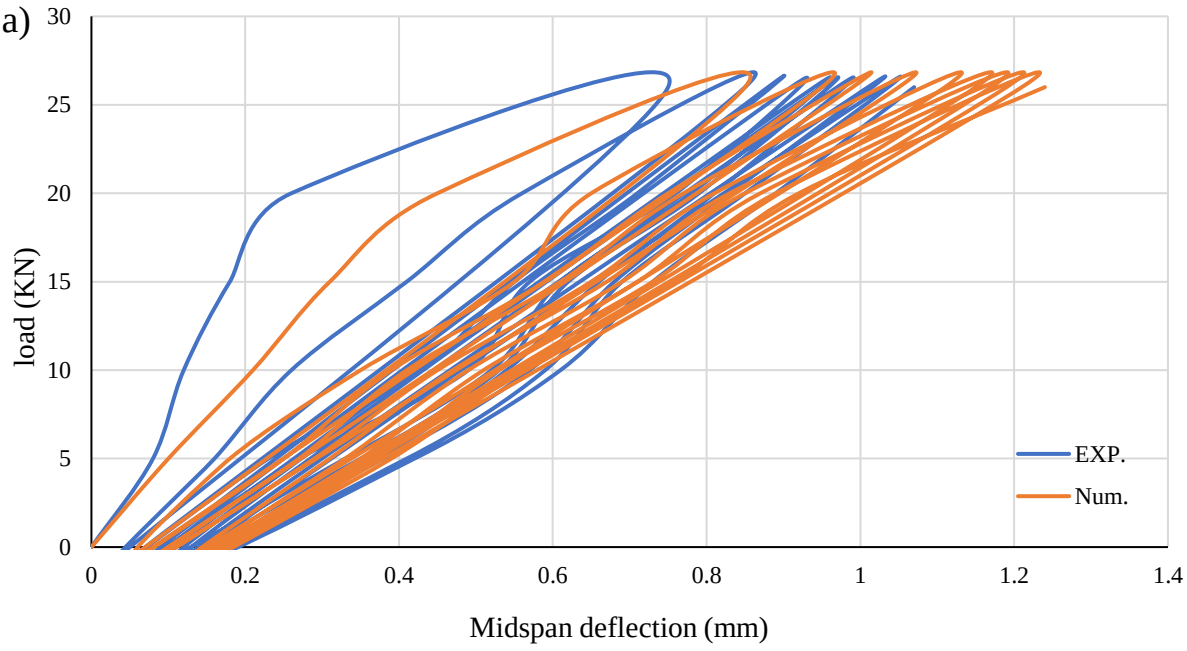
load (KN)
30
25
20
15
10
5
0
0
0.2
0.4
0.6
0.8
1
1.2
1.4
Midspan deflection (mm)
EXP.
Num.

b)

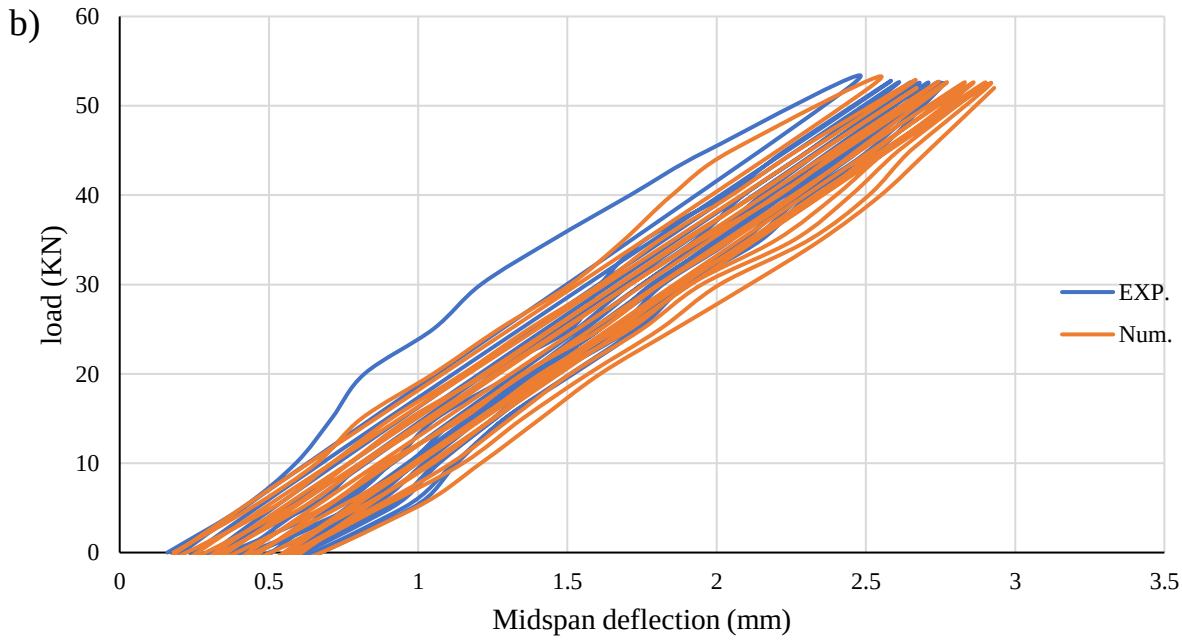
load (KN)
60
50
40
30
20
10
0
0
0.5
1
1.5
2
2.5
3
3.5
Midspan deflection (mm)
EXP.
Num.

c)

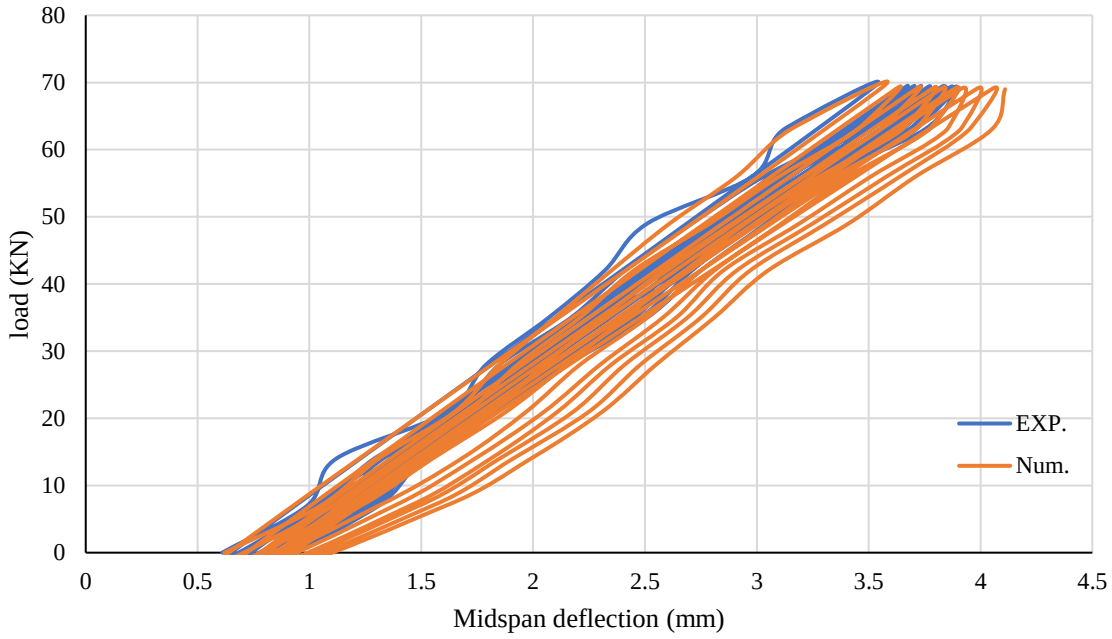

d)

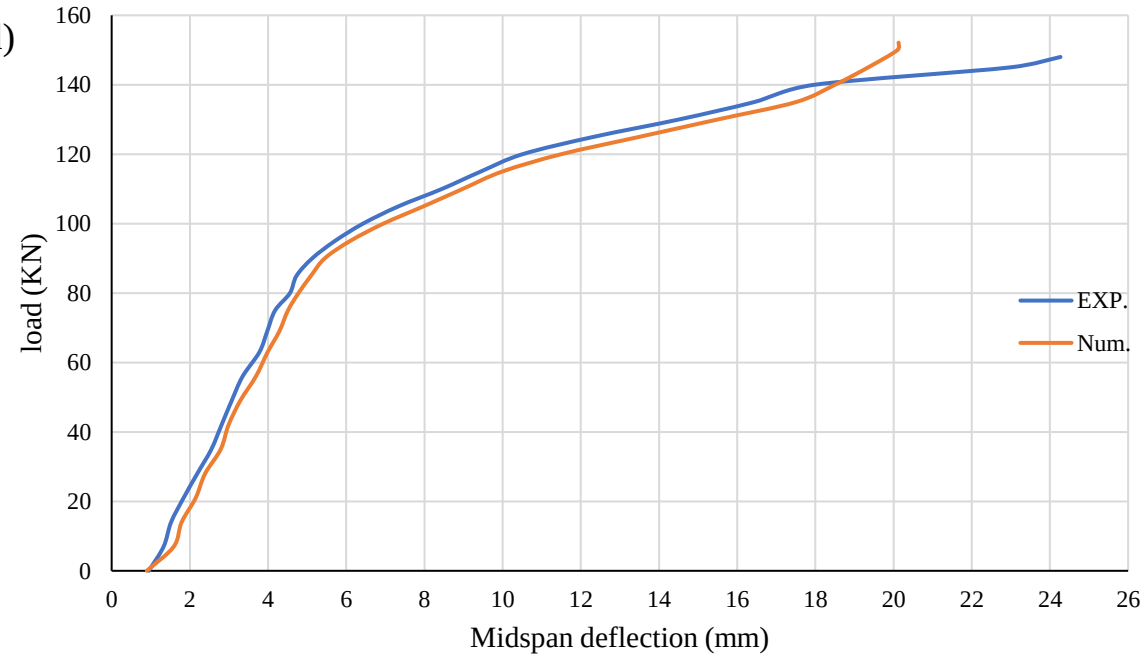

Figure 5-16: Load-Deflection Curves for beam B14F10C10L a) first 10 cycles from repeated load . b) second 10 cycles from 10 cycles from repeated load c) third 10 cycles from repeated load . d) up to failure load.

5.5 Parametric study

The primary goal of the parametric study is to cover research objectives with much more detailed information while also examining the effects of certain parameters, such as geometric changes in structure, and parameters that are not examined in laboratory tests for real members but would have a significant impact on the structural behavior. The following parameters were examined in this study:

1. Diameter of CFRP bar
2. Thickness of CFRP strip
3. Number of CFRP bars

5.5.1 Effect of diameter of CFRP bar

The diameter of the CFRP bar was taken as 8 mm, and the model was analyzed while keeping the rest of the variables constant.

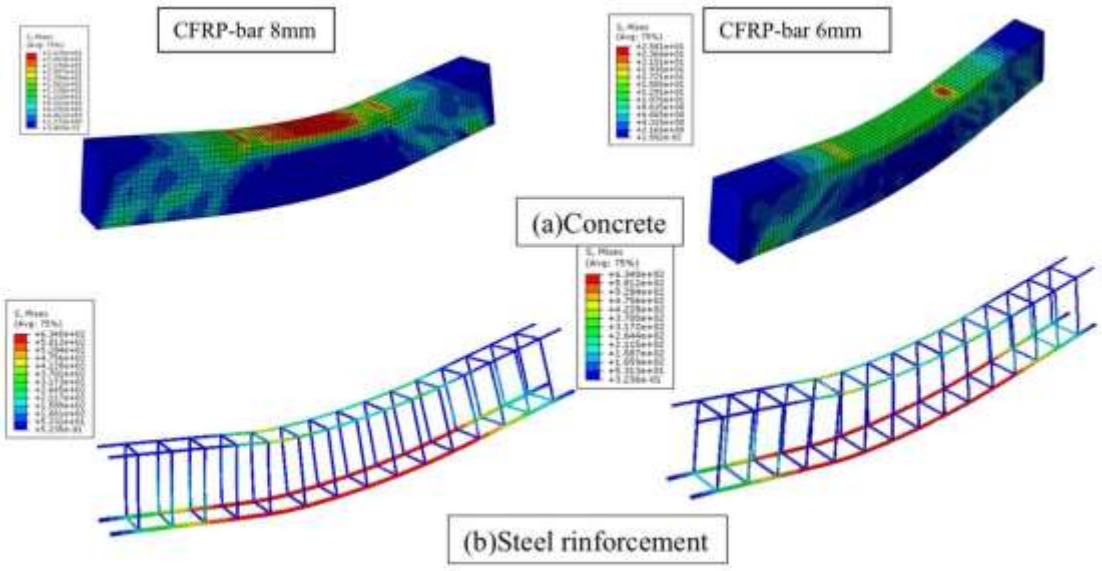

Figure 5-17: Comparison between CFRP-bar 8mm and CFRP-bar 6mm on von Mises Stresses.

Increasing the diameter of the NSM-CFRP bars used for strengthening affects the stress distribution and load bearing capacity. Increasing the diameter enhances the maximum load bearing capacity. Notice that the stresses are distributed more widely between the two load application areas when strengthening with a diameter of 8 mm. This indicates that when increasing the diameter, the stresses increase in the middle of the model, while when strengthening with a diameter of 6 mm, the high stresses appear only in the load application area, as shown in Figure 5-17.

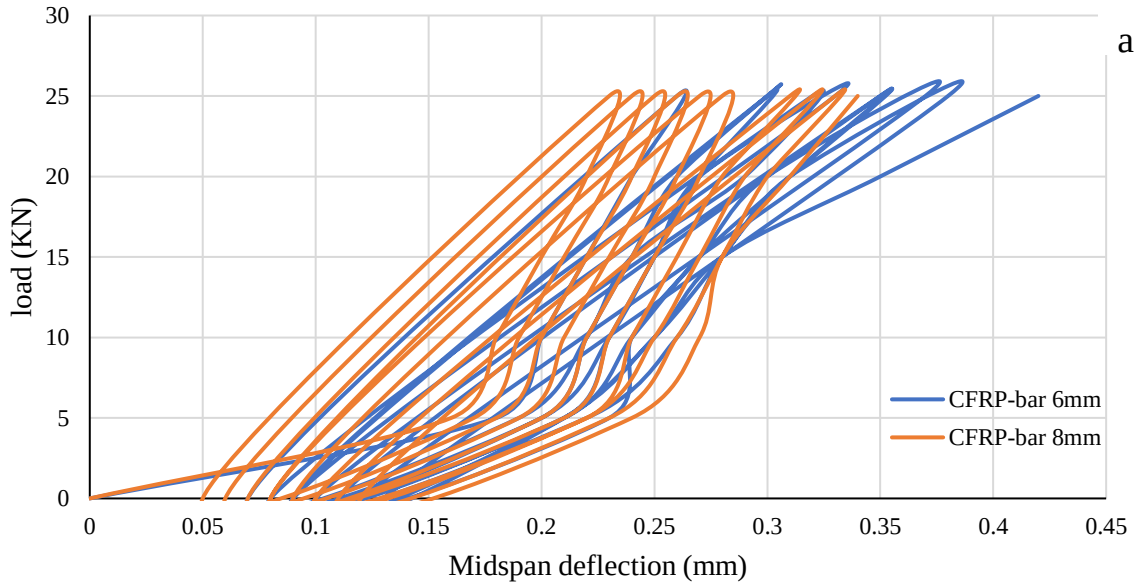

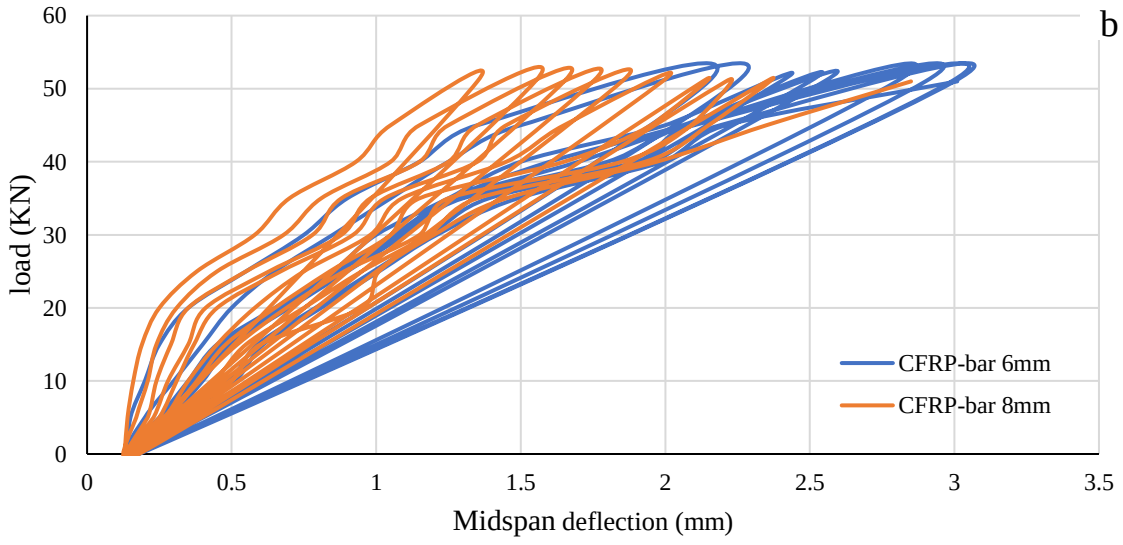

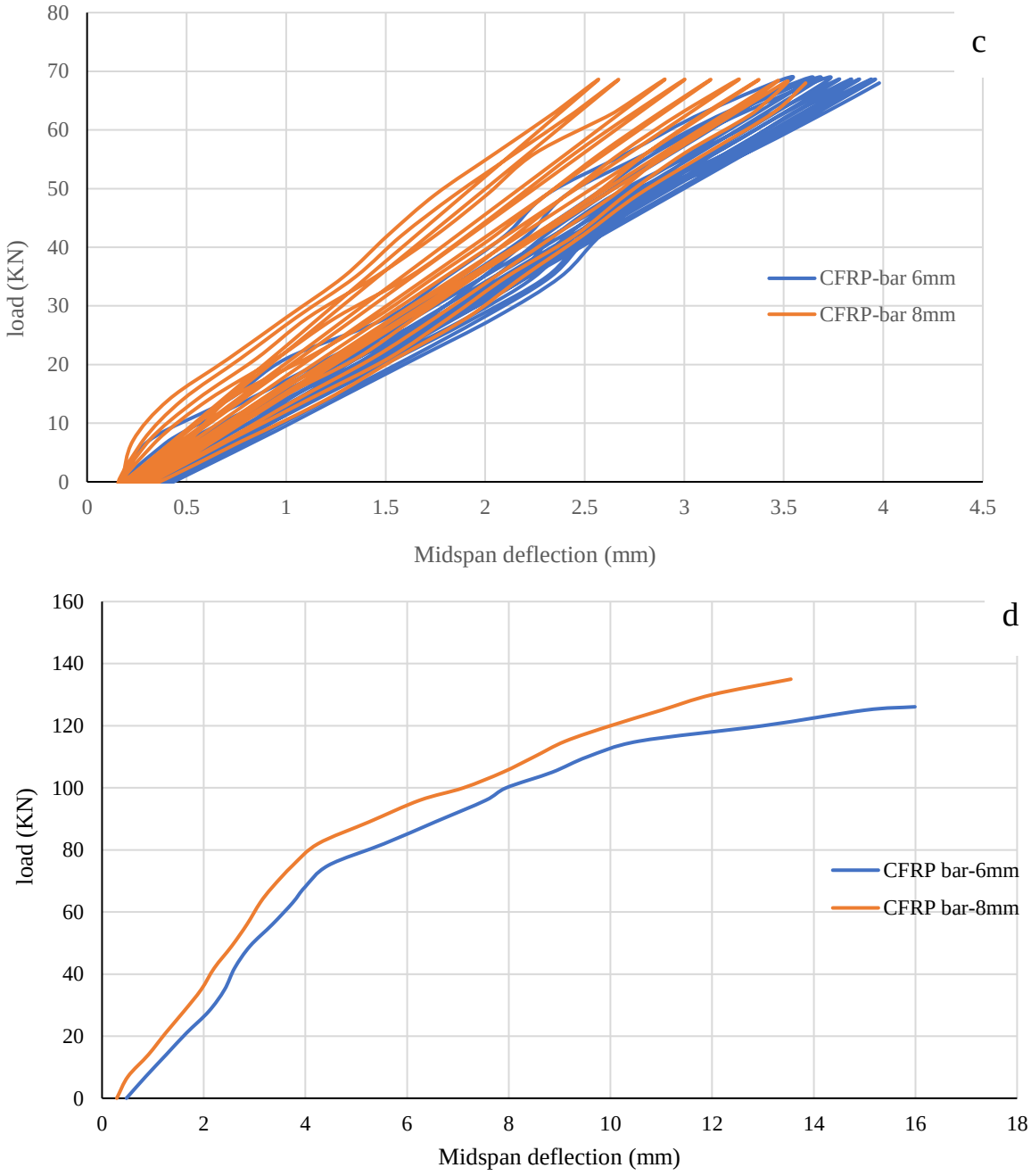

Figure 5-18: Comparison between CFRP-bar 8mm and CFRP-bar 6mm on Load-Deflection Curves for beam B4 F10b a) first 10 cycles from repeated load , b) second 10 cycles from repeated load ,c) third 10 cycles from repeated load .d) up to failure load.

In general, it is observed that the beam strengthening with NSM-CFRP bar 8 mm bears a greater load with less displacement compared to the beam strengthening with NSM-CFRP bar 6 mm. Whereas the maximum load before failure at bar 8 mm is about 136 KN while the maximum load before failure at bar 6 mm is estimated at 126.1 KN.

5.5.2 Effect of thickness of CFRP strip

The thickness of the CFRP strip was taken as 2 mm, and the model was analyzed keeping the other variables constant.

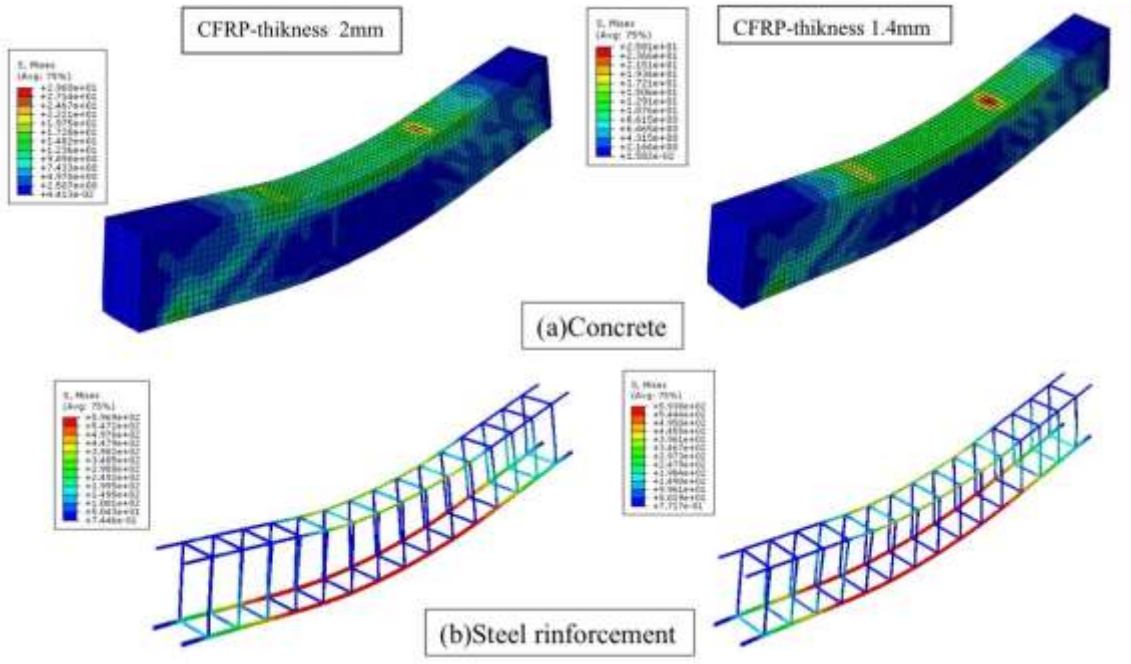

Figure 5-19: Comparison between CFRP-thikness 2mm and CFRP-thickness 1.4mm on von mises stresses.

Increasing the thickness of the CFRP strip (from 1.4 mm to 2 mm) reduced the stress concentration on the concrete surface and distributed it better. The 2 mm thick reinforced model provided higher resistance to bending and stress than the 1.4 mm thick model. Using a larger strip thickness

improves the structural performance but may add additional weight or costs. It is important to achieve a balance between economic efficiency and the required strength.

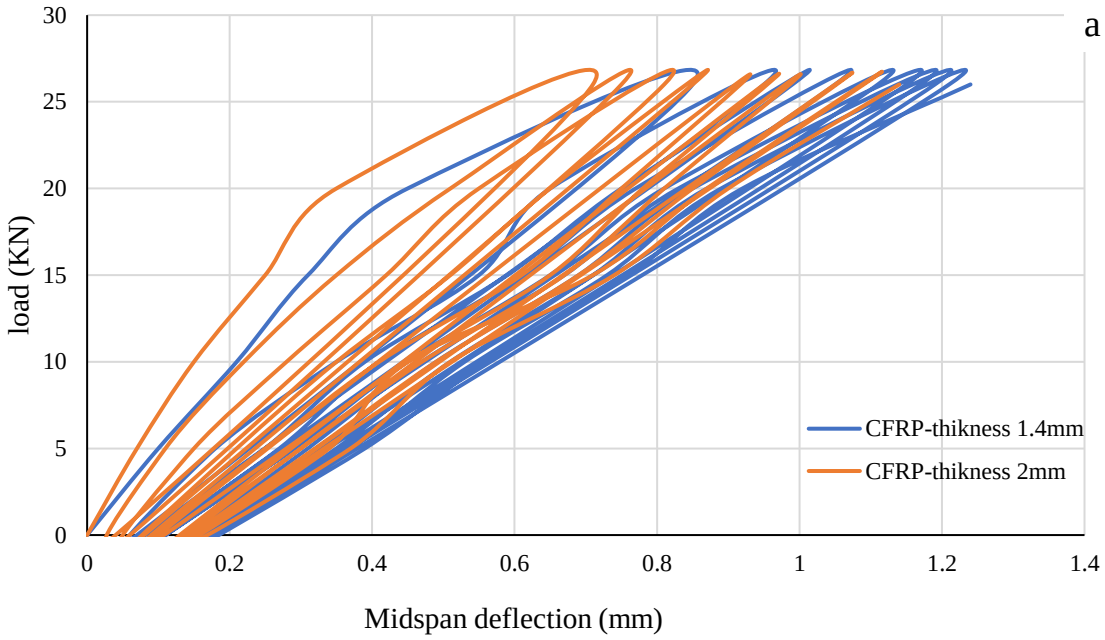

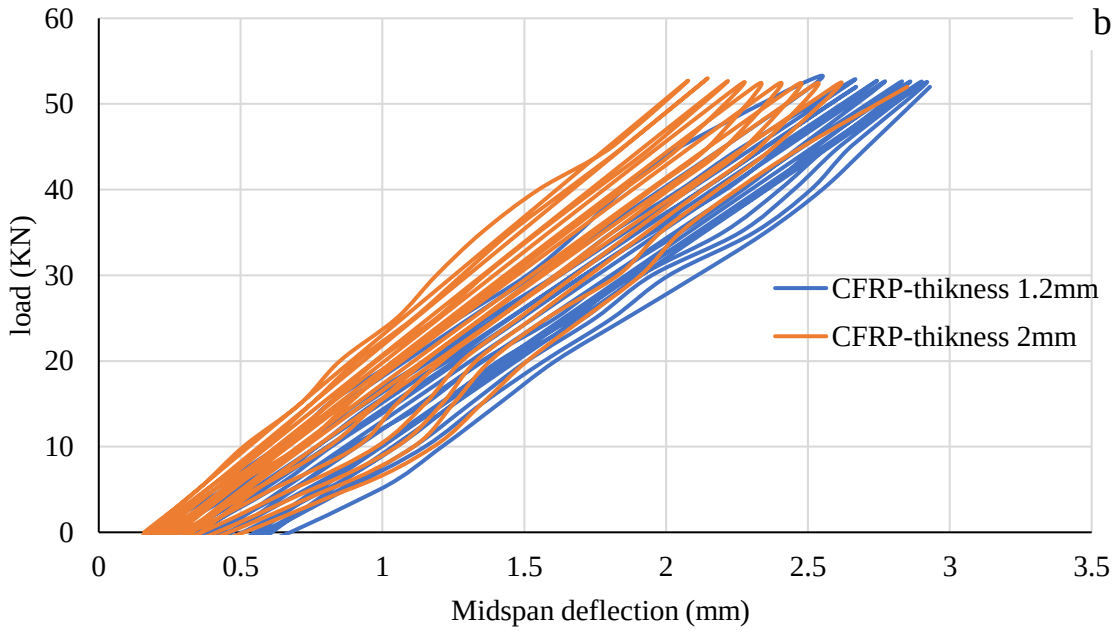

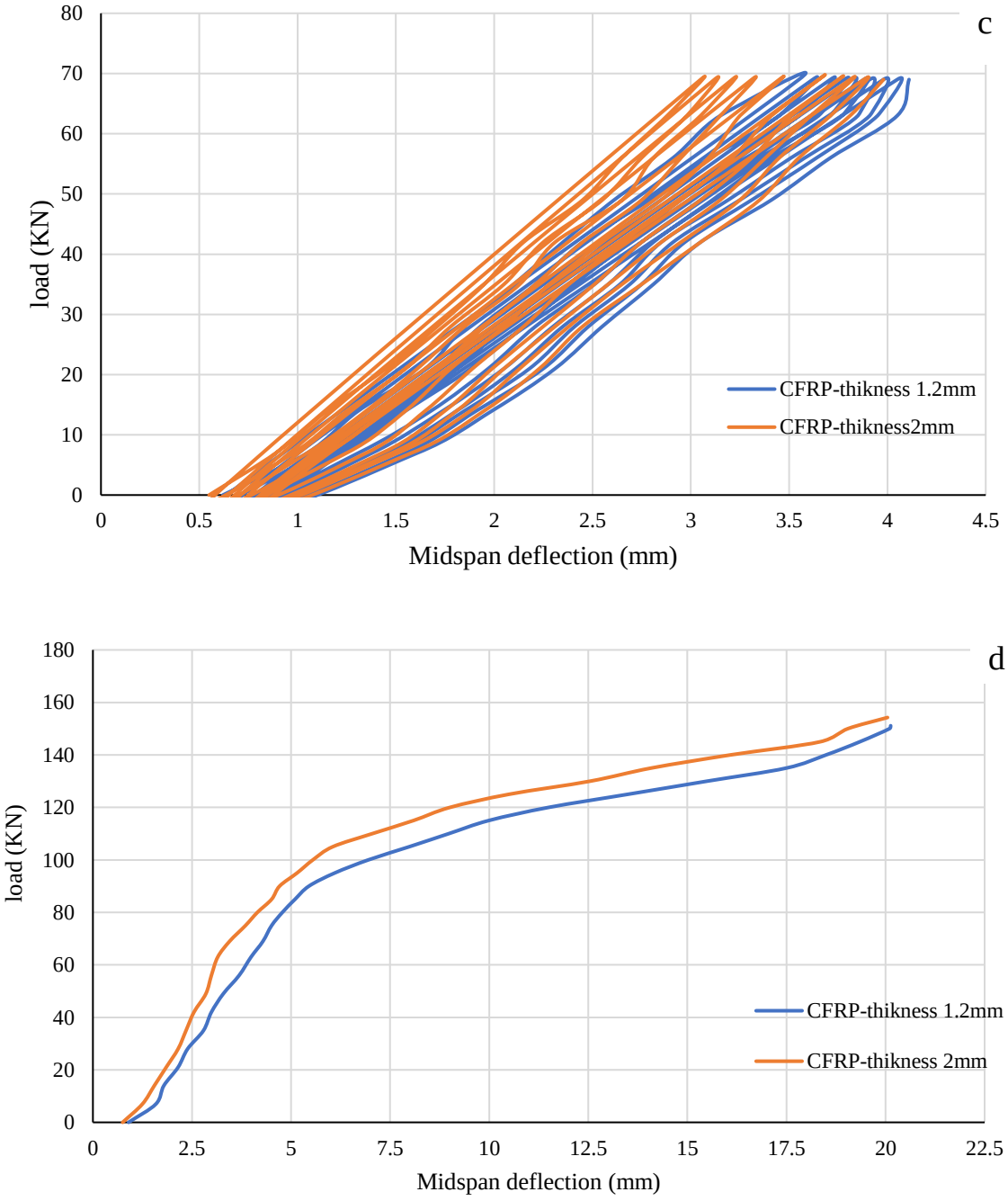

Figure 5-20: Comparison between CFRP-thikness 2mm and CFRP-thickness 1.2mm on Load-Deflection Curves for beam B14F10C10L a) first 10 cycles from repeated load, b) second 10 cycles from 10 cycles from repeated load, c) third 10 cycles from repeated load ,d) up to failure load.

In general, they note that the use of a thicker CFRP strip 2 mm improves the deflection resistance and improves the performance of the structure against repeated loads and ultimate failure. The maximum load before failure at 2 mm strip is about 154.25 KN while the maximum load before failure at 1.4 mm strip is estimated at 151.13 KN.

5.5.3 Effect of number of CFRP bars

In this parametre the number of bars will be changed and 3 CFRP bars will be used and the model will be analyzed while keeping the rest of the variables constant.

The analysis of the obtained results indicates that increasing the number of CFRP bars from two to three leads to a reduction in the overall deflection of the model under the same loading conditions. This improvement is attributed to the enhanced structural stiffness resulting from the increased flexural resistance provided by the additional CFRP bars. Furthermore, the partial replacement of fine aggregate with rubber at a ratio of 10% influenced the overall stiffness of the model, making the material more flexible. However, its impact on deflection was less pronounced in the model containing three CFRP bars, highlighting the mitigating effect of the additional strengthening in counteracting the adverse influence of rubber replacement.

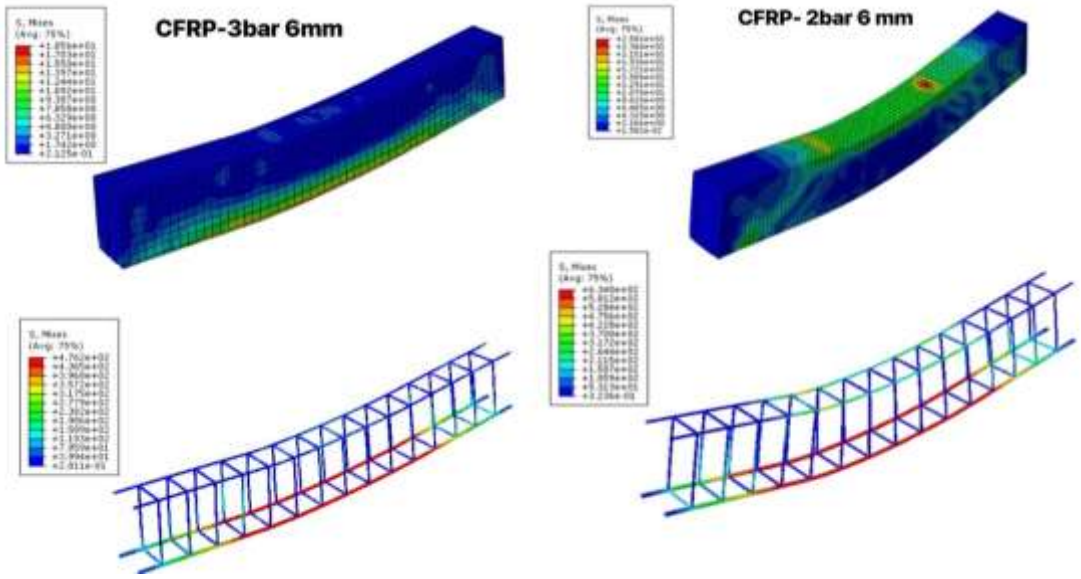

Figure 5-21: Comparison between CFRP-2bar and CFRP-3 bar on von mises stresses.

The results also demonstrated that the distribution of Von Mises stresses was more uniform in the model with three CFRP bars compared to the model with only two. A higher number of CFRP bars reduces stress concentration at specific locations, thereby enhancing structural performance and minimizing the likelihood of crack initiation or localized failure. Conversely, the model reinforced with only two CFRP bars exhibited higher stress concentrations in certain regions, indicating a relatively lower load-bearing capacity. This analysis underscores the significance of CFRP bar quantity in improving stress distribution and mitigating the negative effects associated with the partial replacement of fine aggregate with rubber.

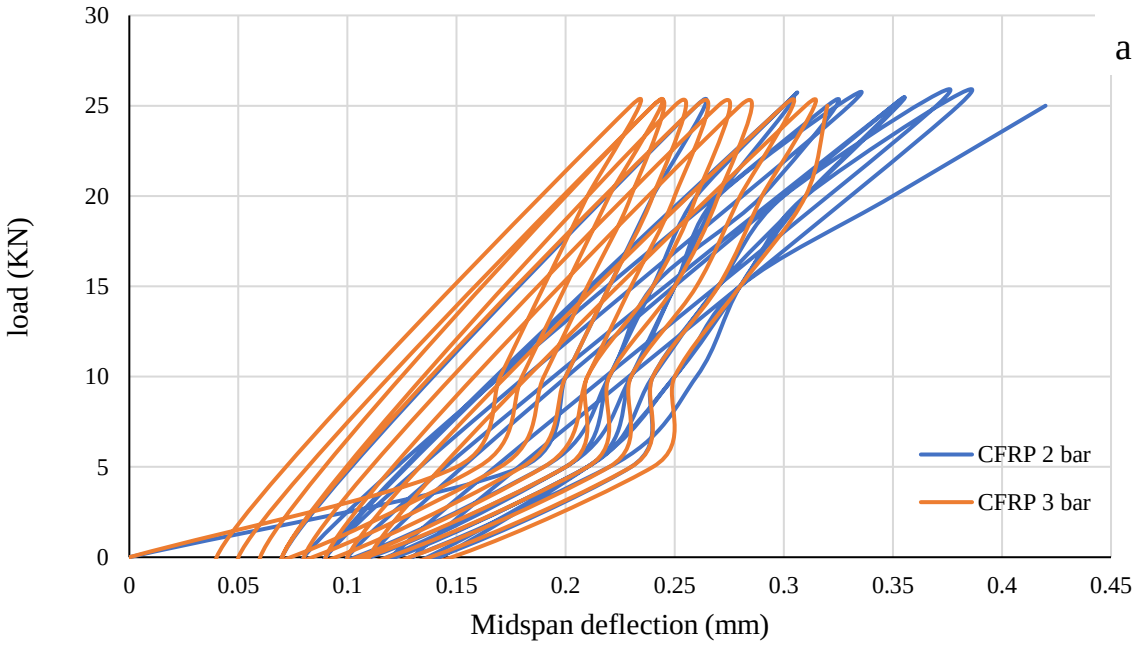
a
load (KN)
30
25
20
15
10
5
0
0
0.05
0.1
0.15
0.2
0.25
0.3
0.35
0.4
0.45
Midspan deflection (mm)
CFRP 2 bar
CFRP 3 bar

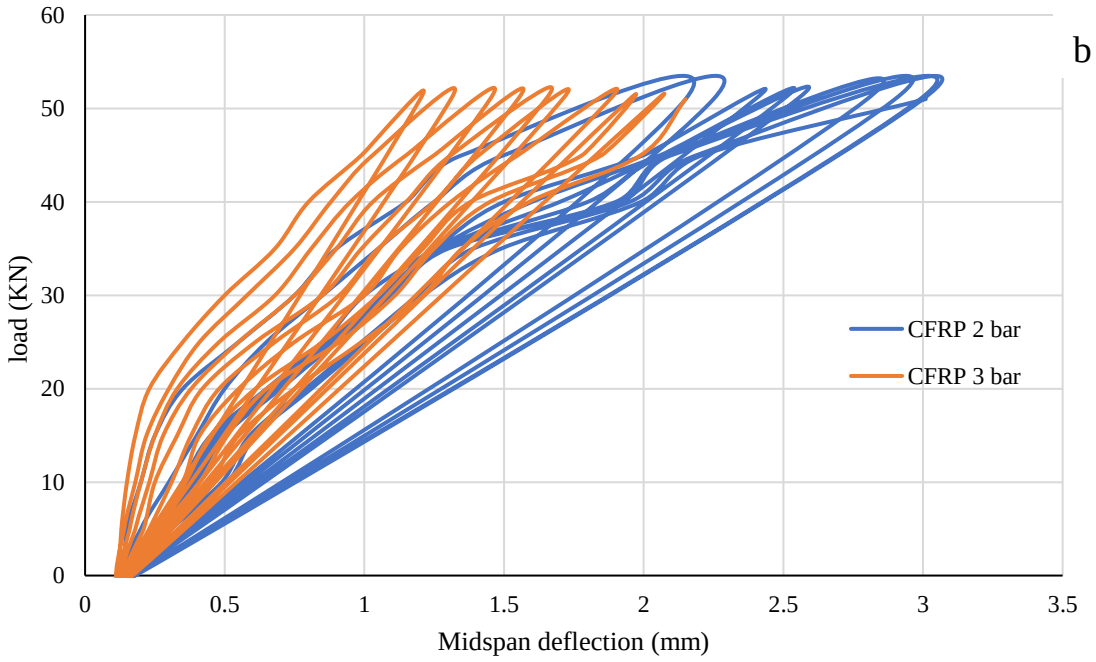
b
load (KN)
60
50
40
30
20
10
0
0
0.5
1
1.5
2
2.5
3
3.5
Midspan deflection (mm)
CFRP 2 bar
CFRP 3 bar

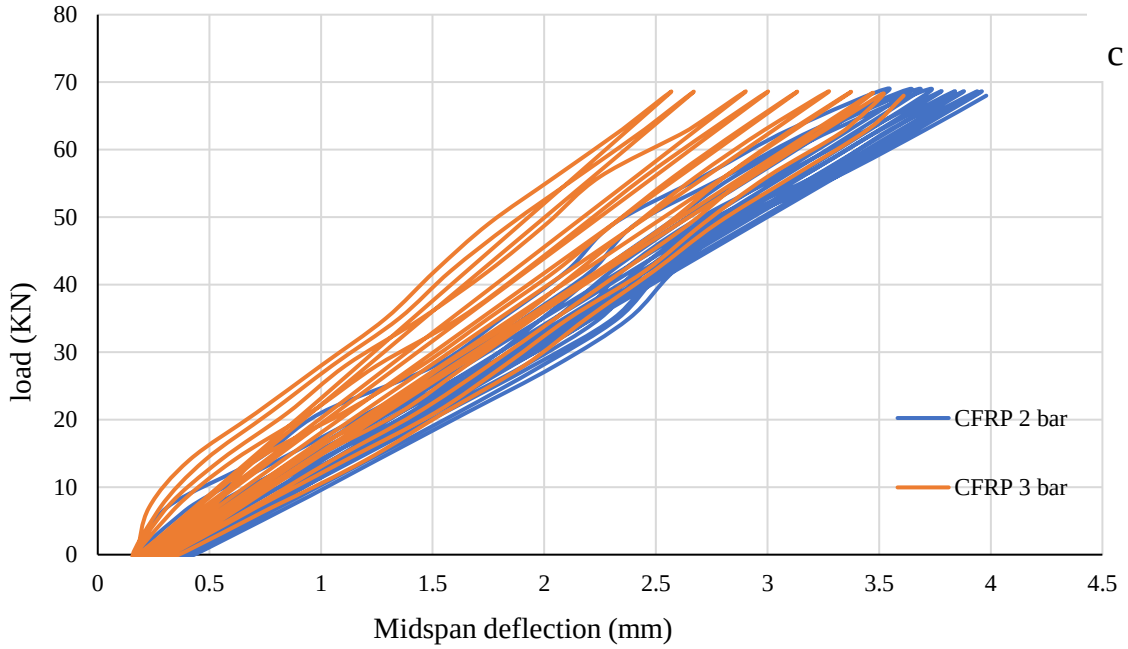

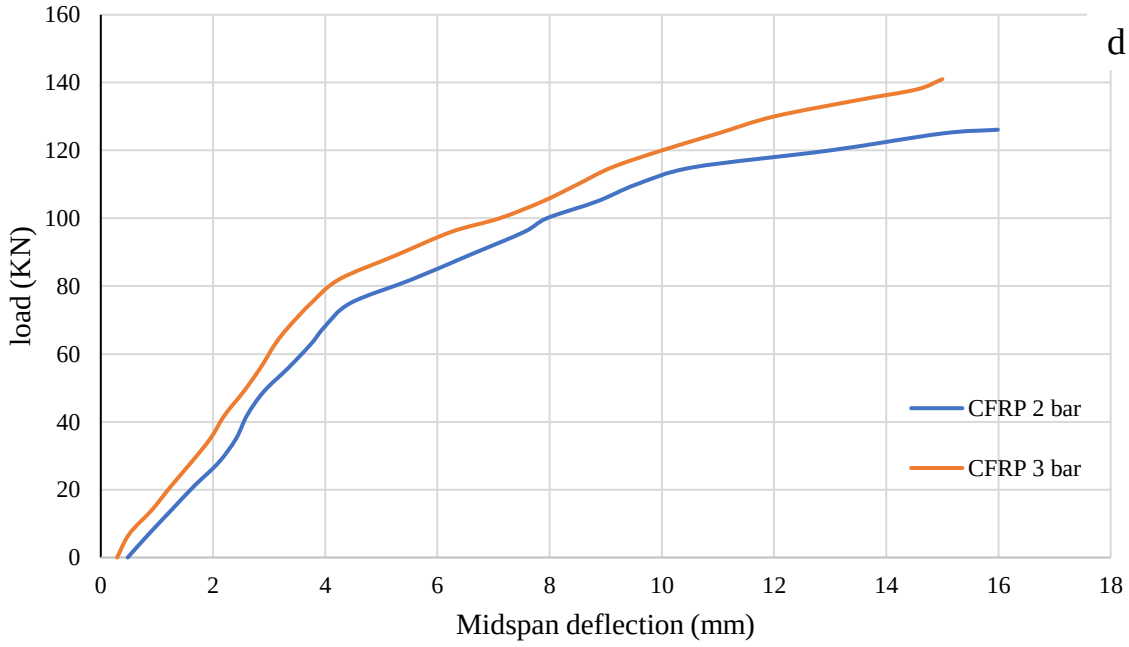

Figure 5-22: Comparison between CFRP-2 bar 6mm and CFRP-3 bar 6mm on Load-Deflection Curves for beam B4 F10b a) first 10 cycles from repeated load , b) second 10 cycles from 10 cycles from repeated load ,c) third 10 cycles from repeated load .d) up to failure load.

The increase in the number of CFRP bars contributed to an overall enhancement in the specimen's stiffness, leading to an increase in the ultimate load-bearing capacity before failure. Initially, both load-displacement curves exhibited a similar slope, indicating comparable initial stiffness. However, as the applied load increased, the 3-bar NSM-CFRP configuration demonstrated superior performance, enabling it to withstand higher stress levels before failure. This suggests that the additional reinforcement enhanced the structural capacity and delayed the onset of significant deformations, ultimately improving the beam's overall load resistance.

5.6 Summary

- Model Validation and Accuracy: The study utilized ABAQUS/Explicit for finite element analysis and demonstrated a strong correlation between numerical predictions and experimental results. This suggests that the numerical model is valid.
- Mesh Size Optimization: A convergence study determined that a mesh size of 30 mm strikes a balance between computational efficiency and result accuracy. This optimized mesh size was used consistently across all beams in the analysis.
- Load-Deflection Consistency: The load-deflection curves obtained through finite element analysis closely matched the experimental data. This consistency indicates that the numerical model effectively captures the structural response of the composite beams.
- Ultimate Load Prediction: The comparison between experimental and numerical ultimate loads revealed a high level of agreement, with variations remaining within a reasonable.

- The numerical study showed that using a CFRP bar diameter of 8 mm instead of the practically used diameter of 6 mm increases the ultimate load by 7.85% and reduces the displacement by 2.20%. Although this is good, its effect is very small.
- The numerical analysis demonstrated that increasing the CFRP strip thickness from the commonly used 1.4 mm to 2 mm results in a 2.06% increase in ultimate load and a 0.40% reduction in displacement. While these improvements are positive, their effect is relatively minor.
- Numerical analysis shows that increasing the number of CFRP bars from 2 to 3 bars increases the ultimate load by 11.82% and decreases the displacement by 6.19%.

Chapter Six: Conclusions and Recommendations

6.1 Introduction

This chapter presents the findings and recommendations for further research based on the experimental and numerical data collected in the current study.

6.2 Conclusions

This section provided a concise summary of the study's findings for rubberised concrete beams subjected to repeated loads using different strengthening techniques, including both experimental and numerical data.

1. The addition of rubber particles as a partial volumetric replacement for natural aggregates in reference concrete mixtures results in a reduction in fresh density and unit weight of rubberized concrete. This reduction is linear for replacement ratios of 10%-20% of fine and coarse aggregates, with fresh density decreasing by 3.30%-6.44% for fine aggregate and 2.44%-4.57% for coarse aggregate. When both fine and coarse aggregates are replaced by 10%-20% rubber, the fresh density decreases by 10.83%-11.57%..
2. Compressive strength . The reference mixture of coarse and fine blocks was substituted with crumb rubber and chips, resulting in a drop in fc', splitting tensile stress fsp, and modulus of rupture fr. Increasing the replacement ratio of worn tyre rubber led to a steady and steady decline in combined strength. By increasing the chip-to-crumb rubber ratio in the same mixture from 0% to 20%, the hardenite characteristics (fc', fsp, and fr) were decreased by 51.66%, 22.59%, and 38%, respectively.

3. According to the results, replacing 5% coarse and fine rubber particles to the concrete mixture reduced the compressive strength by -35.89 and the new unit weight by 10.83.
4. CFRP strips improved the ultimate load capacity of the specimens more effectively than CFRP bars. For example, in sample B5, the ultimate load capacity 127 kN, and in B11, the ultimate load capacity 165 kN. The strip gave an improvement of about 30% in the ultimate load capacity for the same rubber replacement ratio.
5. Repeated loading reduces the ultimate load capacity of beams compared to monotonic loading, as observed between two control samples. The ultimate load decreases by 8.05% due to repeated cycles.
6. In the load-displacement curves, rubber plays a major role in improving the ductility, allowing the material to absorb more deformation before failure.
7. The failure modes in the mid-span region are the primary site for initiating and developing major cracks, including the first visible crack, indicating that all of them are within the compression zone failure.
8. Compared with the normal numerical concrete beams, increasing the diameter of CFRP-bar 8mm lead to increased the ultimate strength of the specimen by 2.25%; although the increase occurred, it was very small.
9. Increasing the thickness of CFRP strips to 2 mm lead to increased the ultimate load by 0.74%, which is very small compared to its prices.
10. Increasing the number of CFRP bars from 2 to 3 bars expanded maximum load capacity by 30.56%, in contrast to practical model B4 F10b. Although this increase is reasonable, the use of 2 or 3 bars depends on the required load capacity and the required economic efficiency.

6.3 Ideas for upcoming projects

1. The behaviour of rubberized beams under the influence of vibration loads.
2. Study the behavior of other structural rubber elements, such as slabs and beam-column joints, under repeated loads.
3. Studying shear behavior of rubberized beams under repeated loads .
4. Study of the Behavior of Rubberized Concrete Treated by Physical and Chemical Methods Under Bending Effects and Strengthened with Near-Surface Mounted (NSM) Reinforcement

References

Abbara, A.A. *et al.* (2022) 'Uniaxial compressive stress-strain relationship for rubberized concrete with coarse aggregate replacement up to 100%', *Case Studies in Construction Materials*, 17, p. e01336.

Abdulameer Kadhim, A. and Mohammed Kadhim, H. (2023) 'Experimental investigation of rubberized reinforced concrete continuous deep beams', *Journal of King Saud University - Engineering Sciences*, 35(3), pp. 174–184. Available at: https://doi.org/10.1016/j.jksues.2021.03.001.

AL-Hajjar, K.R.M. and AL-Khafaji, A.G.A. (2024) 'Behavior of Rubberized Reinforced Concrete Beams Under', 050006.

Al-khafaji, A.G.A., Muhammed, S.H. and Jadooe, A. (2024) 'Effect of strengthening by carbon fi ber reinforced polymer sheets on the fl exural behavior of reinforced self-compacting concrete beams under repeated loads'. Available at: https://doi.org/10.1177/13694332241237587.

Al-Obaidi, S., Saeed, Y.M. and Rad, F.N. (2020) 'Flexural strengthening of reinforced concrete beams with NSM-CFRP bars using mechanical interlocking', *Journal of Building Engineering*, 31(August 2019), p. 101422. Available at: https://doi.org/10.1016/j.jobe.2020.101422.

Al-zu'bi, H., Abdel-Jaber, M. and Katkhuda, H. (2022) 'Flexural strengthening of reinforced concrete beams with variable compressive strength using near-surface mounted carbon-fiber-reinforced polymer strips [NSM-CFRP]', *Fibers*, 10(10), p. 86.

Alfayez, S.A., Suleiman, A.R. and Nehdi, M.L. (2020) 'Recycling tire rubber in asphalt pavements: State of the art', *Sustainability*, 12(21), p. 9076.

Ali, A.S. and Hasan, T.M. (2019a) 'Properties of different types of concrete containing waste tires rubber- a review Properties of different types of concrete containing waste tires rubber- a review'. Available at: https://doi.org/10.1088/1757-899X/584/1/012051.

Ali, A.S. and Hasan, T.M. (2019b) 'Properties of different types of concrete containing waste tires rubber-a review', in *IOP Conference Series: Materials Science and Engineering*. IOP Publishing, p. 12051.

Antil, E.Y. (2014) 'An Experimental Study on Rubberized Concrete', 4(2), pp. 309–316.

Barris, C. *et al.* (2020) 'Flexural behaviour of FRP reinforced concrete beams strengthened with NSM CFRP strips', *Composite Structures*, 241, p. 112059.

Batayneh, M., Marie, I. and Asi, I. (2007) 'Use of selected waste materials in concrete mixes', *Waste management*, 27(12), pp. 1870–1876.

Batayneh, M.K., Marie, I. and Asi, I. (2008) 'Promoting the use of crumb rubber concrete in developing countries', *Waste Management*, 28(11), pp. 2171–2176. Available at: https://doi.org/10.1016/j.wasman.2007.09.035.

Eisa, A.S., Elshazli, M.T. and Nawar, M.T. (2020) 'Experimental investigation on the effect of using crumb rubber and steel fibers on the structural behavior of reinforced concrete beams', *Construction and Building Materials*, 252, p. 119078. Available at: https://doi.org/10.1016/j.conbuildmat.2020.119078.

Fazli, A. and Rodrigue, D. (2020) 'Recycling waste tires into ground tire rubber (GTR)/rubber compounds: A review', *Journal of Composites Science*, 4(3), p. 103.

Ghanim, A. *et al.* (2016) 'Experimental Study on the Flexural Strengthening of Reinforced Concrete Beams Using NSM CFRP Bars Experimental Study of Using Ferro-Cement and Steel Plates in Repairing Reinforced Concrete Beams View project Experimental Study on the Flexural Strengthenin'. Available at: https://www.researchgate.net/publication/323639383.

Ghoneim, M. and Sharobim, K. (1997) 'Flexural behavior of high-strength fiber reinforced concrete beams', *Journal of Engineering and Applied Science*, 44(2), pp. 279–294. Available at: https://doi.org/10.14359/4186.

Goldstone, M. (2012) 'CFRP Strengthening of Reinforced Concrete Beams for Blast and Impact Loads', *Faculty of Engineering, University of Wollongong* [Preprint], (November). Available at: https://www.researchgate.net/profile/Matt_Goldston/publication/313350360_CFRP_Strengthening_of_Reinforced_Concrete_Beams_for_Blast_and_Impact_Loads/links/5896f33aaca2721f0dabd6f9/CFRP-Strengthening-of-Reinforced-Concrete-Beams-for-Blast-and-Impact-Loads.p.

Hassan, T. and Rizkalla, S. (2004) 'Bond mechanism of NSM FRP bars for flexural strengthening of concrete structures', *ACI Structural Journal* [Preprint], (1). Available at: http://www.ce.ncsu.edu/centers/rb2c/Publications/BondMechanismOfNSMFRPBarsForFlexuralStrengtheingOfConcreteStructures_Tarek_ACI_II_figures_included.pdf.

Hussein, N.K., Al-Abbas, B.H. and Al-Khafaji, A.G.A. (2024) 'Experimental and numerical behavior of composite castellated beams under repeated loads', *AIP Conference Proceedings*, 3219(1). Available at: https://doi.org/10.1063/5.0236468.

Jadooe, A., Al-Mahaidi, R. and Abdouka, K. (2017) 'Experimental and numerical study of strengthening of heat-damaged RC beams using NSM CFRP strips', *Construction and Building Materials*, 154, pp. 899–913.

Jevtić, D., Zakić, D. and Savić, A. (2012) 'Achieving sustainability of concrete by recycling of solid waste materials', *Mechanical Testing and Diagnosis*, 2(1), pp. 22–39.

Kadhim, A.A. and Hayder Mohammed Kadhim (2020) 'Experimental Behavior of Rubberized Reinforced Concrete Continuous Deep Beams By Ali Abdulameer Kadhim Al-Humairi'.

Khalaf, M.R. and Al-Ahmed, A.H.A. (2021) 'Effect of large openings on the behavior of reinforced concrete continuous deep beams under static and repeated load', in *E3S Web of Conferences*. EDP Sciences, p. 3012.

Khorami, M., Ganjian, E. and Vafaii, a (2007) 'Mechanical Properties of Concrete with Waste Tire Rubbers as Coarse Aggregates', *Proceeding of Special sections on International conference on Sustainable Construction Materials and Technologies*, pp. 85–90.

Muthuswamy, K.R. and Thirugnanam, G.S. (2014) 'Experimental investigation on behaviour of hybrid fibre reinforced concrete column under axial loading', *Asian Journal of Civil Engineering*, 15(2), pp. 169–178.

Olubunmi, A., Olamoju, R.O. and Taiye, A. (2023) 'Partial Replacement of Coarse Aggregates with Plastic Waste in Paver Blocks', *Journal of Sustainability and Environmental Management*, 2(2), pp. 92–97. Available at: https://nepjol.info/index.php/josem/article/view/55201.

Pomeroy, C.D. (1993) 'Rehabilitation of concrete structures', *Materials and Structures*, 26(3), pp. 185–189. Available at: https://doi.org/10.1007/bf02472937.

Russell, J.S. (2003) *Perspectives in Civil Engineering: Commemorating the 150th Anniversary of the American Society of Civil Engineers*. ASCE Publications.

Senouci, A.B. and Member, A. (1994) 'By Nell N . Eldin , ~ Member , ASCE , TABLE 1 . Control-Mix Proportions Material Quantity (kg / m 3) Coarse aggregate Sand Cement Water FIG . 1 . Typical Size and Shape of Rubber Aggregates Each group consisted of several batches , in which the mineral ', *Journal of Materials*, 5(4), pp. 478–496.

Sharaky, I.A. *et al.* (2014) 'Flexural response of reinforced concrete (RC) beams strengthened with near surface mounted (NSM) fibre reinforced polymer (FRP) bars', *Composite Structures*, 109, pp. 8–22.

Sibiyone, K.P. and Sundar, M.L. (2017) 'Experimental Study on Replacing Waste Rubber as Coarse Aggregate', *International Journal of ChemTech Research*, 10(14), pp. 287–293.

Soren, A.K. *et al.* (2023) 'A Laboratory Study of Use of Crumb Rubber as Partial Replacement of Fine Aggregate in Concrete', (June).

Strukar, K. *et al.* (2018) 'Experimental study of rubberized concrete stress-strain behavior for improving constitutive models', *Materials*, 11(11), p. 2245.

Su, H. (2022) 'Analysis of Cube Compressive Strength on Concrete with Recycled Aggregate and Rubber Particles', *IOP Conference Series: Earth and Environmental Science*, 1050(1). Available at: https://doi.org/10.1088/1755-1315/1050/1/012029.

Tehrani, F.M. and Miller, N.M. (2018) 'Tire-derived aggregate cementitious materials: A Review of Mechanical Properties', *Cement-based Materials* [Preprint].

Vijayan, D.S. *et al.* (2023) 'Carbon fibre-reinforced polymer (CFRP) composites in civil engineering application—a comprehensive review', *Buildings*, 13(6), p. 1509.

Zhang, S.S., Yu, T. and Chen, G.M. (2017) 'Reinforced concrete beams strengthened in flexure with near-surface mounted (NSM) CFRP strips: Current status and research needs', *Composites Part B: Engineering*, 131, pp. 30–42.

Zhu, H. *et al.* (2022a) 'Flexural performance of concrete beams reinforced with continuous FRP bars and discrete steel fibers under cyclic loads', *Polymers*, 14(7), p. 1399.

Zhu, H. *et al.* (2022b) 'Flexural Performance of Concrete Beams Reinforced with Continuous FRP Bars and Discrete Steel Fibers under Cyclic Loads', *Polymers*, 14(7). Available at: https://doi.org/10.3390/polym14071399.

Iraqi Specification, No. 45/1984, "Aggregate from Natural Sources for Concrete and Construction.,"

47. ASTM C33-03, Standard Specification for Concrete Aggregates, ASTM ASTM A615M-05a, "Standard Specification for Deformed and Plain Billet-Steel Bars for Concrete Reinforcement, ASTM

Committee A01 on Steel, Stainless Steel, and Related Alloys, West Conshohocken; PA 19428-2959; United States; 2005; 5 pp. 2005. International, West Conshohocken, PA, 2003, www.astm.org. 2003.

ACI committee 318M-19 (2019). Building code Requirements for structural concrete and commentary. ACI Farmington Hill.

ACI 440.2R-17 : Guide for the Design and Construction of Externally Bonded FRP Systems for Strengthening Concrete Structures

APPENDIX A

Design Examples of The Tested Beams

Here the design method was explained, the control beam was chosen, and the American code ACI 318M-14 was relied upon in the specifications for the designs.

A. Design and Analysis :-

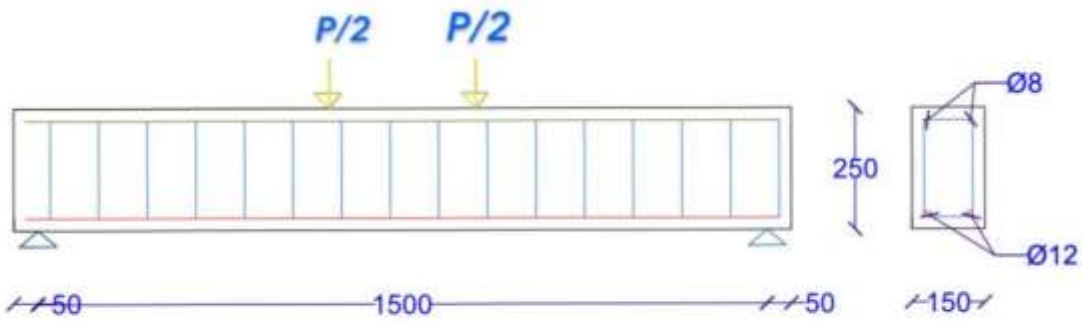

Assume :-

f'c =30 MPa

fy = 400 MP

Now find ρ_{min} and ρ_{max}

$$\rho_{min} = \frac{\sqrt{f'c}}{4fy} \geq \frac{1.4}{fy}$$

$$\rho_{min} = \frac{\sqrt{30}}{4*400} = 0.0034,\ \rho_{min} = \frac{1.4}{400} = 0.0035$$

$\therefore\ \rho_{min} = 0.0035$

$\rho_{max} = 0.85\ \beta 1\ \frac{f'c}{fy}\ \frac{\varepsilon u}{\varepsilon u + 0.004}$

$\rho_{max} = 0.85^2\ \frac{30}{400}\ \frac{0.003}{0.003+0.004}$

$\rho_{max} = 0.0232$

$\rho_t = 0.85\ \beta 1\ \frac{f'c}{fy}\ \frac{\varepsilon u}{\varepsilon u + 0.005}$

$\rho_t = 0.85^2\ \frac{30}{400}\ \frac{0.003}{0.003+0.005}$

$\rho_t = 0.0203$

Must be $\rho_{req} < \rho_t$ and $\rho_{min} < \rho_{req} < \rho_{max}$

Assume $\rho_{req} = 0.0100$

- Find AS

$As = \rho_{req} * b * d$

d = 250-6-30-8 = 206 mm

As =0.01*150*206

AS=309 mm^2

No. of bar = $\frac{AS}{Abar}$

Assume bar Ø12

Abar=113

No. of bar = $\frac{309}{113} = 2.7$

:. Use 2 bar 2Ø12

Now chick spacing

125-2*(30+8)-2*12 = 50 > 25 (OK)

-To Analysis this section

Assume

fy = 400 MP

f'c =30 MPa

As = 2*113 = 226 mm^2

$\rho_{act} = \frac{As}{bd} = \frac{226}{150*211} = 0.00714$

$\rho_{min} = 0.0035 < \rho_{act} = 0.00714 < \rho_{max} = 0.0232$ (OK)

$Mn = \rho\ b\ d^2\ fy\ (1 - 0.59\ \rho\ \frac{fy}{f'c})$

$Mn = 0.00714*150*211^2*400\ (1-0.59*0.00714*\frac{400}{30})\ *10^{-6}$

Mn = 18.001 KN.M

$R_1 = \frac{18}{0.6} = 30kN$

$\sum M_2 = 0$

$\frac{P}{2}*(600) + \frac{P}{2}*(900) - R_1*(1500) = 0$

$P(750) = R_1(1500)$

P=60 KN

A. Design of reinforced concrete beam with NSM-FRP bars ;-

Here the design method for strenthening with near-surface mounted systems is explained, relying on the American code ACI440.2R-17 in the design specifications.

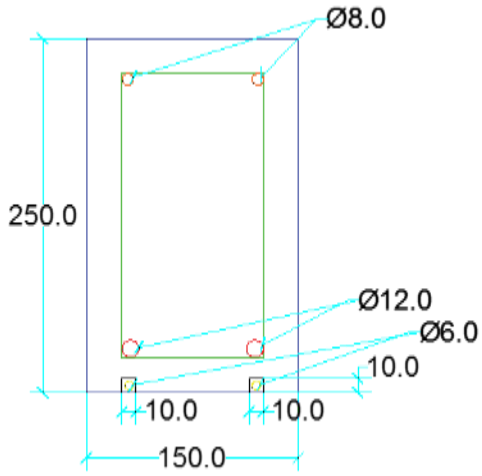

Procedure for flexural strengthening of an interior reinforced concrete beam with NSM FRP bars:-

Step 1-Calculate the FRP system design material properties

$F_{fu}=C_E\ F_{fu}^{*}=0.95*1725=1639\ N/mm^2$

$\varepsilon_{fu}=C_E\ F_{fu}^{*}=0.95*0.013=0.0123 mm/mm$

Step 2—Preliminary calculations

Properties of the concrete:

β_1 from ACI 318-14, Section 22.2.2.4.3

$\beta_1=1.05-0.05\frac{f c\prime}{6.9}=0.832$

$E_C=4700\sqrt{FC'}=4700\sqrt{30}=25742.96 N/mm^2=25.74\ N/mm^2$

$A_S=\frac{\pi}{4}D^2*2=226\ mm^2$

$A_f=\frac{\pi}{4}6^2*2=57\ mm^2$

Step 3—Determine the existing state of strain on the soffit

$\varepsilon_{bi} = M_{DL}(d_f - kd)/ I_{cr} E_C$

$M_{DL} = W L^2/8$ W=0.150*0.250*24000=900N/m

= 900*1.5/8 =168.75N. m =168.75 KN.mm

$I_{cr} = (b h^3/3) + n A_s$ (space frome crnter to N.A)

$n = E_S/E_C = \frac{200000}{4700*\sqrt{30}} = 8$

$I_{cr} = \frac{150*250^3}{3} + 8(226)*(86^2) = 794.621* 10^6 mm^4$

$K= \sqrt{(p\ n)^2 + 2(p\ n)} - p\ n$

$P = A_S/b\ d = \frac{226}{150*211} = 0.00741$

$K= \sqrt{(0.00714 * 8)^2 + (0.00714 * 8)} - (0.00714*8) = 0.285$

:. $\varepsilon_{bi} = M_{DL}(d_f - kd)/ I_{cr} E_C$

$\varepsilon_{bi} = \frac{168.75(245-0.285*211)}{794.621*10^6*25.74} = 0.0000015$

Step 4—Determine the bond-dependent coefficient of the FRP system

K_m is 0.7

Step 5—Estimate c

Assume C= 64

Step 6-Determine the effective level of strain in the FRP reinforcement

$\varepsilon_{fe} = \varepsilon_{bi} \left(\frac{d_f - C}{C}\right) - \varepsilon_{bi} < K_m * \varepsilon_{fd}$

$= 0.003\left(\frac{245-42.2}{42.2}\right) - 0.0000051 < 0.7 * 0.0123$

$= 0.00848 < 0.00861$

:. $\varepsilon_{fe} = 0.00848$

$\varepsilon_c = (\varepsilon_{fe} + \varepsilon_{bi}) \frac{c}{d_f - c}$

$= (0.00848 + 0.0000015) \frac{64}{245-64}$

$= 0.003$

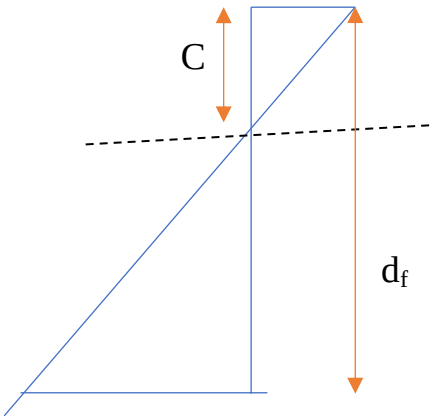

Step 7—Calculate the strain in the existing reinforcing steel

$\varepsilon_s = (\varepsilon_{fe} + \varepsilon_{bi}) \frac{d-c}{d_f-c}$

$= (0.00848 + 0.0000015) (\frac{211-64}{245-64})$

$= 0.00688$

Step 8—Calculate the stress level in the reinforcing steel and FRP.

$F_s = E_S \varepsilon_s \leq F_y$

$= 200000 * 0.00716 \leq 400$

$= 1432 > 400$

:. $F_s = 400$ N/ mm^2

F_{fe} =2200N/ mm

Step 9_ Calculate the internal for sultants and check equilibriu

Concrete stress block factors may be alculated using ACI 318. Approximate stress block factors may also be calculated based on the parabolic stress-strain relationship for concrete as follows:

$\beta_1 = \frac{4\varepsilon_c' - \varepsilon_c}{6\varepsilon_c' - 2\varepsilon_c}$

$\varepsilon_c' = \frac{1.7 * f_c'}{E_c}$

$= \frac{1.7*30}{25742.96} = 0.00198 = 0.002$

$\beta_1 = \frac{4(0.002)-0.003}{6(0.002)-2(0.003)} = 0.83$

$\alpha_1 = \frac{3\ \varepsilon'_c\ \varepsilon_c - \varepsilon_c{}^2}{3\ \beta_1\ \varepsilon'^2_c}$

$= \frac{3(0.002)*(0.003)-0.003^2}{3\ (0.75)0.002^2} = 0.90$

For equl by checking the intial estimate of C with (10.3.1.6g)

$C = \frac{A_S\ F_S + A_F F_{fe}}{\alpha\ f'_c\ \beta_1 b}$

$= \frac{226*400+57*1142.5}{0.89*30*0.75*150}$

C = 63.94 $\approx$ 64 :. O.K

Step 10—Calculate flexural strength components:-

The design flexural strength is calculated using (10.2.10d) . An additional reduction factor $\psi_f = 0.85$, is applied to the contribution of the FRP system:-

$M_n = A_S F_S (d - \frac{\beta\ C}{2}) + \psi f\ A_F F_{fe} (d_{fe} - \frac{\beta\ C}{2})$

$= 226 * 400 (211 - \frac{0.83*64}{2}) + 0.85 * 57 * 2200 (245 - \frac{0.83*64}{2})$

= 42271612.01 N. mm

M_n = 42.27 KN. m

42.27 = R_1 0.6

R_1 = 70.45 KN

$M_{@2} = 0$

$\frac{P}{2} * 0.6 + \frac{P}{2} * 0.9 - R_1 (1.5) = 0$

P = 140.9 KN

A. Design of reinforced concrete beam with NSM-FRP strips ;-

Here the design method for strenthening with near-surface mounted systems is explained, relying on the American code ACI440.2R-17 in the design specifications.

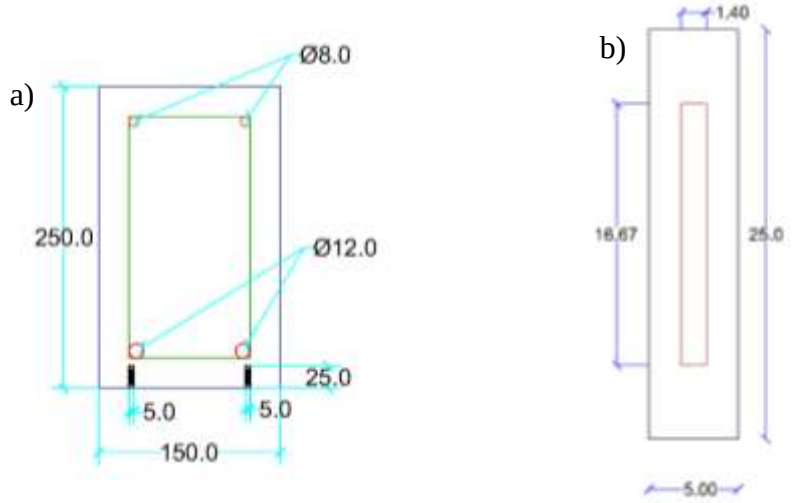

Procedure for flexural strengthening of an interior reinforced concrete beam with NSM FRP strip :-

Step 1-Calculate the FRP system design material properties

$F_{fu}=C_E\ F_{fu}^{*}= 0.95*1725=1639\ N/mm^2$

$\mathcal{E}_{fu}=C_E\ F_{fu}^{*} = 0.95*0.013=0.0123mm/mm$

Step 2—Preliminary calculations

Properties of the concrete:

β_1 from ACI 318-14, Section 22.2.2.4.3

$\beta_1=1.05-0.05\frac{fc'}{6.9}= 0.832$

$E_C=4700\sqrt{FC'}=4700\sqrt{30}\ =25742.96N/mm^2\ =25.74\ N/mm^2$

$A_S=\frac{\pi}{4}\ D^2\ *2=226\ mm^2$

A_f = =16.67*1.4*2 = 46.66 mm^2

Step 3—Determine the existing state of strain on the soffit

$\varepsilon_{bi} = M_{DL}(d_f - kd)/ I_{cr} E_C$

$M_{DL} = W L^2/8$ W=0.150*0.250*24000=900N/m

= 900*1.5/8 =168.75N. m =168.75 KN.mm

I_{cr} = (b h^3 /3)+ n A_s (space frome crnter to N.A)

n = E_S/E_C =$\frac{200000}{4700*\sqrt{30}} = 8$

$I_{cr} = \frac{150*250^3}{3}$ + 8(226)*(86 ^{2}) = 794.621* 10^6 mm^4

K= $\sqrt{(p\ n)^2 + 2(p\ n)}$ – p n

P = A_S/b d = $\frac{226}{150*211}$ = 0.00741

K= $\sqrt{(0.00714 * 8)^2 + (0.00714 * 8)}$ –(0.00714*8) = 0.285

:. $\varepsilon_{bi} = M_{DL}(d_f - kd)/ I_{cr} E_C$

$\varepsilon_{bi} = \frac{168.75(237.5-0.285*211)}{794.621*10^6*25.74} = 1.463*10^{-6}$

Step 4—Determine the bond-dependent coefficient of the FRP system

K_m is 0.7

Step 5—Estimate c, the depth to the neutral axis

Assume C= 65.5

Step 6-Determine the effective level of strain in the FRP reinforcement

$\varepsilon_{fe} = \varepsilon_{bi} \left(\frac{d_f - C}{C}\right) - \varepsilon_{bi} < K_m * \varepsilon_{fd}$

$= 0.003\left(\frac{237.5-65.5}{65.5}\right) - 0.0000051 < 0.7 * 0.0123$

= 0.00787 > 0.00861

:. ε_{fe} = 0.00787

$\varepsilon_c = (\varepsilon_{fe} + \varepsilon_{bi}) \frac{c}{d_f - c}$

$= (0.00787 + 1.463*10^{-6}) \frac{65.5}{237.5-65.5}$

$= 0.003$

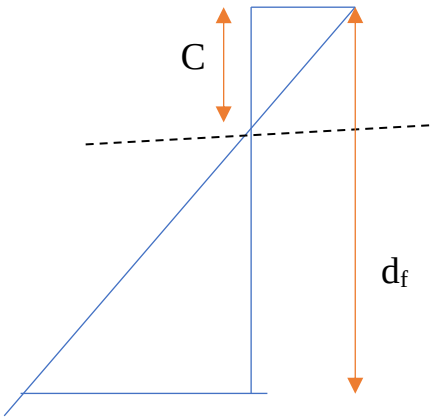

Step 7—Calculate the strain in the existing reinforcing steel

$\varepsilon_s = (\varepsilon_{fe} + \varepsilon_{bi}) \frac{d-c}{d_f-c}$

$= (0.00787 + 1.463*10^{-6}) (\frac{211-65.5}{237.5-65.5})$

$= 0.00665$

Step 8—Calculate the stress level in the reinforcing steel and FRP.

$F_s = E_S \varepsilon_s \leq F_y$

$= 200000 * 0.00739 \leq 400$

$= 1479.5 > 400$

$\therefore F_s = 400$ N/ mm^2

$F_{fe} = 2800$N/ mm

Step 9_ Calculate the internal for sultants and check equilibriu

Concrete stress block factors may be alculated using ACI 318. Approximate stress block factors may also be calculated based on the parabolic stress-strain relationship for concrete as follows:

$\beta_1 = \frac{4\varepsilon_c' - \varepsilon_c}{6\varepsilon_c' - 2\varepsilon_c}$

$\varepsilon_c' = \frac{1.7 * f_c'}{E_c}$

$= \frac{1.7*30}{25742.96} = 0.00198 = 0.002$

$\beta_1 = \frac{4(0.002)-0.003}{6(0.002)-2(0.003)} = 0.83$

$\alpha_1 = \frac{3\ \varepsilon_c'\ \varepsilon_c - \varepsilon_c^2}{3\ \beta 1\ \ \varepsilon_c'^2}$

$= \frac{3(0.002)*(0.003)-0.003^2}{3\ (0.75)0.002^2} = 0.90$

For equl by checking the intial estimate of C with (10.3.1.6g)

$C = \frac{A_S\ \ F_S + A_F F_{fe}}{\alpha\ f_c'\ \ \beta 1\ b}$

$= \frac{226*400+46.66*2800}{0.90*30*0.83*150}$

C = 65.49 $\approx$ 65.5 :. O.K

Step 10—Calculate flexural strength components:-

The design flexural strength is calculated using (10.2.10d) . An additional reduction factor $\psi_f = 0.85$, is applied to the contribution of the FRP system:-

$M_n = A_S F_S (d - \frac{\beta\ C}{2}) + \psi f\ \ A_F F_{fe} (d_{fe} - \frac{\beta\ C}{2})$

$= 226 * 400 (211 - \frac{0.83*65.5}{2}) + 0.85 * 46.66 * 2800 (245 - \frac{0.83*65.5}{2})$

= 42343878.73 N. mm

M_n = 42.34 KN. m

$42.34 = R_1\ 0.6$

R_1 = 70.57 KN

$M_{@2} = 0$

$\frac{P}{2} * 0.6 + \frac{P}{2} * 0.9 - R_1 (1.5) = 0$

P = 141.14 KN

APPENDIX B

MATERIAL DATASHEETS

وزارة الاعمار والاسكان والبلديات العامة
المركز الوطني للمختبرات الانشائية
مختبر بغداد المركزي

العدد: ٣/ف/١٥٧
التاريخ: ١/٢٤/٢٠٢٤

No. : 0022982

الـى/العتبة العباسية المقدسة / قسم المشاريع الهندسية / شعبة الصناعات الانشائية

تقرير فحص/ السمنت البورتلاندي المقاوم

ش ع / ٣٧

بموجب المواصفة القياسية العراقية رقم ٥ لسنة ٢٠١٩

نرج لاحقاً نتائج فحص العينة / العينات المبينة تفاصيلها لاحقاً راجين الاطلاع وتسديد كلفة الفحص بموجب قائمة طلب المرفقة .. مع التقدير

رقم	تاريخ	رقم وتاريخ ورود العينة	التسلسل	التاريخ	تاريخ تسلم العينة	عدد العينات	اسم المشروع وموقع العينة
٩٣٧	٢٠٢٣/١٢/٤	٣٠٢٠ في ٢٠٢٣/١٢/٢٦	-	-	٢٠٢٣/١٢/٢٦	١	العتبة العباسية المقدسة - موقع الخاطفة المركزية

الرقم المختبري	٧٤٠٧	-
الرقم الحقلي	C-SRC-12-23-L	-
نوع السمنت :	مقاوم قلار كربلاء	-

الملاحظات: تم اجراء الفحوصات الفيزياوية بموجب درجة الحرارة والرطوبة المطلوبة ضمن المواصفة

	الفحص		نتائج الفحص
الخواص الفيزيائية	١- النعومة بطريقة بلين (م²/كغم)		٣٨٦
	٢- بوقت التماسك (بجهاز فيكات) أ- الابتدائي (دقيقة)		١٢٠
	ب- النهائي (ساعة)		٤:٠٠
	٣- السلامة (الثبات)	بطريقة المعجم (%)	٠,٠٤-
		بطريقة لي شاتليه (مم)	-
	٤- تحمل الضغط (ميكانيوتن/م²)	أ- بعمر يومين	٢٢,١
		ب- بعمر ثمانية وعشرون	٤٦,٣
الخواص الكيمياوية	١- ($\%SiO_2$)		١٧,٦١
	٢- ($\%Al_2O_3$)		٣,٢٩
	٣- ($\%Fe_2O_3$)		٤,٣١
	٤- ($\%CaO$)		٦٠,٠٩
	٥- ($\%MgO$)		١,٧٥
	٦- الأملاح الكبريتية على شكل ($\%SO_3$)		٢,٠٢
	٧- المواد غير القابلة للذوبان (%)		٠,٥٦
	٨- الفقدان بالحرق (%)		٣,٩٧
	٩- ($\%C_3A$)		١,٤٣
	١٠- الكلورايد ($\%Cl$)		-

المختبر حاصل على شهادة الخبرة حسب المواصفة الدولية ISO 17025

الملاحظات والتوصيات:

اعتمدت بتاريخ ٢٠٢٢/٦/٧

Ministry of construction, housing, municipalities and public works. National Center for Construction Laboratories

ISO/IEC 17025-2017

وزارة الاعمار والاسكان والبلديات والاشغال العامة
المركز الوطني للمختبرات الانشائية
مختبر كربلاء المقدسة الانشائي

مختبر حاصل على شهادة الجودة
حسب المواصفة الدولية ISO 17025

العدد: م/ ٥٧٨
التاريخ: ٦/٥/٢٠٢٤

No. : 0034760

الى/ العتبة العباسية المقدسة /قسم المشاريع الهندسية /شعبة الصناعات الانشائية

تقرير فحص / التدرج والمواد الضارة والناعمة للركام الناعم ت ح/ ٤/ ١

بموجب المواصفة القياسية العراقية رقم ٤٥ لسنة ١٩٨٤ وتعديلاتها (رقم ١ لسنة ٢٠١٥ ورقم ٢ لسنة ٢٠١٦)
ندرج نتائج فحص النموذج المبين تفاصيله لاحقا راجين الاطلاع وتسديد كلفة الفحص بموجب قائمة الطلب ......مع التقدير

كتاب طلب الفحص			قائمة الطلب		تاريخ تسلم العينة	عدد العينات	اسم المشروع وموقع العينة
الرقم	التاريخ	رقم وتاريخ الوارد	التسلسل	التاريخ			
٣٢٥	٢٠٢٤-٤-١٣	ف/٢٥٧ في ٢٠٢٤-٤-٢٥	١/٩ ٤٢٧	٢٠٢٤	٤-٢٥	١	موقع الخباطة المركزية التابع للعتبة العباسية

	الرقم المختبري	١٤٦١			الملاحظات
	رقم الكدس	رمل (S-4-24-A)			
التدرج	مقاس المنخل (مم)				رمل منطقة تدرج(٢)
	١٠	١٠٠			١٠٠
	٤.٧٥	٩٦			١٠٠ - ٩٠
	٢.٣٦	٩٠			١٠٠ - ٨٥
	١.١٨	٨٤			١٠٠ - ٧٥
	٠.٦	٧٣			٧٩ - ٦٠
	٠.٣	٤٤			٤٠ - ١٢
	٠.١٥	١٤			١٠ - صفر

المواد الضارة والناعمة	الفحص				الملاحظات
	المواد المارة من منخل ٧٥ مايكرون %	١.٨			٥% حد اعلى
	الاملاح الكبريتية (%)	٠.٣٢٢			

الملاحظات: العلامة (-) تشير الى ان الانحراف ضمن الحدود المسموح بها بالمواصفة
النمذجة : تم جلب النموذج من قبل ممثلكم السيد(محمد جمال حسون) والمختبر غير مسؤول عن تمثيل واقع الحال
التقويم : النموذج اعلاه مطابق للمواصفات الفنية المطلوبة في كافة الفحوصات اعلاه
التوصيات:
تم اجراء الفحص الفيزياوي بموجب (م.ق.ع رقم ٣٠)لسنة ١٩٨١ والدليل الاسترشادي المرجعي ٢٠١٥/١) والفحص الكيمياوي بموجب الدليل الاسترشادي المرجعي ٣٠٥٠٠/ ٢٠١٨)
قورنت النتائج بموجب م.ق.ع رقم ٤٥ لسنة ١٩٨٤ وتعديلاتها (رقم ١ لسنة ٢٠١٥ ورقم ٢ لسنة ٢٠١٦)
التقرير مختوم بالختم الفسفوري بالاضافة الى الختم الاعتيادي ولايحتوي على اي حك او شطب او تزييف
رقم الوصل //٢٤١٩٣

م.فيزياوي سجى
اعتمدت بتاريخ ٢٠٢٢.١١.٢٩

يمنع الحك والشطب والاضافة على النتائج و...))

المدير
م. مهندس ... كاظم
علي كاظم علوان
٦/ ٥/ ٢٠٢٤

التقرير يعد ... ولا يسمح استنساخه

Ministry of construction and housing municipalities and public works. National Center for Construction Laboratories
AL- E-mail headoffice@mokhtabarat.moch Website https// www.moktabarat.moch.gov.iq

المختبر المركزي معتمد من قبل الهيئة العراقية للاعتماد للفحوصات الانشائية والم... ISO/IEC 17025-2017 رقم الشهادة TL 009
العراق – بغداد – كمب سارة – قرب جسر الطابق – ص.ب:20061

وزارة الاعمار والاسكان والبلديات والاشغال العامة
المركز الوطني للمختبرات الانشائية
مختبر كربلاء المقدسة الانشائي

العدد: ع/٩٣٢
التاريخ: ٢٠٢٤/٦/١١

No.: 0025296

ISO 17025

الى / العتبة العباسية المقدسة / قسم المشاريع الهندسية / شعبة الصناعات الانشائية

تقرير فحص / التدرج والمواد الضارة والناعمة للركام الخشن

بموجب المواصفة القياسية العراقية رقم ٤٥ لسنة ١٩٨٤ وتعديلاتها (رقم ١ لسنة ٢٠١٤ ورقم ٢ لسنة ٢٠١٦)

نرفق نتائج فحص النموذج المبين تفاصيله لاحقاً راجين الاطلاع وتسديد كلفة الفحص بموجب قائمة الطلب ..... مع التقدير

اسم المشروع موقع العينة	عدد العينات	تاريخ تسلم العينة	قائمة الطلب: التاريخ	قائمة الطلب: التسلسل	كتاب طلب الفحص: رقم وتاريخ الوارد	كتاب طلب الفحص: التاريخ	كتاب طلب الفحص: الرقم
موقع الغابة المركزية	١	٦/٩	٢٠٢٤	[illegible]	[illegible]	٢٠٢٤	[illegible]

الملاحظات			١٩٣١	الرقم المختبري
			حصى سورة مكسر (G-6-24-A)	رقم الكتاب
حدود المواصفة المقاس الاسمي الاحادي المرتبة (٢٠-٥) ملم	النسبة المئوية للمواد المارة %			مقاس المنخل (ملم)
				٧٥
				٦٣
١٠٠			١٠٠	٣٧.٥
١٠٠-٩٥			٩٧	٢٠
—			/	١٤
٦٠-٣٠			٣٦	١٠
١٠-٠			٢	٥
—			/	٢.٣٦
٣٥% حد اعلى			١٦	التآكل الميكانيكي

الملاحظات	نتيجة الفحص			الفحص
٣% حد اعلى			٠.٠٦	المواد المارة من منخل ٧٥ مايكرون (%)
٠.١% حد اعلى			٠.٠٤٣	املاح الكبريتات SO3 (%)

الملاحظات:

النمذجة: جلبت العينة من قبل ممثلكم السيد (محمد جمال حسون) والمختبر غير مسؤول عن تمثيل واقع الحال

التقويم: النموذج بالرقم المختبري اعلاه مطابق للمواصفات الفنية في كافة الفحوصات اعلاه

التوصيات:
- تم اجراء الفحص الفيزياوي بموجب (م.ق.ع رقم ٣٠ لسنة ١٩٨٤ والدليل الاسترشادي المرجعي ٢٠١٥/٤-٥٠٠) والفحص الكيمياوي بموجب الدليل الاسترشادي المرجعي (٢٠١٨/٣-٥٠٠) م.ق.ع رقم (١) لسنة ١٩٨٤
- قورنت النتائج بموجب م.ق.ع رقم ٤٥ لسنة ١٩٨٤ وتعديلاتها (رقم ١ لسنة ٢٠١٥ ورقم ٢ لسنة ٢٠١٦)
- التقرير مختوم بالختم الفسفوري بالاضافة الى الختم الاعتيادي ولا يحتوي على اي حك او شطب او تزييف

((يمنع الحك او الشطب او الاضافة على النتائج ويعتبر التقرير غير رسمي))

رقم الوصل / ٠٢٤٣٧١
المدير
م. مهندسين اقدم
علي كاظم علوان
٢٠٢٤/٦/١١

التقرير يمثل نتيجة الفحص ولا يمنع استنساخه

المختبر المركزي معتمد من قبل الهيئة العراقية للاعتماد للفحوصات الانشائية والمعدنية وفق المواصفة ISO/IEC 17025-2017 رقم الشهادة TL 009
العراق – بغداد – كتب نسارة – قرب جسر الطير – ص.ب: 20061

Ministry of construction and housing municipalities and public works, National Center for Construction Laboratories
AL- E-mail headoffice@moh... Website https://www.mokhtabarat.moch.gov.iq

G.Carbon fiber Rebar

Carbon fiber rebar, also known as carbon fiber reinforced polymer (CFRP) rebar, is a type of reinforcement material used in construction and civil engineering projects. It is a lightweight and high-strength alternative to traditional steel reinforcement which provides exceptional tensile strength, stiffness, and corrosion resistance. The combination of these properties makes carbon fiber rebar an attractive choice for applications where weight reduction, high strength, and durability are desired.

Advantages of carbon fiber rebar:

- High strength-to-weight ratio.
- Corrosion resistance.
- Excellent fatigue performance.
- Non-magnetic and non-conductive.
- Dimensional stability.
- Design flexibility.
- Easy installation.
- Longevity and durability

Product Data:

DIAMETER:	4-26 mm
TENSILE STRENGTH:	1800-2200 Mpa
ELASTIC MODULUS:	140-155 Gpa
ELONGATION:	1.3-1.5%
DENSITY:	1.6-1.8g/m^3
COEFFICIENT OF THERMAL EXPANSION	0 (x10-6/° C)
SURFACE:	Ribbed/wrapped/sand coated
MATERIAL:	Carbon Roving & Epoxy Additives



D.Carbon fiber Laminates / Plate

Carbon fiber laminates / Plate are typically made by pressing multiple layers of carbon fiber fabric or unidirectional carbon fiber together under high pressure and temperature using a high-strength epoxy resin. Carbon fiber laminates are increasingly being used in construction applications as a strengthening material due to their high strength-to-weight ratio, excellent stiffness, and durability. They are typically used to reinforce structures such as concrete, masonry, or steel that require additional support to withstand heavy loads, seismic forces, or other stresses.
In concrete structures, carbon fiber plates are commonly used to increase the flexural strength, shear strength and stiffness of beams, columns and slabs. In masonry structures, carbon fiber plates are used to reinforce walls and improve their resistance to seismic and wind loads. In steel structures, carbon fiber plates can be used to reinforce steel members and increase their load-carrying capacity. They can be anchored to the surface of the steel using mechanical fasteners, adhesive anchors, or a combination of both.

Product Data:

THICKNESS:	1.4 MM I 2 MM I 3 MM
TENSILE STRENGTH:	2400-2800Mpa
TENSILE MODULUS:	⩾ 200 GPA
ELONGATION:	⩾ 1.6%
WIDTH:	5 CM I 10 CM I 20 CM
LENGTH:	50 M I 100 M



BUILDING TRUST

PRODUCT DATA SHEET

Sikadur®-30 LP

Thixotropic adhesive for bonding reinforcement

DESCRIPTION

Sikadur®-30 LP is a thixotropic, structural 2-component adhesive, based on a combination of epoxy resins and especially designed for use at higher temperatures between +25 °C and +55 °C.
Suitable for use in hot and tropical climatic conditions.

USES

Sikadur®-30 LP may only be used by experienced professionals.

Adhesive for bonding structural reinforcement, particularly in structural strengthening works. Especially for the following uses:
- Sika® CarboDur® Plates to concrete, brickwork, timber and steel (for details see the Sika® CarboDur® Product Data Sheet, the "Method Statement for Sika® CarboDur® Externally Bonded Reinforcement" and the "Method Statement for Sika® CarboDur® Near Surface Mounted Reinforcement").
- Steel plates to concrete (for details see the relevant Sika Technical information).

FEATURES

Sikadur®-30 LP has the following advantages:
- Long pot life
- High temperature resistance at elevated curing temperatures
- Easy to mix and apply
- No primer needed
- High creep resistance under permanent load
- Very good adhesion to concrete, masonry, stonework, steel, cast iron, aluminium, timber and Sika® CarboDur® Plates
- Hardening is not affected by high humidity
- High strength adhesive
- Thixotropic: non-sag in vertical and overhead applications
- Hardens without shrinkage
- Different coloured components (for mixing control)
- High initial and ultimate mechanical resistance
- High abrasion and shock resistance
- Impermeable to liquids and water vapour

SUSTAINABILITY

Sikadur®-30 LP is certified according "Low Emitting Materials as per Al Sa'fat - Dubai Green Building Evaluation System" by Dubai Central Laboratory (DCL) certificate No. CL17020432

CERTIFICATES AND TEST REPORTS

- Adhesive for structural bonding tested according to EN 1504-4.

PRODUCT INFORMATION

Composition	Epoxy resin	
Packaging	6 kg (A + B)	Pre-batched unit
	12 kg (A + B)	Pre-batched unit
Shelf life	24 months from date of production	
Storage conditions	Store in original, unopened, sealed and undamaged packaging in dry conditions at temperatures between +5 °C and +30 °C. Protect from direct sunlight.	
Colour	Component A: white Component B: black Component A + B: light grey	
Density	~1.8 kg/l (+23 °C) (components A + B)	

SYSTEM INFORMATION

System structure	Sika® CarboDur® System: For Application Details of Sika® CarboDur® plates with Sikadur®-30 LP, see the "Method Statement for Sika® CarboDur® Externally Bonded Reinforcement" and the "Method Statement for Sika® CarboDur® Near Surface Mounted Reinforcement"

TECHNICAL INFORMATION

Compressive strength (DIN EN 196)

Curing time	Curing temperature	
	+25 °C	+55 °C
12 h	–	~90 N/mm²
1 d	> 75 N/mm²	~100 N/mm²
3 d	> 85 N/mm²	~110 N/mm²

Modulus of elasticity in compression ~10 000 N/mm² (+25 °C) (ASTM D 695)

Flexural-strength (DIN EN 196)

Curing time	Curing temperature	
	+25 °C	+55 °C
1 d	> 12 N/mm²	~38 N/mm²
3 d	> 20 N/mm²	~40 N/mm²
7 d	> 25 N/mm²	~42 N/mm²

Tensile strength (ISO 527)

Curing time	Curing temperature	
	+25 °C	+55 °C
1 d	–	~26 N/mm²
3 d	~14 N/mm²	~28 N/mm²
7 d	~17 N/mm²	~28 N/mm²

Modulus of elasticity in tension ~10 000 N/mm² (+25 °C) (ISO 527)

Shear strength (FIP 5.15: Fédération Internationale de la Précontrainte)

Curing time	Curing temperature		
	+25 °C	+44 – 55 °C	+80 °C
> 1 h	–	–	*~17 N/mm²
7 d	*~7 N/mm²	~19 N/mm²	–

*(DIN EN 1465)

Tensile adhesion strength (EN ISO 4624)

Curing time	Substrate	Curing temperature +25 °C	Curing temperature +55 °C
1 d	Concrete	> 4 N/mm² (Concrete fracture)	> 4 N/mm² (Concrete fracture)
1 d	Steel	~15 N/mm²	~25 N/mm²
3 d	Steel	~22 N/mm²	~28 N/mm²

Shrinkage ~0.04 % (FIP: Fédération Internationale de la Précontrainte)

Coefficient of thermal expansion 2.5 x 10^{-5} per °C (Temperature range: -20 °C min. / +40 °C max.) (EN 1770)

Service temperature -40 °C min. / +45 °C max. (when cured at > +23 °C)
-40 °C min. / +72 °C max. (when cured > 2 h at +80 °C within 7 d)

Glass transition temperature (EN 12614)

Curing time	Curing temperature	TG
3 d / 1 d	+23°C / +80 °C	+90 °C
3 d / 1 d	+23°C / +50 °C	+80 °C
30 d	+30 °C	+70 °C

Heat deflection temperature (FIP 5.10: Fédération Internationale de la Précontrainte, ASTM D 648)

Curing time	Curing temperature	HDT
2 h	+80 °C	+84 °C
7 d	+55 °C	+82 °C
7 d	+23 °C	+55 °C

APPLICATION INFORMATION

Mixing ratio Component A : Component B = 3 : 1 (by weight or volume)
Only mix complete pre-batched units of Sikadur®-30 LP.

Layer thickness 30 mm max.

Sag flow On vertical surfaces it is non-sag up to 3 – 5 mm thickness at +55 °C. (FIP: Fédération Internationale de la Précontrainte)

Squeezability 5 500 mm² at +25 °C at 15 kg (FIP: Fédération Internationale de la Précontrainte)

Material temperature Sikadur®-30 LP must be applied at temperatures between +20 °C and +40 °C.

Ambient air temperature +25 °C min. / +55 °C max.

Dew point Beware of condensation.
Substrate temperature during application must be at least 3 °C above dew point.

Substrate temperature +25 °C min. / +55 °C max.

Substrate moisture content Maximum 4 % pbw
When applied to mat damp concrete, brush the adhesive well into the substrate.

Pot Life (FIP: Fédération Internationale de la Précontrainte)

Temperature	Potlife	Open time
+25 °C	~60 min	~90 min
+55 °C	~30 min	~60 min

The potlife begins when the resin and hardener are mixed. It is shorter at high temperatures and longer at low temperatures. The greater the quantity mixed, the shorter the potlife. To obtain longer workability at high temperatures, the mixed adhesive may be divided into portions. Another method is to chill components A and B before mixing them (not below +5 °C).

BASIS OF PRODUCT DATA

All technical data stated in this Data Sheet are based on laboratory tests. Actual measured data may vary due to circumstances beyond our control.

IMPORTANT CONSIDERATIONS

Sikadur® resins are formulated to have low creep under permanent loading. However, due to the creep behavior of all polymer materials under load, the long term structural design load must account for creep. Generally the long term structural design load must be lower than 20 – 25 % of the failure load.
A structural engineer must be consulted for load calculations for the specific application.

ECOLOGY, HEALTH AND SAFETY

User must read the most recent corresponding Safety Data Sheets (SDS) before using any products. The SDS provides information and advice on the safe handling, storage and disposal of chemical products and contains physical, ecological, toxicological and other safety-related data.

APPLICATION INSTRUCTIONS

SUBSTRATE QUALITY

See the Product Data Sheet of Sika® CarboDur® Plates and Sika® CarboDur® BC rods.

SUBSTRATE PREPARATION

See the "Method Statement for Sika CarboDur® Externally Bonded Reinforcement" and the "Method Statement for Sika CarboDur® Near Surface Mounted Reinforcement".

MIXING

Pre-batched units:
Mix components A and B together for at least 3 minutes with a mixing spindle attached to a slow speed electric drill (maximum 300 rpm) until the material becomes smooth in consistency and a uniform grey colour. Avoid aeration while mixing. Then, pour the whole mix into a clean container and stir again for approximately 1 more minute at low speed to keep air entrapment at a minimum. Mix only that quantity which can be used within its potlife.

APPLICATION METHOD / TOOLS

See the "Method Statement for Sika® CarboDur® Externally Bonded Reinforcement" and the "Method Statement for Sika® CarboDur® Near Surface Mounted Reinforcement".

CLEANING OF EQUIPMENT

Clean all tools and application equipment with Sika® Colma Cleaner immediately after use. Hardened / cured material can only be mechanically removed.

LOCAL RESTRICTIONS

Note that as a result of specific local regulations the declared data and recommended uses for this product may vary from country to country. Consult the local Product Data Sheet for exact product data and uses.

LEGAL NOTES

The information, and, in particular, the recommendations relating to the application and end-use of Sika products, are given in good faith based on Sika's current knowledge and experience of the products when properly stored, handled and applied under normal conditions in accordance with Sika's recommendations. In practice, the differences in materials, substrates and actual site conditions are such that no warranty in respect of merchantability or of fitness for a particular purpose, nor any liability arising out of any legal relationship whatsoever, can be inferred either from this information, or from any written recommendations, or from any other advice offered. The user of the product must test the product's suitability for the intended application and purpose. Sika reserves the right to change the properties of its products. The proprietary rights of third parties must be observed. All orders are accepted subject to our current terms of sale and delivery. Users must always refer to the most recent issue of the local Product Data Sheet for the product concerned, copies of which will be supplied on request.

Sika Gulf B.S.C. (c)
Tel: +973 177 38188
Email: info@bh.sika.com
Sika Kuwait Cons. Mat. & Paints Co WLL
Tel: +965 22 282 296
Email: sika.kuwait@kw.sika.com
Web: gcc.sika.com

Sika UAE LLC
Sika MB Construction Chemicals LLC
Sika International Chemicals LLC
Tel: +971 4 439 8200
Email: info@ae.sika.com
Web: gcc.sika.com

Sika Saudi Arabia Limited
Riyadh / Jeddah / Dammam / Rabigh
Tel: +966 11 217 6532
Email: info@sa.sika.com
Web: gcc.sika.com

Sika LLC - Oman
Master Builders Solutions LLC
(part of Sika)
Tel. +968 22 826 500
Email: info@om.sika.com
Web: gcc.sika.com

Structuro 502

FOSROC constructive solutions

A high performance concrete hyperplasticiser based on polycarboxylate technology

Uses

- Self-compacting concrete
- Pumped concrete
- Concrete requiring long workability retention
- High performance concrete

Advantages

- Increased early and ultimate compressive strengths
- Increased flexural strength
- Improved adhesion to reinforcing and stressing steel
- Improved resistance to carbonation
- Lower permeability
- Increased resistance to aggressive atmospheric conditions
- Reduced shrinkage and creep
- Increased durability

Description

Structuro 502 is differentiated from conventional superplasticisers in that it is based on a unique carboxylic ether polymer with long lateral chains. This greatly improves cement dispersion. At the start of the mixing process an electrocstatic dispersion occurs but the presence of the lateral chains, linked to the polymer backbone, generate a steric hindrance which stabilises the cement particle's capacity to separate and disperse. This mechanism considerably reduces the water demand in flowable concrete.

Structuro 502 combines the properties of water reduction and workability retention. It allows the production of high performance concrete and/or concrete with high workability.

Structuro 502 is a particularly strong hyperplasticiser allowing production of consistent concrete properties around the required dosage.

Properties

Appearance:	Light brown coloured liquid
pH value:	6.5
S.G. @ 20°C	1.06 ± 0.02
Chloride content:	Nil
Alkali content:	Typically less than 1.5 gm Na_2O equivalent per litre of admixture

Dosage

The optimum dosage of Structuro 502 to meet specific requirements should always be determined by trials using the materials and conditions that will be experienced in use. The normal dosage range is between 0.2 to 3.0 litres/100 kg of cementitious material.

Use at other dosages

Dosages outside the normal range quoted above can be used to meet particular mix requirements. Contact Fosroc Technical Service Department for advice in these cases.

Effects of Overdosing

Over-dosage may cause delay in the setting time.

Technical support

Fosroc offers a comprehensive technical support service to specifiers, end users and contractors. It is also able to offer on-site technical assistance.

Instructions for use

Compatibility

Structuro 502 should not be used in conjunction with any other admixture unless prior approval is obtained from local Fosroc office.

Structuro 502 is suitable for use with all types of Portland cements and cement replacement materials such as PFA, GGBFS, and SRC and micro-silica.

Mixing

When used at the mixing plant, Structuro 502 should be added in the mixing water.

In some instances, e.g. addition to ready mix concrete on site, Structuro 502 can be added directly in the truck mixer and mixed at maximum speed for an extra 5 minutes.

Structuro 502

Dispensing

The correct quantity of Structuro 502 should be measured by means of a recommended dispenser. The admixture should then be added to the concrete with the mixing water to obtain the best results. Contact Fosroc for advice regarding suitable equipment and its installation.

Estimating – Packaging

Structuro 502 is available in 200 litre drums and 1000 tanks.

Storage

Structuro 502 has a minimum shelf life of 6 months provided the temperature is kept within the range of $2^{o}C$ to $50^{o}C$. Should the temperature of the product fall outside this range then contact Fosroc for advice.

Precautions

Health and Safety

Structuro 502 does not fall into the hazard classifications of current regulations. However, it should not be swallowed or allowed to come into contact with skin and eyes.

Suitable protective gloves and goggles should be worn. Splashes on the skin should be removed with water. In case of contact with eyes rinse immediately with plenty of water and seekmedical advice. If swallowed seek medical attention immediately - Do not induce vomiting.

For further information consult the Material Safety Data sheet available for this product.

Fire

Structuro 502 is water based and non-flammable.

Cleaning and disposal

Spillages of Structuro 502 should be absorbed onto sand, earth or vermiculite and transferred to suitable containers. Remnants should be hosed down with large quantities of water.

The disposal of excess or waste material should be carried out in accordance with local legislation under the guidance of the local waste regulatory authority.

FOSROC

Fosroc Jordan

Head Office
P.O Box 253,
King Abdullah II Industrial State
Sahab 11512, Jordan
www.fosroc.com

Regional Offices **email:**enquiryjordan@fosroc.com

Amman - Khalda Offices:	Tel: (06) 535 9562	Fax: (06) 535 9563
Amman – Sahab Factory:	Tel: (06) 402 2665	Fax: (06) 402 9475
Aqaba Showroom:	Tel: (03) 205 0061	Fax: (03) 205 0062

الخلاصة

تتناول هذه الدراسة سلوك العتبات الخرسانية المسلحة المعززة بالمطاط عند تعرضها لأحمال متكررة، والمعززة باستخدام قضبان وألواح البوليمر المقوى بالألياف الكربونية (CFRP) المرفقة بالقرب من السطح (NSM). تهدف الدراسة إلى معالجة القضية البيئية المتزايدة الناتجة عن النفايات من إطارات المركبات التالفة ، التي يصعب التخلص منها بسبب طبيعتها غير القابلة للتحلل البيولوجي. من خلال إعادة تدوير مطاط الإطارات واستخدامه كبديل جزئي للركام الخشن والناعم في الخرسانة، تسعى الدراسة إلى تقليل نفايات الإطارات وتقييم تأثيرها على خصائص الخرسانة والأداء الهيكلي.

تضمن البرنامج التجريبي استبدال الركام الناعم والخشن بجزيئات المطاط بنسب حجمية قدرها 10% و20% بشكل منفصل ومجتمعة. تم إعداد أربعة عشر عينة من العتبات (250 × 150 × 1600 مم)، بما في ذلك عتبتين مرجعيتين (تم اختبار واحدة تحت تحميل أحادي والأخرى تحت تحميل متكرر) واثني عشر عتبة معززة. تم تقسيم العتبات إلى مجموعتين: ستة عتبات معززة باستخدام قضبان NSM-CFRP وستة معززة باستخدام ألواح NSM-CFRP. اتبع اختبار الأحمال المتكررة بروتوكولًا يتضمن 30 دورة، بدءًا من 30%، 60%، و80% من الحمل الأقصى، تلتها تحميلات حتى الفشل.

أظهرت النتائج أن استبدال الركام بالمطاط أدى إلى تقليل كبير في الخصائص الميكانيكية، بما في ذلك القوة الانضغاطية، قوة الشد، والقوة المرنة بنسبة 51.66% و22.59% و38% على التوالي عند نسبة استبدال 20%. أظهرت الخرسانة المعززة بالمطاط قدرة تحميل نهائية أقل، خاصة عند مستويات الاستبدال العالية. ومع ذلك، أظهر استبدال الركام الخشن بالمطاط مقاومة أفضل للتشقق مقارنةً باستبدال الركام الناعم.

ساهم التعزيز باستخدام ألواح NSM-CFRP في تحسين قدرة التحميل النهائية تحت الأحمال المتكررة أكثر من القضبان NSM-CFRP. أظهر النموذج العددي باستخدام برنامج ABAQUS توافقًا جيدًا مع النتائج التجريبية مع انحرافات طفيفة. كشفت التحليلات أن زيادة قطر قضبان CFRP من 6 مم إلى 8 مم أدى إلى تحسين قدرة التحميل النهائية بنسبة 2.25%، بينما أسفرت زيادة سماكة الألواح من 1.2 مم إلى 2 مم عن تحسين طفيف بنسبة 0.74%، مما يشير إلى محدودية الجدوى الاقتصادية للألواح الأكثر سمكًا.

تسلط هذه الدراسة الضوء على إمكانيات الخرسانة المعززة بالمطاط كمواد مستدامة وفعالية أنظمة التعزيز باستخدام NSM-CFRP في تحسين أداء العتبات الخرسانية تحت ظروف التحميل المتكرر.

جمهورية العراق

وزارة التعليم العالي و البحث العلمي

جامعة كربلاء

كلية الهندسة

قسم الهندسة المدنية

تقوية العوارض الخرسانية المطاطية المسلحة بواسطة تقنية NSM-CFRP التي تتعرض لأحمال متكررة

رسالة مقدمة الى مجلس كلية الهندسة / جامعة كربلاء وهي جزء من متطلبات نيل درجة الماجستير في علوم الهندسة المدنية

المؤلف:

شهد عدنان عبد الكاظم

باشراف :

أ. م.د علي غانم عباس الخفاجي

شوال - 1446

نيسان - 2025